UDK 621.3:(53+54+621+66)(05)(497.1)=00 ISSN 0352-9045

INFORMACIJE MIDEM

Strokovno društvo za mikroelektroniko elektronske sestavne dele in materiale

3°2008

Strokovna revija za mikroelektroniko, elektronske sestavne dele in materiale
Journal of Microelectronics, Electronic Components and Materials

INFORMACIJE MIDEM, LETNIK 38, ŠT. 3(127), LJUBLJANA, september 2008

LMFE Laboratorij za Mikroelektroniko
FAKULTETA ZA ELEKTROTEHNIKO
UNIVERZA V LJUBLJANI

UDK 621.3:(53+54+621+66)(05)(497.1)=00 ISSN 0352-9045

INFORMACIJE MIDEM 3 ◦ 2008

INFORMACIJE MIDEM LETNIK 38, ŠT. 3(127), LJUBLJANA, SEPTEMBER 2008
INFORMACIJE MIDEM VOLUME 38, NO. 3(127), LJUBLJANA, SEPTEMBER 2008

Revija izhaja trimesečno (marec, junij, september, december). Izdaja strokovno društvo za mikroelektroniko, elektronske sestavne dele in materiale - MIDEM.
Published quarterly (march, june, september, december) by Society for Microelectronics, Electronic Components and Materials - MIDEM.

Naslov uredništva
Headquarters
Uredništvo Informacije MIDEM
MIDEM pri MIKROIKS
Stegne 11, 1521 Ljubljana, Slovenija
tel.: + 386 (0)1 51 33 768
faks: + 386 (0)1 51 33 771
e-pošta: Iztok.Sorli@guest.arnes.si
http://www.midem-drustvo.si/

Letna naročnina je 100 EUR, cena posamezne številke pa 25 EUR. Člani in sponzorji MIDEM prejemajo Informacije MIDEM brezplačno.
Annual subscription rate is EUR 100, separate issue is EUR 25. MIDEM members and Society sponsors receive Informacije MIDEM for free.

Znanstveni svet za tehnične vede je podal pozitivno mnenje o reviji kot znanstveno-strokovni reviji za mikroelektroniko, elektronske sestavne dele in materiale. Izdajo revije sofinancirajo ARRS in sponzorji društva.
Scientific Council for Technical Sciences of Slovene Research Agency has recognized Informacije MIDEM as scientific Journal for microelectronics, electronic components and materials.
Publishing of the Journal is financed by Slovene Research Agency and by Society sponsors.

Znanstveno-strokovne prispevke objavljene v Informacijah MIDEM zajemamo v podatkovne baze COBISS in INSPEC.

Prispevke iz revije zajema ISI® v naslednje svoje produkte: Sci Search®, Research Alert® in Materials Science Citation Index™

Scientific and professional papers published in Informacije MIDEM are assessed into COBISS and INSPEC databases.

The Journal is indexed by ISI® for Sci Search®, Research Alert® and Material Science Citation Index™

Po mnenju Ministrstva za informiranje št.23/300-92 šteje glasilo Informacije MIDEM med proizvode informativnega značaja.

Grafična priprava in tisk
Printed by
BIRO M, Ljubljana

Naklada
Circulation
1000 izvodov
1000 issues

Poštnina plačana pri pošti 1102 Ljubljana
Slovenia Taxe Percue

UDK621.3:(53+54+621+66), ISSN0352-9045 Informacije MIDEM 38(2008)3, Ljubljana

VSEBINA CONTENT

Obnovitev članstva v strokovnem društvu MIDEM in iz tega izhajajoče ugodnosti in obveznosti

Spoštovani,

V svojem več desetletij dolgem obstoju in delovanju smo si prizadevali narediti društvo privlačno in koristno vsem članom.Z delovanjem društva ste se srečali tudi vi in se odločili, da se v društvo včlanite. Življenske poti, zaposlitev in strokovno zanimanje pa se z leti spreminjajo, najrazličnejši dogodki, izzivi in odločitve so vas morda usmerili v povsem druga področja in vaš interes za delovanje ali članstvo v društvu se je z leti močno spremenil, morda izginil. Morda pa vas aktivnosti društva kljub temu še vedno zanimajo, če ne drugače, kot spomin na prijetne čase, ki smo jih skupaj preživeli. Spremenili so se tudi naslovi in način komuniciranja.

Ker je seznam članstva postal dolg, očitno pa je, da mnogi nekdanji člani nimajo več interesa za sodelovanje v društvu, se je Izvršilni odbor društva odločil, da stanje članstva uredi in **vas zato prosi, da izpolnite in nam pošljete obrazec priložen na koncu revije.**

Naj vas ponovno spomnimo na ugodnosti, ki izhajajo iz vašega članstva. Kot član strokovnega društva prejemate revijo »Informacije MIDEM«, povabljeni ste na strokovne konference, kjer lahko predstavite svoje raziskovalne in razvojne dosežke ali srečate stare znance in nove, povabljene predavatelje s področja, ki vas zanima. O svojih dosežkih in problemih lahko poročate v strokovni reviji, ki ima ugleden IMPACT faktor.S svojimi predlogi lahko usmerjate delovanje društva.

Vaša obveza je plačilo članarine 25 EUR na leto. Članarino lahko plačate na transakcijski račun društva pri A-banki : 051008010631192. Pri nakazilu ne pozabite navesti svojega imena!

Upamo, da vas delovanje društva še vedno zanima in da boste članstvo obnovili. Žal pa bomo morali dosedanje člane, ki članstva ne boste obnovili do konca leta 2008, brisati iz seznama članstva.

Prijavnice pošljite na naslov:

MIDEM pri MIKROIKS

Stegne 11

1521 Ljubljana

Ljubljana, september 2008

Izvršilni odbor društva

SAFETY MARGIN AT MAMMALIAN NEUROMUSCULAR JUNCTION - AN EXAMPLE OF THE SIGNIFICANCE OF FINE TIME MEASUREMENTS IN NEUROBIOLOGY

Jože Trontelj*, Janez Trontelj** and †Lojze Trontelj**

*Institute of Clinical Neurophysiology, University Medical Centre of Ljubljana, Slovenia;
**Laboratory for Microelectronics, Faculty of Electrical Engineering,
University of Ljubljana, Slovenia

Key words: neuromuscular transmission, neuromuscular junctions, single fibre electromyography, jitter, safety factor.

Abstract: Single fibre electromyography with axonal microstimulation was used to study the margin of safety of neuromuscular transmission in human and in rat muscle. The latter has been claimed to have a significantly wider safety margin compared to man. There is an inverse relationship between the jitter of the neuromuscular junction (NMJ) and its safety factor. Jitter was measured at 498 NMJs of the extensor communis muscle of 16 healthy human volunteers and at 177 NMJs in the tibialis anterior of 6 Wistar rats. The mean jitter expressed as MCD was 17.1 μs (SD 8.2) and 17. 7 μs (SD 6.1) for the human and the rat muscle, respectively. Moreover, the scatter of the individual jitter values was remarkably similar. These closely similar findings ($P < 0.5$) demonstrate that no significant difference exists in the safety margin of neuromuscular transmission between the two muscles in man and in the rat. An essential condition for studies of this kind has been adequate resolution of time measurement, < 1 μs. This could have been achieved by using a home-designed system for finely adjustable microstimulation amplitude at pulse width ≤ 0.01 ms and for jitter measurement at a resolution of 0.0001 ms, both of which is still unsurpassed by the commercially available equipment for single fibre electromyography.

Varnostni rob na živčno-mišičnem stiku sesalcev, primer pomembnosti natančnega merjenja časa v nevrobiologiji

Kjučne besede: živčno-mišični prenos, živčno-mišični stik, elektromiografija posamičnih vlaken, živčno-mišični drget, varnostni koeficient

Izvleček: V raziskavi varnostnega roba živčno–mišičnega prenosa v človeški in podganji mišici je bila uporabljena elektromiografija posamičnih vlaken z mikrostimulacijo motoričnih aksonov. Ta je po splošnem prepričanju pri podgani mnogo širši kot pa pri človeku. Obstaja obratno sorazmerje med razponom drgeta živčno–mišičnega stika (NMJ) in varnostnim koeficientom. Razpon drgeta je bil merjen v mišici extensor digitorum communis na 498 motoričnih ploščicah 16 zdravih prostovoljcev in na 177 motoričnih ploščicah v mišici tibialis anterior 6 podgan rase Wistar. Povprečni drget, izražen kot MCD, je bil 17.7 μs (SD 8.2) pri človeški mišici in 17.8 μs (SD 6.1) pri podganji mišici. Tudi raztros posameznih vrednosti drgeta je bil zelo podoben. Ti zelo podobni rezultati ($P<0.5$) kažejo, da ni pomembne razlike med varnostnim koeficientom za pregledani mišici pri človeku in podgani. Ključni pogoj za take raziskave pa je ustrezna ločljivost in natančnost merjenja časa, ki mora biti boljša od ene mikrosekunde. To je bilo možno doseči z lastno zasnovo fino nastavljive amplitude mikrostimulacije pri širinah impulza ≤ 0.01ms in merjenje latenc z ločljivostjo 0.0001 ms, kar je veliko boljše, kot je dosegljivo s komercialno dostopnimi napravami za elektromiografijo posamičnih mišičnih vlaken.

1. Introduction

Single fibre EMG is a method which allows recording of action potentials of single muscle fibres in humans or animals, *in vivo* and *in situ*. The method, originally developed by Ekstedt and Stålberg (1964 and 1966) and later supplemented by axonal microstimulation (Trontelj and Stålberg 1992), has been introduced in clinical neurology as a highly sensitive and specific diagnostic technique, mainly for the diagnosis of disorders of neuromuscular transmission. In research, it has contributed many new observations regarding the microphysiology and structure of the motor unit (Stålberg, Trontelj 1994).

The essence of the technique is in its high selectivity of recording, higher than with the conventional needle electrodes used in standard clinical electromyography. The physical dimensions and the input impedance of the active electrode, 25 mm platinum surface exposed in a side port of a cannula, provide a happy compromise resulting in relatively high amplitudes of the recorded single muscle fibre action potentials (most often 1-7 mV, and up to 15 mV). On the other hand, the size of the recording area is comparatively small (a hemisphere of about 300 μm) and is well suited to record from only a limited number of closely adjacent muscle fibres (1-3, rarely up to 10). Later it became apparent that this number does not change much in muscle atrophy in spite of the smaller fibre size, since atrophic fibres are weaker electric generators, and the recording area also becomes smaller. Thus a restricted, more or less standard fraction of the motor unit territory can be investigated. With some experience, the intramuscular position of the electrode can be manually adjusted and maintained for periods of up to more than an hour, thus allowing prolonged recordings from individual muscle fibres. With constant position, the amplitude, shape, and duration of single fibre action potentials clear-cut biphasic spikes remain remarkably constant on consecutive discharges. This makes it possible to accurately identify the moment of depolarization of muscle fibre membrane at the

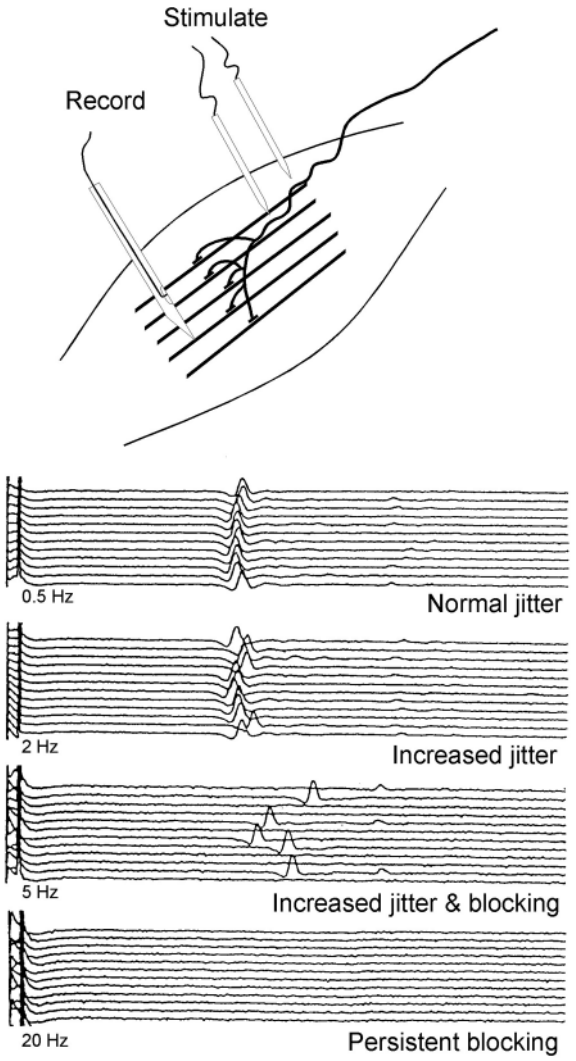

Fig. 1. Jitter study with axonal stimulation technique. The jitter is measured between the stimulus and the action potentials from one muscle fibre. Different degrees of jitter at the same myasthenic NMJ are produced in this case by changing stimulation rate. With 50 % block in the 3rd pane the safety margin of neuromuscular transmission is zero. (From Trontelj et al. 2001, with permission).

electrode surface. Time measurements, e.g. between stimulus and response or between two action potentials from neighbouring fibres with a resolution as high as 100 nanoseconds are not only possible but may, in certain cases, have a physiological significance (Trontelj et al, 1990).

When a motor axon is stimulated repetitively above its threshold and responses are recorded from a single muscle fibre there is latency *variability* of the order of tens of microseconds. This phenomenon is called *the jitter*. The term jitter was introduced to denote variation of neuromuscular transmission time at a single or a pair of neuromuscular junctions (NMJs). It is usually expressed as *mean of consecutive differences* of delay, the *MCD* (Stålberg, Trontelj 1994).

The main source of the jitter in normal muscle is at the NMJ. The jitter is discussed in detail elsewhere (e. g., Stålberg and Trontelj 1994). At the normal NMJ, it is mainly due to small fluctuations in the firing threshold of the subsynaptic sarcolemma, which result in variable neuromuscular transmission time. Moreover, minor variations in amplitude and therefore slope of the end-plate potential, which are due to the variable number of released ACh quanta, contribute to the variability of this synaptic delay in normal muscle (Fig. 2a).

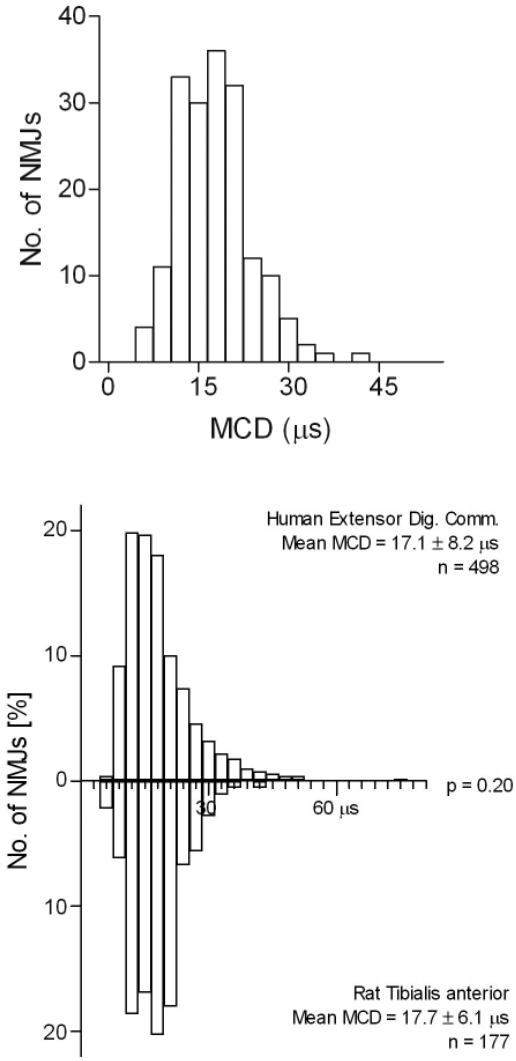

Fig. 2. A. Jitter values of the 177 rat tibialis anterior NMJs. B. Jitter of 498 NMJs in the human extensor digitorum muscle of 16 subjects plotted against jitter values at 177 tibialis anterior NMJs of 6 rats. The means and distributions are closely similar.

Normal jitter varies among different NMJs in the same muscle, and the normal range of mean jitter values varies among muscles. In a study of the effects of regional curarization (Schiller, Stålberg and Schwartz 1975) it was shown that the magnitude of the jitter is related to *the safety margin* of neuromuscular transmission. In other words, the jitter depends on the height of the tip of the endplate potential above

Muscle	Number of NMJs	Minimum [µs]	95% centile [µs]	Mean [µs]	SD [µs]
Extensor dig. comm. (man)	498	5	35.5	17.1	8.2
Tibialis ant. (rat)	177	6	30.5	17.7	6.1

the muscle fibre firing threshold, i.e., on the excess of the acetylcholine receptors activated per nerve impulse. This means that in a normal muscle, the NMJs have a rather different safety margin. When a disease process, such as myasthenia gravis, affects the structure and function of the NMJs, the jitter becomes increased and at a certain point, most often with jitter values between 60 and 120 µs, intermittent blocking of transmission sets in. At this point, the safety margin is close to zero. With increasing jitter values, for example during continued activity, the blocking becomes more frequent and may finally persist.

This safety margin can be semi-quantitatively estimated in vivo in experiments with axonal stimulation during ischaemia or treatment with neuromuscular blocking agents (Dahlbäck et al. 1970; Ekstedt, Stålberg 1969; Schiller et al. 1975; Trinkaus et al. 2007).

Jitter measurement was originally described during voluntary muscle contraction, where the phenomenon is displayed as changing intervals between action potentials of two muscle fibres of the same motor unit during repetitive discharges. The technique was later made simpler and independent of patient's cooperation by replacing voluntary contraction with axonal microstimulation. In this way it became possible to use it also in animals (Trontelj et al. 1986). Moreover, the perfect control of firing patterns and rates over a wide range exceeding that of physiological discharge rates combined with high resolution time measurement made possible new types of in vivo research into physiology and pathology of neuromuscular transmission in intact man or animal.

The purpose of this study was to compare the jitter, and thus the safety margin of neuromuscular transmission, in a human and the rat limb muscle.

2. Materials and Methods

2.1. Human subjects

Sixteen normal subjects participated in the study, their ages ranging between 25 and 45 years. All were in good health and without evidence or past history of neurological problems. The jitter measurement was performed at 10 Hz stimulation at 498 NMJs in the extensor communis muscle. The details of the technique are described elsewhere (Trontelj, Stålberg 1992, Stålberg, Trontelj 1994). Part of the data has been published (Trontelj et al. 2002).

2.2. Animals

Adult male rats (Wistar strain, 200-300 g) were used. The animals were maintained on a standard diet with food and water ad libitum and all efforts were made to assure their comfort. Uretan (Fluka, EU) in 25 % normal saline solution was applied i.p. in a dose of 1.75 g per kg of animal weight for anaesthesia. Tibialis anterior muscle was used; the jitter was measured at 177 NMJs of 6 animals.

The same standard stimulation SFEMG technique was used on the human subjects as well as in the animals (Trontelj, Stålberg 1992). A pair of Teflon coated monofilar needle electrodes were inserted into the belly of the muscle just proximally to its middle, so that the uninsulated tips were 3-6 mm apart. Stimuli were 0.04 µs rectangular pulses of 0.1 - 5.0 mA, adjusted to be suprathreshold for the studied motor axon. They were presented at 10 Hz, although rates of 0.5, 1, 15 and 20 Hz were tried on some NMJs to examine the presence of intratetanic potentiation or exhaustion. Recording was made with a standard SFEMG electrode inserted proximally or distally into the twitching portion of the muscle, between 5 and 12 mm away from the tips of the stimulating needle electrodes (Fig. 1). The stimulation, recording and jitter measurement were performed on a Keypoint EMG system by Medtronic. The jitter programme in this equipment uses a peak-detection algorithm, so the jitter is measured between the stimulus and the negative peak of the single muscle fibre action potential. The jitter is expressed in the standard way as the mean of absolute latency differences between consecutive responses (MCD) to a series of 100 stimuli. The accuracy of measurement was tested by measuring the jitter on simulated single fibre action potentials delivered by a pulse generator with zero jitter, and the measurement error for the conditions used was < 3 µs (MCD). This degree of time resolution was considered less than an optimum, but still adequate for recognising so called low jitter, which indicates direct stimulation of muscle fibres (i.e., not via the nerve and the NMJ). Responses with jitter < 5 µs (MCD) were excluded (Trontelj et al. 1990), but they were infrequent with the position of the stimulating and recording electrodes used.

In accordance with the national guidelines, the study was approved by the National Medical Ethics Committee of Slovenia and the Veterinary Administration of the Slovene Ministry for Agriculture, Forestry and Food, for the human and animal part, respectively.

3. Results

The results obtained are shown in Fig. 2 and in Table. The mean of all MCD values for the 498 NMJs of the human EDC muscle was 17.1 µs (SD 8.2), and for the 177 NMJs of the rat tibialis anterior muscle it was 17.7 µs (SD 6.1). The difference between the two sets of values is nonsignificant (P = 0.20). Even the distribution of the individual values within the two muscles closely resembled each other (Fig. 2). It is obvious that the jitter in the rat tibialis anterior muscle is nearly identical with that in the human extensor digitorum communis muscle. The scatter of the results among the individual animals was small (Fig. 3), again similar to the findings in the human subjects.

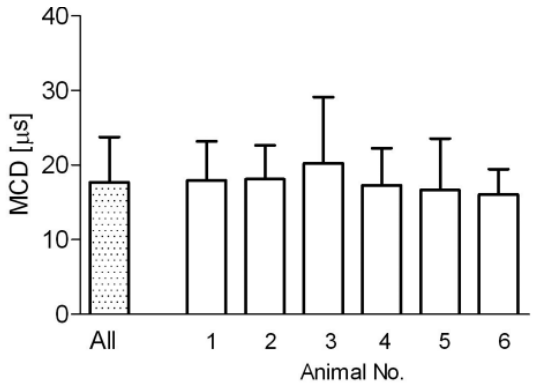

Fig. 3. The variation of the mean jitter values and the SD between the individual animals is relatively small.

With the position of the stimulating and recording electrodes used, there were few responses that could be suspected to be due to direct stimulation of the muscle fibres. As indicated above, the equipment used was barely satisfactory to measure the jitter with the precision required, so some doubt remained with the responses with the jitter in the neighbourhood of 5 µs. Experience gained with the original equipment that served during the development of the technique and the criterion to exclude any slightly 'noisy' action potentials with jitter just above 5 µs were helpful in eliminating direct responses, and were not considered to have introduced a bias towards higher jitter values.

4. Discussion

The jitter of normal neuromuscular transmission at NMJs of human muscles is between 5 and 55 ms. It has been shown that the size of the jitter at a NMJ reflects the amplitude of the end-plate potentials and is inversely related to the safety margin of impulse transmission at that NMJ.

A MCD value of less than 5 ms measured between two different single fibre action potentials or between a stimulus and the response is termed *low jitter*; the impulse in this case has not crossed a NMJ, as neuromuscular jitter always exceeds this value (Trontelj et al. 1986). An example of this is the jitter between action potentials of branches of a split muscle fibre. The jitter of a directly stimulated muscle fibre is low, provided that the stimulus is above the threshold. This could be reliably confirmed by using specially designed equipment and measuring technique (Mihelin et al. 1975) allowing an accuracy of 100 ns (Trontelj et al. 1990). With stimulation pulse width of 10 ms (Trontelj et al. 1967) and good recording conditions this system makes it possible to accurately identify cases of direct muscle fibre stimulation. Commercially available EMG equipment does not provide this degree of temporal resolution. Yet, the test of the equipment indicated an acceptable error of measurement, provided that the noise was kept at a low level.

On the other hand, the jitter of a directly stimulated muscle fibre activated at threshold may be large, between a few tens and a few hundreds of ms, when the discharge rhythm is disturbed by intermittent drop out of the responses and the discharge rate is higher than 1 Hz. This variation in latency is due to changes in muscle fibre conduction velocity (Stålberg 1966, Trontelj et al. 1990).

A similar situation arises when stimulation is via the motor axon and threshold stimulus intensity is used, so that some of the responses fail (false blocking due to insufficient stimulus). Such situations were carefully avoided by adjusting the stimulus strength well above the threshold.

The jitter of neuromuscular transmission results from variability of the time needed for the end-plate potential (EPP) to reach the depolarization threshold of the juxta-junctional sarcolemma (Fig. 4). A part of this variability is due to oscillation of the depolarization threshold of the muscle fibre (the *JUXTA-junctional* component of the jitter). This is not known to be associated with any pathology and is assumed to represent a significant share of the normal jitter.

Moreover, the EPP slope varies from discharge to discharge in a random fashion. The EPP slope in the region of threshold depends on the (extrapolated) EPP amplitude. The mean EPP amplitude and the variation of the EPP slope determine the *junctional* component of the jitter. This component depends on the amount of ACh released per nerve impulse and on the sensitivity of the postsynaptic membrane. The junctional part of the jitter thus reflects the safety margin of neuromuscular transmission, and is proportional to the (excess) amplitude of the extrapolated EPP potential above the level of muscle fibre discharge threshold. The *effect* of fluctuation of the discharge threshold (the juxta-junctional component of jitter) is inversely proportional to the EPP slope. The combination of these factors actually determines the safety margin of neuromuscular transmission (Stålberg, Trontelj 1994).

The *postjunctional* part of the jitter, mainly due to changes in muscle fibre conduction velocity resulting from different degrees of "supernormality" following previous activity, is largely avoided by the uniform discharge rates during electrical stimulation. (The contribution of this factor may be large when intermittent blocking occurs, resulting in disrupted rhythm.)

There is a possibility for a pre-junctional contribution to the jitter, seen as latency variation of the end-plate potential. The *end-plate potential jitter* is usually negligible (<1-2 µs); it may however become large after intoxication with some organophosphates (De Blaquiere et al. 1998). A large EPP jitter may also be seen in botulism or experimental intoxication with botulinum toxin B (Maselli et al. 1992; Gansel et al. 1987).

Neither pre- nor postjunctional factors could have influenced the measured jitter in this study. The measured values can therefore be safely considered to reflect the true variation of time taken for transmission at the NMJ itself, and thus its safety margin.

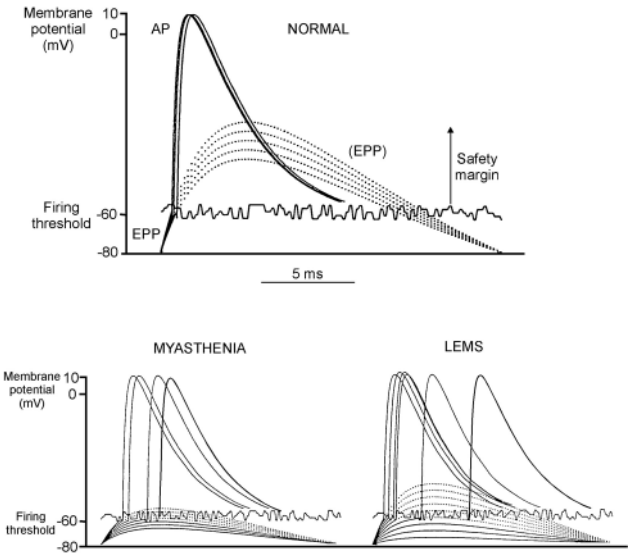

Fig. 4. Schematic explanation of the relationship between the jitter and the safety margin. At the normal NMJ, the variation in neuromuscular transmission time (the jitter) is generated mainly by oscillations of the firing threshold at which muscle fibre action potential (AP) is triggered. High amplitude EPPs have a steeper slope and a shorter course through the firing threshold range, and the jitter generated is smaller. Another source of the jitter is the variation in endplate potential (EPP) amplitude and therefore slope. The amplitude of the extrapolated EPPs exceeding the firing threshold represents the safety margin. In cases of postsynaptic dysfunction (such as myasthenia gravis), the variation of neuromuscular transmission time is increased due to lower EPPs, which take a longer path through the firing threshold range; some EPPs do not reach the threshold and the transmission is blocked. In cases of presynaptic dysfunction (such as the Lambert Eaton syndrome, LEMS), the EPP amplitude is not only low but is also excessively variable.

The safety margin at the individual NMJs has been semi-quantitatively estimated *in vivo* in experiments with axonal stimulation during ischaemia or treatment with neuromuscular blocking agents (Schiller et al. 1975; Stålberg et al. 1975). However, the exact relationship between the magnitude of the jitter and the safety factor is difficult to establish. A computer simulation study suggested an exponential-like relationship, which was supported by the actual data from myasthenic NMJs (Lin, Cheng 1998b, Trontelj et al. 2002). It suggested a safety factor of 8-10 for human NMJs. In contrast, it was estimated at up to 20 or more in some animals (Waud, Waud 1975; Lin, Cheng 1998b).

In this study, the rat tibialis anterior muscle has been found to have practically identical jitter as the human extensor digitorum muscle and therefore equally wide safety margin. On the other hand, the NMJs in the rat tibialis anterior muscle have a narrower safety margin than those of the human orbicularis oculi or mentalis muscle.

One might argue that comparison should be made between identical muscles of man and the rat. However, the human tibialis anterior muscle has rather large jitter values. This has been suggested to be due to subclinical microtraumatisation of the peroneal nerve at the head of the fibula, for example while sitting with crossed legs. As a result, some denervation and reinnervation is going on in the peroneal supplied muscle. New NMJs are known to have larger jitter (Stålberg, Trontelj 1994). This mechanism is unlikely to operate in the rat.

Our results are actually similar to those of Lin and Cheng (1998a), who studied the rat gastrocnemius muscle. Yet they found some NMJs with small jitter (about 5 µs) which they took as evidence of extremely high safety factor of neuromuscular transmission in the rat. However, such values can be recorded in human muscles and are seen in a similar (small) proportion of the NMJs in a muscle. Indeed, the jitter and thus the safety margin of neuromuscular transmission may vary in one and the same muscle of a single individual quite considerably. In the human extensor digitorum communis muscle, about 20 % of the NMJs are found to have relatively larger jitter (Trontelj et al 2002).

Slightly smaller jitter was reported for 81 gluteus medius NMJs of 8 Lewis rats (Verschuuren et al. 1990). The mean MCD at 10 Hz stimulation in this study was 11.5 µs (SD 4.0). Considerably smaller jitter was found in the mouse gastrocnemius muscle: MCD 5-15 µs; mean 7.9, 11.3 and 6.1; SD 3, 4 and 2, respectively, for mice of three different strains (Gooch, Mosier 2001). Such low values would be compatible with a significantly wider safety margin.

However, one has to exclude technical reasons. The gastrocnemius muscle in the mouse is small and the position of both stimulating and recording electrodes is more critical. One possibility for obtaining small jitter values is unrecognized direct stimulation of muscle fibres (rather than through their axons), which would result in 'low' jitter. With less than optimal recording conditions, and in particular with unsatisfactory resolution of time measurement, the values may exceed the 5 µs criterion and be erroneously considered as normal NMJ jitter. As a result, false-low readings will shift the calculated mean towards lower figures.

Another possible explanation for relatively small mean jitter values found in some studies could be superimposition of action potentials from several fibres. The resulting spike, when well synchronised, may in fact resemble a single fibre action potential. However, the jitter of the composite potential may be smaller than that of the individual muscle fibre components, as has been demonstrated by a computer simulation (Stålberg et al. 1992). In our experience, such recordings are common in the rat tibialis anterior muscle, and their inadvertent inclusion could result in a significantly underestimated mean jitter. Good recording

conditions, including absence of noise are an essential prerequisite for a reliable distinction between an axonal and a direct muscle fibre stimulation. Single fibre action potentials used for measurement of jitter should have a peak-to-peak amplitude of at least 1.0 mV. Criteria for single fibre action potentials must be strictly observed, in order to avoid measurements on composite spikes. The effective resolution of latency measurement should be at least 1 µs. Jitter measurement based on peak detection algorithm used in some equipment for diagnostic SFEMG, is reliable and convenient for clinical use, where the aim is to detect and measure large jitter, but may, near the low jitter values, become unreliable.

In conclusion, this study failed to confirm the assumption of a wider safety margin of neuromuscular transmission in the limb muscle of the rat compared to a similar muscle in man. On the contrary, there does not seem to be any difference between the mean safety factors of human and rat NMJs.

Acknowledgements

This study is part of a research project on the protection and treatment of intoxication with neurochemical warfare agents (M3-0142). The contributions of Dr. Janez Sketelj, Dr. Miha Trinkaus, Dr. Špela Glišovič, Dr. Marjan Mihelin, Mrs. Tatjana Trontelj, Mr. Ignac Zidar and Tone Žakelj to the experimental work, data collection and analysis are gratefully acknowledged.

References

/1/ De Blaquiere GE, Williams FM, Blain PG, Kelly SS (1998). A comparison of the electrophysiological effects of two organophosphates, mipafox and ecothiopate, on mouse limb muscles. *Toxicol Appl Pharmacol* 150(2): 350-360.

/2/ Dahlbäck L-O, Ekstedt J, Stålberg E (1970). Ischemic effect on impulse transmission to muscle fibres in man. *Electroencephalogr Clin Neurophysiol* 29: 579-591.

/3/ Ekstedt J (1964). Human single muscle fibre action potentials. *Acta Physiol Scand*, Suppl 226, 61: 1-96.

/4/ Ekstedt J, Stålberg E (1969). The effect of non-paralytic doses of d-tubocurarine on individual motor endplates in man, studied with a new neurophysiological method. *Electroencephalogr Clin Neurophysiol* 27: 557-562.

/5/ Gansel M, Penner R, Dreyer F (1987). Distinct sites of clostridial neurotoxins revealed by double-poisoning of mouse motor nerve terminals. *Pflügers Arch* 409: 533-539.

/6/ Gooch CL, Mosier DR (2001). Stimulated single fibre electromyography in the mouse: technique and normative data. *Muscle Nerve* 24: 941-945.

/7/ Lin TS, Cheng KS (1998b). Characterization of the relationship between motor end-plate jitter and the safety factor. *Muscle Nerve* 21: 628-636.

/8/ Lin TS, Cheng TJ (1998a). Stimulated single fibre electromyography in the rat. *Muscle Nerve* 21: 482-489.

/9/ Maselli RA, Burnet MA, Tongaard JH (1992). *In vitro* microelectrode study of neuromuscular transmission in a case of botulism. *Muscle Nerve* 15: 273-276.

/10/ Mihelin M, Trontelj JV, Trontelj JK (1975). Automatic measurement of random interpotential intervals in single fibre electromyography. *Int J Biomed Comput* 6: 181-191.

/11/ Schiller HH, Stålberg E, Schwartz MS (1975). Regional curare for the reduction of the safety factor in human motor endplates studied with single fibre electromyography. *J Neurol Neurosurg Psychiatry* 38: 805-809.

/12/ Stålberg E (1966) Propagation velocity in single human muscle fibres in situ. *Acta Physiol Scand,* Suppl 287, 1-112.

/13/ Stålberg E, Schiller HH, Schwartz MS (1975). Safety factor of single human motor end plates studied in vivo with single fibre electromyography. *J Neurol Neurosurg Psychiatry* 38: 799-804.

/14/ Stålberg E, Trontelj JV (1994) *Single Fibre Electromyography. Studies in Healthy and Diseased Muscle*, 2nd edition. New York: Raven Press, pp. 291.

/15/ Stålberg E, Trontelj JV, Mihelin M (1992). Electrical microstimulation with single-fibre electromyography: a useful method to study the physiology of the motor unit. *J Clin Neurophysiol* 9: 105-119.

/16/ Trinkaus M, Sketelj J, Mihelin M, Trontelj J. Jitter in organophosphate intoxicated rats. *Proceedings, XVIth International SFEMG and QEMG Course and IXth Quantitative EMG Conference* with the 23rd Dr. Janez Faganel Memorial Lecture, Ljubljana, Slovenia, June 2-6, 2007: 181 (FC-16).

/17/ Trontelj JV, Khuraibet A, Mihelin M (1988). The jitter in stimulated orbicularis oculi muscle: technique and normal values. *J Neurol Neurosurg Psychiatry* 51: 814-819.

/18/ Trontelj JV, Mihelin M, Fernandez JM, Stålberg E (1986). Axonal stimulation for end-plate jitter studies. *J Neurol Neurosurg Psychiatry* 49: 677-685.

/19/ Trontelj J.V., Mihelin M., Khuraibet A (2002). Safety margin at single neuromuscular junctions*. Muscle Nerve*, Suppl 11: S21-27.

/20/ Trontelj JV, Stålberg E (1992). Jitter measurements by axonal stimulation. Guidelines and technical notes. *Electroencephalogr Clin Neurophysiol, EMG and Motor Control* 85: 30-37.

/21/ Trontelj JV, Stålberg E (2002). Single fibre and macro electromyography. In: Bertorini TE (Ed.), *Clinical Evaluation and Diagnostic Tests for Neuromuscular Disorders*. Butterworth-Heineman / Elsevier Science, Woburn, MA, USA, pp. 417-447.

/22/ Trontelj JV, Stålberg E, Mihelin M (1990). Jitter in the muscle fibre. *J Neurol Neurosurg Psychiatry* 53: 49-54.

/23/ Trontelj JK, Trontelj L, Trontelj JV (1967). A voltage-controlled multi- channel electrical stimulator for programmed afferent functional stimulation. Digest of the 7th Internat Conf on Medical and Biological Engineering. Stockholm: 356.

/24/ Verschuuren JJ, Spans F, De Baets MH (1990). Single fiber electromyography in experimental autoimmune myasthenia gravis. *Muscle Nerve* 1990;13:485–492.

/25/ Waud DR, Waud BE (1975). In vitro measurement of margin of safety of neuromuscular transmission. *Am J Physiol* 229: 1632-1634.

akademik dr. Jože Trontelj, dr. med.,
profesor, višji svetnik
Inštitut za klinično nevrofiziologijo, Nevrološka klinika,
Univerzitetni klinični center v Ljubljani
Zaloška 7, SI-1525 Ljubljana, Slovenija.
Tel. (01) 522 1525, 041 576 218. Faks (01) 522 1533
elektronski naslov: joze.trontelj@kclj.si

dr. Janez Trontelj, univ. dipl. ing., profesor,
Laboratorij za mikroelektroniko
Fakulteta za elektrotehniko
Tržaška 25, 1000 Ljubljana

†dr. Lojze Trontelj, univ. dipl. ing., profesor emeritus,
Laboratorij za mikroelektroniko
Fakulteta za elektrotehniko
Tržaška 25, 1000 Ljubljana

Prispelo (Arrived): 01.09.2008 Sprejeto (Accepted): 15.09.2008

NEWTON, RUNGE-KUTTA AND SCIENTIFIC SIMULATIONS

Zvonko Fazarinc

Palo Alto, California, USA

Key words: Scientific simulations, accelerated motion, numeric integration of Newton's equations, fourth order Runge-Kutta, Heun algorithm

Abstract: Scientific simulations of natural phenomena are powerful predictors of likely experimental outcomes. Improvement of their reliability and accuracy translates directly into time savings. Simulations are also powerful supporters of education. Created as teaching tools, simulations provide unique insights into mechanisms of addressed phenomena and can serve as experimental breadboards to the student.

Visual display of simulated behaviour is usually the last step in writing a simulation code. The relevant algorithms that convert forces into motion to be displayed are seldom given the attention of the expert scientist. His focus is understandably elsewhere and the simulation of motion has to draw on previous work or on libraries of integration algorithms.

This paper addresses the motion algorithm from the viewpoint of Newton's Laws and deals with the haphazard usage of pre-computer integration formulas such as the high order Runge-Kutta schemes. As these are offered as the'' high accuracy'' and conveniently packaged answer to all integration needs, these formulas have gained high acceptance without a demonstrated justification.

The goal of this paper is to highlight the mismatch with the computer age of the fourth order Runge-Kutta (FORK) integration formula and to analyze its performance in light of simpler formulas with more transparency and less expenditure of computer cycles.

I wish to dedicate this paper to the memory of my late friend and colleague professor dr.Lojze Trontelj with whom I had the pleasure to discuss the potential value of scientific simulations in the early days of computer evolution.

Newton, Runge-Kutta in simulacije v znanosti

Kjučne besede: simulacije v znanosti, pospešeno gibanje, numerična integracija Newtonovih enačb, metoda Runge-Kutta četrtega reda, Heunov algoritem

Izvleček: Znanstvene simulacije naravnih pojavov so pomembni napovedovalci verjetnih eksperimentalnih izidov. Povečanje njihove zanesljivosti in natančnosti ima za neposredno posledico velike prihranke časa. Simulacije so tudi močna podpora pri izobraževanju. Ustvarjene kot orodja za učenje, simulacije omogočajo edinstven vpogled v mehanizme obravnavanih fenomenov in študentom lahko služijo kot eksperimentalni poligon.

Vizualni prikaz simuliranega pojava je navadno zadnji korak pri pisanju simulacijskega računalniškega programa. Relevantnim algoritmom, ki sile prevedejo v prikazano gibanje, izkušeni strokovnjak le redko posveča posebno pozornost. Razumljivo je, da je osredotočen drugam, in simulacija gibanja se mora zato naslanjati na prejšnje raziskovalne rezultate ali na knjižnice integracijskih algoritmov.

Članek obravnava algoritem gibanja s stališča Newtonovih zakonov in nestrogo uporabo integracijskih formul, ki izvirajo iz predračunalniških časov, kot na primer postopke Runge-Kutta višjih redov. Ker jih ponujajo kot ''natančne'' in priročno prirejene odgovore na vse potrebe po integraciji, so te formule splošno sprejete brez dokazne upravičenosti.

Namen tega članka je osvetliti neskladje med računalniško dobo in Runge-Kutta (FORK) integracijsko formulo četrtega reda ter analiza njene uspešnosti v primerjavi s preprostejšimi, preglednejšimi formulami, ki zahtevajo manj računalniških ciklov.

Ta članek posvečam spominu na svojega preminulega prijatelja in kolego, profesorja dr. Lojzeta Trontlja, s katerim sem še v zgodnjih časih evolucije računalnikov razpravljal o potencialni vrednosti simulacij v znanosti

1 Introduction

Scientific simulations of natural phenomena can predict the outcomes of practical experiments if done correctly. For dangerous experiments their value is unprecedented, for expensive ones it is fiscally advantageous. Scientific simulation can also provide unique insights into the underlying mechanisms of phenomena studied. In this mode their educational potential is without precedent.

The task of a simulation designer is to assign relevant natural forces to objects that mimic their natural counterparts. The running simulation allows the objects to mutually interact and their resulting collective behaviour is studied. One of the common tools for tracking the evolution of a simulation is a dynamic visual display. This must contain some algorithm that converts the forces on objects into their velocity and position. This task is the focus of this paper.

The conversion of forces acting on objects into their positional changes would seem quite trivial to Isaac Newton and it may appear trivial to a practitioner of scientific simulations as well. A double integration of the forces acting on the mass in question is all that is necessary to obtain the object's instantaneous position. According to Newton's First Law of Motion /1/, an object's momentum M is preserved. It is defined for an object of mass m moving at velocity v as $M = mv$. The change of momentum dM/dt can be caused only by some force F acting on the object. Their relationship is given by Newton's Second Law of Motion as

$dM/dt = F$. Because we will ignore the change of mass in the continuation of this paper we will assign all changes of momentum to the velocity *v.* Consequently

$$dv(t) = F(t)dt/m \tag{1}$$

Furthermore, the temporal change of an object's position *ds/dt* is equal to its velocity *v*, thus

$$ds(t) = v(t)dt \tag{2}$$

The motion algorithm we employ in a simulation context must conform to equations (1) and (2) in the discrete domain of finite differences

$$\Delta v(t) = v(t+\Delta t) - v(t) = F\Delta t/m \tag{3}$$

and

$$\Delta s(t) = s(t+\Delta t) - s(t) = v\Delta t \tag{4}$$

where Δt is the smallest discrete time resolution of the simulation. Yet, the algorithms that are used to perform the two respective integrations do not necessarily produce the correct answers. In most cases they are chosen from a library of numerical integration routines with poorly defined behaviour, without relevance to the particular problem, sometimes producing inaccurate object positions and always consuming unnecessarily excessive computer resources. The positional accuracy of an object, which is subject to accelerating forces, can be critically important when the force is a function of object's position. Such is the case with gravitational and electromagnetic simulations as well as with all simulations of interacting objects.

In this paper we will use Newton's Laws of Motion /1/ as the reference for a critical analysis of the most frequently recommended integration algorithm known as the Fourth Order Runge-Kutta method /2/ in light of other integration algorithms.

2 Approach

The numerical double integration of forces may be addressed from a mathematician's viewpoint without regard to the physics of the problem. This approach had led to the majority of the numeric integration formulas in existence today and was driven by the quest for reduction of manual computation effort without compromising the accuracy of the approximation. We will elaborate on this in later sections.

The same integration question may also be addressed from the physicist's viewpoint and be driven by the demand for a match between Newton's Laws of Motion and the results produced by its discrete mimicry. This will be our approach in the search for the ideal algorithm. Let us first put on the mathematician's hat.

2.1 Discrete Integration Method from Mathematicians Viewpoint

All numeric integration formulas are based on the definition of the derivative's integral over a finite interval Δt

$$\int_{t}^{t+\Delta t} y'(t)dt = y(t+\Delta t) - y(t)$$

Various approximations of this integral lead to different families of numeric integration formulas. Newton's Interpolation formula, for example, leads to the Adams family while Taylor's expansion gives rise to the Runge-Kutta family. We will focus on the latter, which is based on

$$y(t+\Delta t) - y(t) = \Delta t\, y'(t) + \frac{\Delta t^2}{2} y''(t) + \\ + \frac{\Delta t^3}{3!} y'''(t) + \frac{\Delta t^4}{4!} y''''(t) + ... \tag{5}$$

The mathematician's task is now to decide where to truncate the infinite expansion, providing an acceptable error. A good guess is that the truncation error /3/ may be in the order of power of Δt of the first neglected term. Retaining then as many terms as reasonable and using as small a time step Δt as practical seems appropriate. Now the former would complicate the formula while the latter would require more repetitive evaluations to cover a desired time span. Neither of these seems to be an overriding consideration for today's computer performance. But we must consider the fact that a vast majority of existing numeric integration formulas were developed before and at the turn of the 20-th century, which this author likes to call the BC (before computers) era. The problems that needed to be addressed by numerical means were usually low order, nonlinear differential equations for which their changes, i.e. the first derivatives were known, arising usually from observations or measurements. When the humans were faced with a choice between numerous repetitive manual evaluations of a simpler formula versus fewer executions of a more complex formula, they would understandably choose the latter. And this is how the more complex integration formulas gained their BC fame.

2.1.1 Newton

We will first choose a driving force function $F(t) = A\cos(\omega t)$, which is representative of all force functions that can be decomposed into Fourier series. This excludes the Dirac function.

First we integrate (1) and (2) to obtain our reference data

$$v(t) = \frac{A}{m\omega}\sin(\omega t) \qquad s(t) = -\frac{A}{m\omega^2}\cos(\omega t) \\ v(0) = 0 \qquad\qquad s(0) = -\frac{A}{m\omega^2} \tag{6}$$

2.1.2 Fourth-Order Runge-Kutta (FORK)

Had we followed the mindset of the BC era we would have included at least the first three or four terms of the expansion (5) thus placing the anticipated truncation error into the fourth or fifth order of Δt, respectively. This would then allow us the choice of a larger time increment as is desir-

able for manual integration. In turn, this would lead to a fairly complex, yet very popular Fourth-Order Runge-Kutta (FORK) formula /2/. Its systematic derivation involves much algebra and the interested reader is directed to this reference. The FORK formula is

$$\begin{aligned} k_0 &= \Delta t\, y'\left[t,\, y(t)\right] \\ k_1 &= \Delta t\, y'\left[t+\Delta t/2\,,\, y(t)+\Delta t\, k_0/2\right] \\ k_2 &= \Delta t\, y'\left[t+\Delta t/2\,,\, y(t)+\Delta t\, k_1/2\right] \\ k_3 &= \Delta t\, y'\left[t+\Delta t,\, y(t)+\Delta t\, k_2\right] \\ y(t) &= y(t-\Delta t)+\frac{k_0+2k_1+2k_2+k_3}{6} \end{aligned} \qquad (7)$$

In (7) the slope is allowed to be the function of time and of the dependent variable *y*(*t*) should such be the case. We will use this formula to evaluate the motion quantities (3) and (4) and will then compute the deviation from Newton's answers in (6).

To evaluate (3) and (4) we must plug the respective values of *F* and *v* into (7). Because these are only functions of time the FORK parameters k_0 through k_3 adopt very simple forms. The result is shown below

$$\begin{aligned} v(t) &= v(t-\Delta t)+\frac{A\Delta t}{6m}\left[\cos\omega(t-\Delta t)+4\cos\omega(t-0.5\Delta t)+\cos\omega t\right] \\ s(t) &= s(t-\Delta t)+\frac{\Delta t}{6}\left[v(t-\Delta t)+4v(t-0.5\Delta t)+v(t)\right] \end{aligned} \qquad (8)$$

In Fig.1 we have superimposed the positions *s(t)* as calculated from (6) and from (8) as functions of the number of time increments Δt.

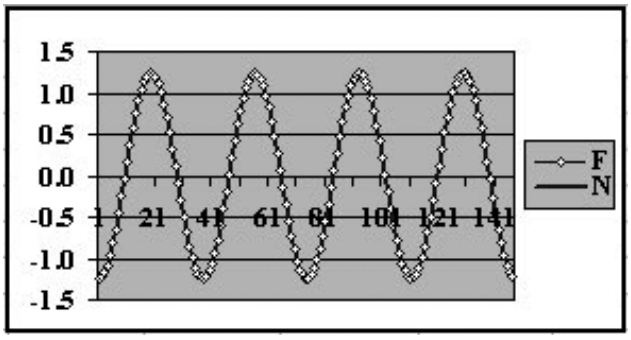

Fig. 1: Newton and FORK position for cosinusoidal driving force.

While deviations are not discernible in Fig.1 we have depicted in Fig.2 the percentage deviation between the FORK evaluated *s(t)* and that predicted by Newton. These are actual errors associated with our particular example and have nothing to do with the elaborate but often meaningless truncation errors /3/

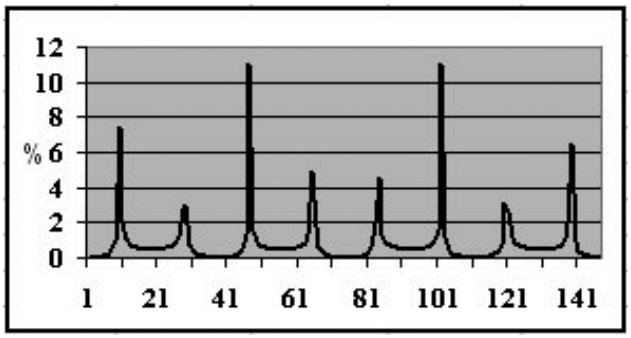

Fig. 2: Fractional error between Newton and FORK positions for cosinusoidal driving force

2.1.3 Second Order Runge-Kutta

Let us now choose to include only the first two terms of the Taylor expansion (5) With this choice we are committing, in the mathematician's mind, to a mere third order accuracy yet we do retain the control over Δt. The second term of expansion (5) calls for *y*''(*t*), which we do not know but can approximate by the central difference $\left[y'(t+\Delta t/2)-y'(t-\Delta t/2)\right]/\Delta t$, by the forward difference $\left[y'(t+\Delta t)-y'(t)\right]/\Delta t$ or by the backward difference $\left[y'(t)-y'(t-\Delta t)\right]/\Delta t$. We will return to this later but choose for now the forward difference and obtain instantly the following second order formula

$$y(t+\Delta t)=y(t)+\Delta t\,\frac{y'(t+\Delta t)+y'(t)}{2} \qquad (9)$$

Expression (9) is known as the trapezoidal but also as the Heun or Second Order Runge-Kutta formula /4/ in which we have replaced the fractional times with their linear approximations. Belonging to the second order brand this formula was discouraged by the BC mathematicians and remained in disrepute ever since. So let us now take a quantitative look at the error issue in light of what we have just learned about the FORK formula behaviour. To this end we adopt the same force function $F(t)=A\cos(\omega t)$ with its initial conditions spelled out in (6) to obtain from (3) and (4) the following equations

$$\begin{aligned} v(t+\Delta t) &= v(t)+\frac{A\Delta t}{2m}\left[\cos\omega\,(t+\Delta t)+\cos\omega t\right] \\ s(t+\Delta t) &= v(t)+\frac{\Delta t}{2}\left[v(t+\Delta t)+v(t)\right] \end{aligned} \qquad (10)$$

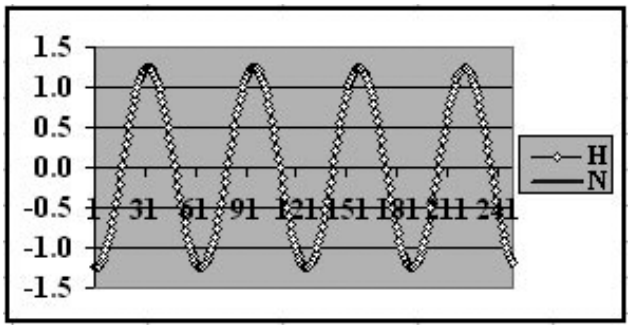

Fig. 3: Superposition of Newton and Heun position for cosinusoidal driving force.

Fig.3 displays the position *s*(*t*) as function of index $t/\Delta t$ and Fig.4 the percentage deviation of *s*(*t*) from the true position given by (6). This time we have experimentally adjusted the time increment Δt in such a way that the errors in Fig.4 and in Fig.2 are about the same.

As discernible from two sets of plots we had to compute almost twice as many points in (10) as we did in (8) to obtain the match of errors. Thus, the FORK formula gives us the same accuracy with fewer passes. No real surprise here but to compare the net computational effort we must establish some measurable criteria. Ignoring the memory accesses and all other overhead and not allowing any duplicate computations, we can count the number of floating point operations (FLOPs) needed for each time step.

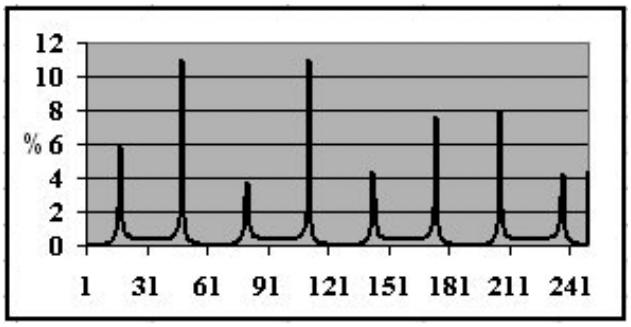

Fig. 4: Fractional error between Newton and Heun positions for cosinusoidal driving force

Formula (10) requires 30 FLOPs while (8) requires 49 provided that we have precomputed the repeating quantities such as $A\Delta t/2m$, $A\Delta t/6m$, $\Delta t/2$, etc. and allotted 10 FLOPs for each trigonometric function evaluation. One could then say that the two formulas are identical in terms of net computational effort for the same accuracy. But formula (10) gives us 70% more individual computed points. We will reexamine this issue after we have completed a more severe comparative test of the two formulas from a physicist's viewpoint.

2.2 Discrete Integration from Physicist's Viewpoint

While the truncation error /3/ might be the sole criterion to a mathematician when judging various integration formulas, to a physicist it is the trustworthiness of the simulated phenomenon that matters. We will therefore subject formulas (7) and (9) to a more realistic scrutiny because in simulations we seldom encounter a simple, clean textbook case of a well defined external force. The force is commonly self induced by the motion and is then fed back to the object involved. We will therefore make the force a function of the object's position and elect the following relationship.

$$\frac{F}{m}=\frac{\Delta v(t)}{\Delta t}=-\omega^2 s(t) \qquad (11)$$

where ω^2 is a proportionality constant for the moment. Such opposing functional dependence of force on position is commonly encountered in gravitational, electromagnetic, Van DerWall and other simulations of natural phenomena /5/, /6/.

2.2.1 Newton

First we solve Newton's equations (1) and (2) for the case of force function (11)

$$\frac{dv(t)}{dt}=-\omega^2 s(t) \qquad \frac{ds(t)}{dt}=v(t) \text{ or}$$

$$\frac{d^2 s(t)}{dt^2}=-\omega^2 s(t)$$

Solving for *s(t)* this second order differential equation yields the harmonic solution

$$\begin{aligned} s(t) &= s(0)\cos\omega t+\frac{v(0)}{\omega}\sin\omega t \\ v(t) &= v(0)\cos\omega t-s(0)\omega\sin\omega t \end{aligned} \qquad (12)$$

Position *s(t)* from equation (12) with *v*(0) = 0 is plotted in Fig.5 as the black solid line.

2.2.2 FORK formula

We introduce the force function (11) into equation (3) and then use the FORK formula (7) in both (3) and (4) to end up with an expression for position *s(t)*. Because the FORK formula integrates only one first order equation at a time, we would need a separate application of (7) to (3) and another to (4). Two sets of distinguishable factors "*k*" would have to be employed in general. But because (3) and (4) are coupled the following simplification is available from /7/

$$\begin{aligned} m_0 &= \Delta t\, y'[t,\ y(t),\ y'(t)] \\ m_1 &= \Delta t\, y'\left[t+\Delta t/2,\ y(t)+y'(t)\Delta t/2,\ y'(t)+m_0/2\right] \\ m_2 &= \Delta t\, y'\left[t+\Delta t/2,\ y(t)+y'(t)\Delta t/2+m_0\Delta t/4,\ y'(t)+m_1/2\right] \\ m_3 &= \Delta t\, y'\left[t+\Delta t,\ y(t)+\Delta t\, y'(t)+m_1\Delta t/2,\ y'(t)+m_2\right] \end{aligned}$$

$$\begin{aligned} y'(t+\Delta t) &= y'(t)+(m_0+2m_1+2m_2+m_3)/6 \\ y(t+\Delta t) &= y(t)+\Delta t\, y'(t)+\Delta t(m_0+m_1+m_2)/6 \end{aligned}$$

Because for our case the slope $y'(t)=v'(t)=-\omega^2 s(t)$ is only a function of time *t* the above equations simplify to

$$\begin{aligned} m_0 &= -\Delta t\,\omega^2 s(t) \\ m_1 &= m_2 = -\Delta t\,\omega^2 s(t+\Delta t/2) \\ m_3 &= -\Delta t\,\omega^2 s(t)+\Delta t \end{aligned} \qquad (13)$$

$$\begin{aligned} s(t+\Delta t) &= s(t)+\Delta t\, v(t)+\Delta t(m_0+m_1+m_2)/6 \\ v(t+\Delta t) &= v(t)+(m_0+2m_1+2m_2+m_3)/6 \end{aligned}$$

At this time we must point out that scientific simulations are commonly run with constant time increments Δt for a variety of practical reasons. One is the preservation of relative temporal occurrences of events under observation while simplicity of coding does not lag far behind. The half increment appearing in m_1 and m_2 must therefore be ap-

proximated by a linear interpolation

$$m_1 = m_2 = -\Delta t\omega^2 \frac{s(t) + s(t+\Delta t)}{2}$$

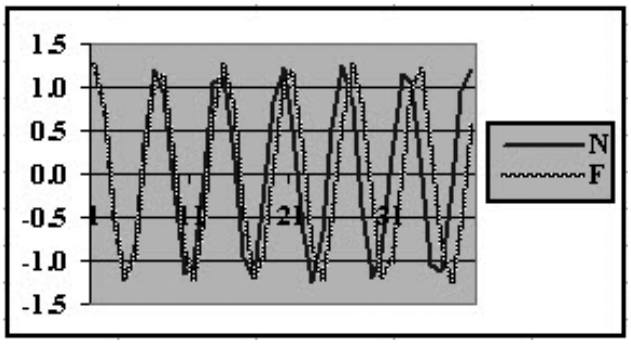

Fig. 5: Newton and FORK position when the driving force depends on position.

With this substitution the Runge-Kutta equation (13) produces the position *s(t),* shown in Fig. 5, superimposed on Newton's prediction from (12). The plot was computed for $\omega\Delta t = 1$, which is just over six points per period of the resulting harmonic motion *s(t)*.

The rugged waveform is the consequence of that. It was chosen intentionally for later comparisons with other options.

Fig. 6: Long term behaviour of Newton and FORK with positional feedback.

In order to gain an insight into the long term stability of the FORK solution we have plotted in Fig.6 the Newton prediction for 8500 time increments and superimposed on it the FORK answer from (13) for 8000 time increments. It is not doubtable that the FORK solution (13) would continue to provide stable answers beyond 8000 points but we will later prove this to be the case.

2.2.3 Second Order Formula

Let us continue to retain the physicist's viewpoint and argue with the mathematician who would want to convince us that only an infinite number of terms in the Taylor expansion would guarantee a perfect match of a numeric algorithm with Newton's formulas. On the other hand there are no doubts that Newton's equations (1) and (2) describe a second order system. Why should a second order numeric formula not suffice to adequately describe the accelerated motion? So, instead of choosing an existing integration algorithm we will force a second order integration formula to conform to Newton's laws of motion.

We start again from formulas (3) and (4). In them we have intentionally avoided the specification of respective temporal arguments of *F* and *v.* The discrete domain, characterized by finite time increments, often confronts us with the question of what happens before something else. We could, for example, compute the new velocity from Equation (3) by using the present force $F(t+\Delta t)$, the previous force *F(t),* their average as seen before or some other more general combination of the two. Similarly, we could compute the position s*(t)* from Equation (4) using some arbitrary combination of the previously evaluated and contemporaneous velocities. Without knowing the outcomes produced by a given choice, we have no reason to prefer one over the other. Therefore we will elect as yet undefined fractions of the force *a* $F(t+\Delta t)$ and (1-*a*) *F(t)* as the contributions to velocity changes as indicated below

$$v(t+\Delta t) = v(t) + \frac{\Delta t}{m}[aF(t+\Delta t) + (1-a)F(t)] \qquad (14)$$

Furthermore we will choose as yet unknown fractions of two primary velocity choices to determine their relative contributions to the change of position

$$s(t+\Delta t) = s(t) + [bv(t+\Delta t) + (1-b)v(t)]\Delta t \qquad (15)$$

Parameters *a* and *b* have values between zero and unity and we will try to extract them by a parameter optimization procedure designed to force a match between the simulated results produced by the above equations and the true accelerated motion expressed by Newton's Laws. We will do this for our specific choice of force defined by (11), which yields the following version of (14)

$$v(t+\Delta t) = v(t) - \omega^2\Delta t[as(t+\Delta t) + (1-a)s(t)] \qquad (16)$$

Expressions (15) and (16) represent the numeric integration algorithm that we are trying to force in compliance with (1) and (2).To this end we must find a closed form solution of the coupled equations (15) and (16). We have done this in the Appendix AP1 with the result

$$\begin{aligned} s(n\Delta t) &= s(0)B^{n/2}\cos n\Omega\Delta t + \\ &+ \frac{s(0)\omega\Delta t(b-a)/4 + v(0)/\omega}{\sqrt{1-\omega^2\Delta t^2(a-b)^2/4}} B^{n/2}\sin n\Omega\Delta t \\ B &= \frac{1+(1-b)(1-a)\omega^2\Delta t^2}{1+ab\omega^2\Delta t^2} \\ \Omega\Delta t &= \tan^{-1}\omega\Delta t\frac{\sqrt{1-\omega^2\Delta t^2(a-b)^2/4}}{1-(a+b-2ab)\omega^2\Delta t^2/2} \end{aligned} \qquad (17)$$

A comparison of position *s*(*t*) in (17) with that in (12) suggests that the quantity $B^{n/2}$ must be unity, calling for $1+(1-b)(1-a)\omega^2\Delta t^2 = 1+ab\omega^2\Delta t^2$, which further entails a + b = 1. The numerator of the second term of the $s(n\Delta t)$ expression in (17) demands b – a = 0 to conform to (12).

These two requirements imply the following overall conclusion of our analysis

$$a = b = 0.5 \tag{18}$$

Our final form of the set (15) and (16) is now highly reminiscnet of the Heun formula

$$\begin{aligned} v(t+\Delta t) &= v(t) - \omega^2 \Delta t \left[s(t+\Delta t) + s(t) \right] / 2 \\ s(t+\Delta t) &= s(t) + \Delta t [v(t+\Delta t) + v(t)]/2 \end{aligned} \tag{19}$$

For *a = b = 0.5* expression (17) takes on the form.which except for the angular frequency Ω matches Newton's prediction (12) in all other details.

$$\begin{aligned} s(n\Delta t) &= s(0)\cos n\Omega\Delta t + \frac{v(0)}{\omega}\sin n\Omega\Delta t \\ \Omega\Delta t &= \tan^{-1}\frac{\omega\Delta t}{\sqrt{1-\omega^2\Delta t^2/4}} \end{aligned} \tag{20}$$

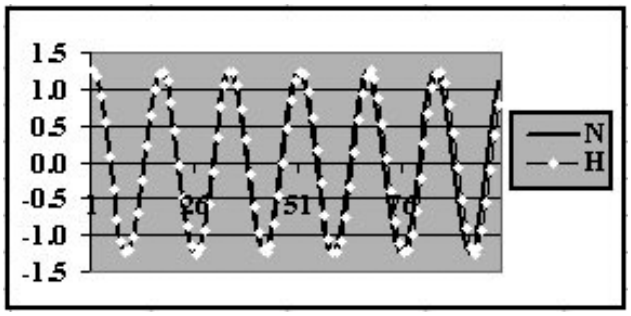

Fig. 7: Newton and Heun position when driving force depends on position

It should therefore not come as a surprise that an evaluation of (20) produces Figs.7 and 8 for which we have chosen the parameter $\omega\Delta t = 0.38$. Figs.5 and 6, on the other hand, were obtained with $\omega\Delta t = 1$ as stated earlier. The ratio of 1 to 0.38 happens to match the ratio 21 to 8 of floating point operations needed to execute (13), versus (19). This, in turn, assures equal computation time for both formulas with (19) providing 2.6 times as many time increments.

Fig. 8: Long term behaviour of Newton and Heun with positional feedback.

A debate over the relative accuracy of one or the other formula is irrelevant since both appear to match the Newton waveform except for the angular frequencies as seen from the graphs. For the Heun case defined in (20), the fractional deviation of Ω from ω is established as $\left(\tan^{-1}\left[\omega\Delta t / \sqrt{1-\omega^2\Delta t^2/4}\right] - 1\right)/\omega\Delta t$ and is plotted in Fig.9 versus $\omega\Delta t$. In the Appendix AP2 we have also found an analytic expression for the angular frequency Ω of the Runge-Kutta case and its relevant deviation from the nominal ω as $\left(\tan^{-1}\left[\omega\Delta t\sqrt{1-\omega^2\Delta t^2/12} / (1-\omega^2\Delta t^2/3)\right] - 1\right)/\omega\Delta t$. This is also plotted in Fig.9 as R..

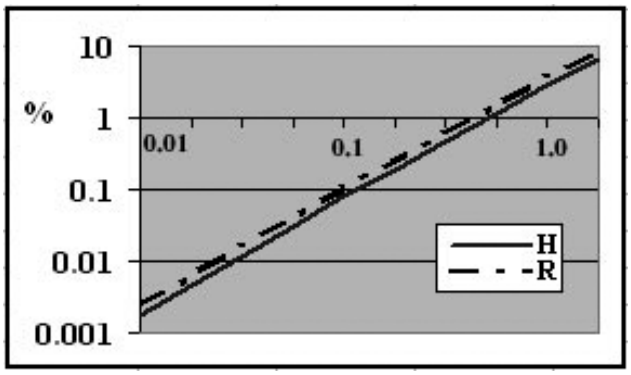

Fig. 9: Fractional error of FORK and Heun simulated frequency.

There is a slight difference in favor of Heun in terms of angular frequencies but more significant is the fact that for same expenditure of computer cycles Heun delivers more computed points with shorter time increments. Both of these are desirable for dynamic simulations, which demand displays of velocities and positions of objects.

3. Conclusion

In summary the Heun algorithm has been found to numerically integrate Newton's laws of motion with the same accuracy as the FORK formula in tests from the highest frequencies down to the Nyquist limit. The superiority of Heun formula over the FORK algorithm is its ability to deliver 260% more computed points at proportionately reduced time increment for same expenditure of computer cycles. Both of these are criteria important to simulation practitioners. Furthermore, its simplicity of implementation leaves the designer in control of the last stage of his dynamic simulation code. i.e. of computing the new velocities $v(t+\Delta t)$ and the new positions $s(t+\Delta t)$ of his objects from forces $F(t+\Delta t)$ currently acting on them. When we consider our starting force (11) we can present the preferred result of our analysis for general force functions as

$$\begin{aligned} v(t+\Delta t) &= v(t) + \frac{\Delta t}{2m}\left[F(t+\Delta t) + F(t)\right] \\ s(t+\Delta t) &= s(t) + \frac{v(t+\Delta t) + v(t)}{2}\Delta t \end{aligned} \tag{21}$$

A simulation program in which (21) was implemented has been tested with 100 spherical particles with randomly assigned initial velocities. They were allowed to interact through mutual gravitation, through three-dimensional collisions and individually by bouncing off the box walls. The gravitational masses of particles were adjusted so that their naturally formed clusters were able to disperse as their rotational velocity increased. This assured a continuous activity of all 100 particles. While there is no method available to evaluate the accuracy of observed simulated behaviour of this many objects, the physics comes to the rescue. Unless a loss mechanism or a source of energy is coded into the system the total energy must remain constant. Therefore we have monitored the overall energy through one million passes, during which each of the 100 particles received an update of position and velocity from the Heun algorithm from formula (21). During the whole observation time of one hour and 23 minutes that was needed for the experiment, the total energy of particles remained unchanged.

Appendix

AP1 Closed form solution of equations (15) and (16)

They are respectively

$$s(t+\Delta t) = s(t) + [bv(t+\Delta t) + (1-b)v(t)]\Delta t \quad \text{(APP1)}$$

$$v(t+\Delta t) = v(t) - \omega^2\left[as(t+\Delta t) + (1-a)s(t)\right]\Delta t \quad \text{(APP2)}$$

Take the first forward difference of (APP1)

$$s(t+2\Delta t) - s(t+\Delta t) = s(t+\Delta t) - s(t) + b\Delta t[v(t+2\Delta t) -$$

$$- v(t+\Delta t)] + (1-b)\Delta t[v(t+\Delta t) - v(t)]$$

Note that the first bracketed term arises directly from (APP2) as $-\omega^2\Delta t^2\,[as(t+2\Delta t) + (1-a)s(t+\Delta t)]$ and the second one as $-\omega^2\Delta t^2[as(t+\Delta t) + (1-a)\,s(t)]$

Substitute these into the above equation and collect contemporaneous terms to obtain

$$s(t+2\Delta t)(1+ab\omega^2\Delta t^2) - 2s(t+\Delta t)[1-(a+b-2ab)\omega^2\Delta t^2/2] +$$

$$+ s(t)[1+(1-a)(1-b)\omega^2\Delta t^2] = 0$$

This equation is equivalent to

$s(t+2\Delta t) - 2A\,s(t+\Delta t) + B\,s(t) = 0$ with

$$A = \frac{1-(a+b-2ab)\omega^2\Delta t^2/2}{1+ab\omega^2\Delta t^2}$$

$$B = \frac{1+(1-a)(1-b)\omega^2\Delta t^2}{1+ab\omega^2\Delta t^2} \quad \text{(APP3)}$$

(APP3) has two closed form solutions dependent on the relative magnitude of *A* and *B*. The case *B*>*A* is of interest to us. Application of the Z-transform /8/ results in the following Z-domain equation for s(*t*) in which the transformed variable is defined as $S(z) = Z[s(t)]$

$$S(z)z^2 - s(0)z^2 - s(\Delta t)z - 2AS(z)z + 2As(0)z + BS(z) = 0$$

From this follows immediately

$$S(z) = \frac{s(0)z^2 + s(\Delta t)z - 2As(0)z}{z^2 - 2Az + B} = \frac{s(0)z^2 + s(\Delta t)z - 2As(0)z}{(z-z_1)(z-z_2)}$$

where

$$z_{1,2} = A \pm j\sqrt{B-A^2} = |z|e^{\pm j\varphi} = \sqrt{B}e^{\pm j\tan^{-1}\frac{\sqrt{B-A^2}}{A}} \quad \text{(APP4)}$$

The inversion is done by the sum of residui since we are dealing with an analytic function /9/. We have discretized time as $t = n\Delta t$ in the following expressions

$$s(n\Delta t) = S(z)(z-z_1)z^{n-1}\big|_{z=z_1} + S(z)(z-z_2)z^{n-1}\big|_{z=z_2}$$

$$= \frac{s(0)z_1 + s(\Delta t) - 2s(0)A}{z_1 - z_2}z_1^n + \frac{s(0)z_2 + s(\Delta t) - 2s(0)A}{z_2 - z_1}z_2^n$$

Because $z_1 - z_2 = 2j\sqrt{B-A^2}$ we get

$$s(n\Delta t) = \frac{s(0)\left(A + j\sqrt{B-A^2}\right)}{2j\sqrt{B-A^2}}z_1^n - \frac{s(0)\left(A - j\sqrt{B-A^2}\right)}{2j\sqrt{B-A^2}}z_2^n +$$

$$+ \frac{s(\Delta t) - 2s(0)A}{2j\sqrt{B-A^2}}(z_1^n - z_2^n)$$

or

$$s(n\Delta t) = \frac{s(0)A}{2j\sqrt{B-A^2}}(z_1^n - z_2^n) + \frac{s(0)}{2}(z_1^n + z_2^n) +$$

$$+ \frac{s(\Delta t) - 2s(0)A}{2j\sqrt{B-A^2}}(z_1^n - z_2^n)$$

From (APP4) it follows

$$z_1^n - z_2^n = \sqrt{B^n}e^{jn\tan^{-1}\frac{\sqrt{B-A^2}}{A}} - \sqrt{B^n}e^{-jn\tan^{-1}\frac{\sqrt{B-A^2}}{A}} =$$

$$= 2j\sqrt{B^n}\sin n\tan^{-1}\frac{\sqrt{B-A^2}}{A}$$

$$z_1^n + z_2^n = \sqrt{B^n}\left[\varepsilon^{jn\tan^{-1}\frac{\sqrt{B-A^2}}{A}} + e^{-jn\tan^{-1}\frac{\sqrt{B-A^2}}{A}}\right] =$$

$$= 2\sqrt{B^n}\cos n\,\tan^{-1}\frac{\sqrt{B-A^2}}{A}$$

Then

$$s(n\Delta t) = s(0)\sqrt{B^n}\cos n\Omega\Delta t + \frac{s(\Delta t) - s(0)A}{\sqrt{B-A^2}}\sqrt{B^n}\sin n\,\Omega\Delta t \quad \text{(APP5)}$$

where $\Omega\Delta t = \tan^{-1}\frac{\sqrt{B-A^2}}{A}$

The denominator of the second right hand term of (APP5) can be found with straightforward but time consuming algebraic manipulations as

$$\sqrt{B-A^2} = \omega\Delta t\frac{\sqrt{1-\omega^2\Delta t^2(a-b)^2/4}}{1+ab\omega^2\Delta t^2} \quad \text{(APP6)}$$

$s(\Delta t)$ is extracted directly from (APP1) as

$$s(\Delta t) = s(0) + b\Delta t v(\Delta t) + (1-b)\Delta t v(0)$$

while $v(\Delta t) = v(0) - \omega^2 \Delta t a s(\Delta t) - \omega^2 \Delta t (1-a) s(0)$ is obtained from (APP2).

From expressions (APP5) and (APP6) and from the definition of *A* in (APP3) we obtain via tedious but elementary algebraic manipulation

$$\frac{s(\Delta t) - s(0)A}{\sqrt{B - A^2}} = s(0) \frac{\omega \Delta t (a-b)/2}{\sqrt{1 - \omega^2 \Delta t^2 (a-b)^2 / 4]}} +$$

$$+ v(0) \frac{1/\omega}{\sqrt{1 - \omega^2 \Delta t^2 (a-b)^2 / 4]}}$$

The argument of Ω is evaluated as follows

$$\frac{\sqrt{B - A^2}}{A} = \omega \Delta t \frac{\sqrt{1 - \omega^2 \Delta t^2 (a-b)^2 / 4}}{1 + ab\omega^2 \Delta t^2}$$

$$\frac{1 + ab\omega^2 \Delta t^2}{1 - (a + b - 2ab)\omega^2 \Delta t^2 / 2} = \omega \Delta t \frac{\sqrt{1 - \omega^2 \Delta t^2 (a-b)^2 / 4}}{1 - (a + b - 2ab)\omega^2 \Delta t^2 / 2}$$

With these values our solution for *s(t)* becomes

$$s(n\Delta t) = s(0) B^{n/2} \cos \Omega t +$$

$$+ \frac{s(0)\omega \Delta t (b-a)/2 + v(0)/\omega}{\sqrt{1 - \omega^2 \Delta t^2 (a-b)^2 / 4}} B^{n/2} \sin \Omega t$$

$$B = \frac{1 + (1-a)(1-b)\omega^2 \Delta t^2}{1 + ab\omega^2 \Delta t^2} \qquad \text{(APP7)}$$

$$\Omega \Delta t = \tan^{-1} \omega \Delta t \frac{\sqrt{1 - \omega^2 \Delta t^2 (a-b)^2 / 4}}{1 - (a + b - 2ab)\omega^2 \Delta t^2 / 2}$$

AP2. Closed Form solution of FORK equation (13)

We reproduce the relevant expressions

$$\begin{aligned} m_0 &= -\Delta t \omega^2 s(t) \\ m_1 &= m_2 = -\Delta t \omega^2 s(t + \Delta t)/2 \\ m_3 &= -\Delta t \omega^2 s(t) + \Delta t \end{aligned} \qquad \text{(APP8)}$$

and

$$s(t + \Delta t) = s(t) + \Delta t v(t) + \Delta t (m_0 + m_1 + m_2)/6 \qquad \text{(APP9)}$$

$$v(t + \Delta t) = v(t) + (m_0 + 2m_1 + 2m_2 + m_3)/6 \qquad \text{(APP10)}$$

When we substitute the *m*-factors from (APP8) into (APP9) we obtain

$$s(t + \Delta t) = s(t) + v(t)\Delta t - \frac{\omega^2 \Delta t^2}{6} [s(t) + 2s(t + \Delta t/2)]$$

In scientific simulations the stepping time increment Δt is commonly maintained at a fixed value and consequently the $s(t + \Delta t/2)$ quantity is simply not available. In the time period when the FORK algorithm was developed, the relevant slopes were extracted from measurements or observations so there was no problem to satisfy the above formulas. But in simulations we are forced to either run at halved increments and use only every second result, do some fancy iteration to extract the fractional time values or approximate the half time quantity. Only a linear interpolation is available in the second order systems so we will make the following substitution:

$s(t + \Delta t/2) = [s(t) + s(t + \Delta t)]/2$ This leads to

$s(t + \Delta t) = s(t) + v(t)\Delta t - \omega^2 \Delta t^2 [2s(t) + s(t + \Delta t)]/6$ A simple collection of terms yields

$$s(t + \Delta t) = s(t)(1 - \omega^2 \Delta t^2 / 3)/(1 + \omega^2 \Delta t^2 / 6) +$$

$$+ v(t)\Delta t / (1 + \omega^2 \Delta t^2 / 6) \qquad \text{(APP11)}$$

Take the first difference, which yields

$$s(t + 2\Delta t) - s(t + \Delta t) = [s(t + \Delta t) - s(t)]$$

$$\frac{1 - \omega^2 \Delta t^2 / 3}{1 + \omega^2 \Delta t^2 / 6} + \frac{[v(t + \Delta t) - v(t)]\Delta t}{1 + \omega^2 \Delta t^2 / 6} \qquad \text{(APP12)}$$

We need the velocity term in (APP12). To this end we insert the *m*-factors from (APP8) into velocity equation (APP10) to get

$$v(t + \Delta t) = v(t) - \frac{\Delta t \omega^2}{6} [s(t) + 4s(t + \Delta t/2) + s(t + \Delta t)],$$

After making the same approximation to the half increment term we obtain

$$v(t + \Delta t) - v(t) = -\frac{\omega^2 \Delta t}{6} [3s(t) + 3s(t + \Delta t)] \qquad \text{(APP13)}$$

Insertion of this into (APP12) yields

$$s(t + 2\Delta t) - s(t + \Delta t) \left[1 + \frac{1 - \omega^2 \Delta t^2 / 3}{1 + \omega^2 \Delta t^2 / 6} - \frac{\omega^2 \Delta t^2 / 2}{1 + \omega^2 \Delta t^2 / 6} \right] +$$

$$+ s(t) \left[\frac{1 - \omega^2 \Delta t^2 / 3}{1 + \omega^2 \Delta t^2 / 6} + \frac{\omega^2 \Delta t^2 / 2}{1 + \omega^2 \Delta t^2 / 6} \right] = 0$$

This equation can be easily rewritten into the form $s(t + 2\Delta t) - 2A s(t + \Delta t) + B s(t) = 0$ with

$$A = \frac{1 - \omega^2 \Delta t^2 / 3}{1 + \omega^2 \Delta t^2 / 6} \qquad B = 1 \qquad \text{(APP14)}$$

Taking advantage of previously recorded derivation between (APP3) and (APP5) we can write down the solution of our FORK equation defined by (APP8),APP(9) and (APP10)as

$$s(n\Delta t) = s(0)\sqrt{B^n} \cos n\Omega \Delta t +$$

$$+ \frac{s(\Delta t) - s(0)A}{\sqrt{B - A^2}} \sqrt{B^n} \sin n\Omega \Delta t$$

$$\Omega \Delta t = \tan^{-1} \frac{\sqrt{B - A^2}}{A}$$

The numerator of the second term is established from expression (APP14) as

$$B - A^2 = 1 - (1 - \omega^2 \Delta t^2 / 3)^2 / (1 + \omega^2 \Delta t^2 / 6)^2 =$$

$$= (1 - \omega^2 \Delta t^2 / 12) / (1 + \omega^2 \Delta t^2 / 6)^2$$

Just as easily we find

$$\sqrt{B - A^2} / A = \omega \Delta t \sqrt{1 - \omega^2 \Delta t^2 / 12} / (1 - \omega^2 \Delta t^2 / 3)$$

The target expression $s(n\Delta t)$ has an undefined numerator in the second term, part of which is obtained from (APP11) by setting the time equal to zero

$s(\Delta t) = s(0) \frac{1 - \omega^2 \Delta t^2 / 3}{1 + \omega^2 \Delta t^2 / 6} + v(0) \frac{\Delta t}{1 + \omega^2 \Delta t^2 / 6}$. Multiplier of the sinusoidal term is found as

$$\frac{s(\Delta t) - s(0) A}{\sqrt{B - A^2}} =$$

$$= \frac{s(0) \frac{1 - \omega^2 \Delta t^2 / 3}{1 + \omega^2 \Delta t^2 / 6} + \frac{v(0) \Delta t}{1 + \omega^2 \Delta t^2 / 6} - s(0) \frac{1 - \omega^2 \Delta t^2 / 3}{1 + \omega^2 \Delta t^2 / 6}}{\frac{\omega \Delta t \sqrt{1 - \omega^2 \Delta t^2 / 12}}{1 + \omega^2 \Delta t^2 / 6}} =$$

$$= \frac{v(0)}{\omega \sqrt{1 - \omega^2 \Delta t^2 / 12}}$$

The closed form solution of the FORK equation (13) is now

$$s(n\Delta t) = s(0) \cos \Omega \Delta t + \frac{v(0)}{\omega \sqrt{1 - \omega^2 \Delta t^2 / 12}} \sin \Omega \Delta t$$

$$\Omega \Delta t = \tan^{-1} \omega \Delta t \frac{\sqrt{1 - \omega^2 \Delta t^2 / 12}}{1 - \omega^2 \Delta t^2 / 3}$$

The fractional angular frequency deviation is

$$\frac{\Omega \Delta t - \omega \Delta t}{\omega \Delta t} = \frac{\tan^{-1} \omega \Delta t \sqrt{1 - \omega^2 \Delta t^2 / 12} / (1 - \omega^2 \Delta t^2 / 3)}{\omega \Delta t} - 1$$

References

/1/ J.S Newton "Philosophiae Naturalis Principia Mathematica", Translation by Andrew Motte, UC CAL Press, Berkeley, CA, 1946 p. 13

/2/ F.B.Hildebrand "Introduction to Numerical Analysis", Second Edition, Dover Publications, New York 1974, p.285-292

/3/ Ibid pp.5-10

/4/ Ibid p.290

/5/ Z.Fazarinc, "Getting Physics into the Bounce", IEEE Potentials Vol.14 No.1, Feb./March 1995, pp.21-25

/6/ Z. Fazarinc, "Potential Theory, Maxwell's Equations, Relativity, Radiation and Computers", CAEE, Vol.7, No.2, John Wiley&Sons, Inc 1999 pp.51-86

/7/ F.B.Hildebrand "Introduction to Numerical Analysis", Second Edition, Dover Publications, New York 1974, pp.291-292

/8/ John A. Aseltine, "Transform Method in Linear Systems Analysis", McGraw-Hill Book Co., Inc. 1958, p.260

/9/ Ibid, p.276.

Dr. Zvonko Fazarinc
Formerly director of R&D laboratory at Hewlett Packard Co in Palo Alto
and Consulting professor of EE at Stanford University, California
620 Sand Hill Road, 417D, Palo Alto, California 94304
Tel.: (001) (650) 330 0310; Fax: (001) (650) 330 1967
E-mail: z.fazarinc@comcast.net

Prispelo (Arrived): 26.06.2008 *Sprejeto (Accepted): 15.09.2008*

4G: WHERE ARE WE GOING?

Ferdo Ivanek

Palo Alto, California, USA

Key words: Mobile communication, broadband communication, communication standards, radio spectrum management, communication system planning.

Abstract: While deployment of 3G broadband cellular mobile systems still leaves ample room for growth and upgrades, recently developed international standards and new spectrum allocation changes, as well as new systems development, stimulate early 4G deployment. The possible impact of these new developments is exemplified and quantified in terms of 4G aggregate throughput to be shared between individual users. The available data indicate that the user experience with the exemplified candidate 4G systems can be expected to be within the range of current wireline ADSL and cable modem broadband services. 2G/3G deployment indicators are presented that apparently have a bearing on the prevailing evolutionary 3G/4G trends among the leading incumbent mobile service providers aiming at 4G deployment to start in 2010, and attention is drawn to announced plans by other mobile service providers planning to start commercial 4G services in 2008 and 2009, respectively. Three possible scenarios for future 4G convergence and competition are submitted and discussed.

4G: Kam gremo?

Kjučne besede: mobilne komunikacije, širokopasovne komunikacije, komunikacijski standardi, upravljanje z radijskim spektrom, načrtovanje komunikacijskih sistemov

Izvleček: Čeprav uporaba širokopasovnih 3G celičnih mobilnih sistemov še vedno omogoča rast in izboljšave, pred kratkim sprejeti mednarodni standardi in spremembe v dodelitvi frekvenc, kot tudi razvoj novih sistemov, vzpodbujajo zgodnjo uvedbo sistemov 4G. Možen vpliv tega napredka ponazarja in kvantificira skupna prepustnost sistemov 4G, ki si jo med seboj naj delijo posamezni uporabniki. Dostopni podatki kažejo, da bi izkušnje uporabnikov s predlaganimi sistemi 4G, ki so navedeni kot primer, lahko bile primerljive s storitvami obstoječih žičnih ADSL in širokopasovnih kabelskih modemskih sistemov. Predstavljene izkušnje z uvajanjem sistemov 2G/3G imajo očitno zelo močan vpliv na razvojne usmeritve sistemov 3G/4G vodilnih obstoječih ponudnikov mobilnih storitev, ki nameravajo začeti z uvajanjem sistemov 4G v letu 2010. Obravnavani so tudi napovedani načrti drugih ponudnikov mobilnih storitev, ki načrtujejo komercialno uvedbo storitev 4G v letu 2008 ali v letu 2009. Opisani in obravnavani so trije možni scenariji bodoče 4G konvergence in konkurence.

Preface

My selection of the subject of this article is based on wishful thinking about still being able to chat with Lojze over the telephone or visiting him in his home. I imagine he could have said: "I read the August 2008 Focused Issue of the IEEE Microwave Magazine that you edited. Timely subject; would also be of interest to the readers of our Journal "Informacije MIDEM". Could you condense the information into a single article and include your comments?" This is what I decided to do.

1. Introduction

A straightforward single answer to the question in the title is elusive due to the complex interplay of a number of technological, regulatory and business issues. To develop an understanding of where we are really going, it is indispensable to direct attention to the activities of the International Telecommunication Union (ITU), the world's supreme standardization and regulatory body for telecommunications, in which the leading regional and national standardization development organizations (SDOs) and regulatory agencies systematically cooperate. ITU's Radiocommunication Sector (ITU-R) is therefore the most authoritative source of relevant information needed to evaluate the progress of cellular mobile communications.

Presenting key relevant information on this subject in a convenient format for use by the membership of the IEEE Microwave Theory and Techniques Society (MTT-S) was the intent of the August 2008 Focused Issue of the IEEE Microwave Magazine, one of the periodicals published by MTT-S. The focus was on convergence and competition on the way toward the 4th generation of cellular mobile communication systems (4G), which are necessarily of great interest to a large segment of MTT-S membership, primarily those involved in or affected by the development of mobile communications. The author of this article served as guest editor /1/, and was fortunate to benefit from the participation of a prominent international group of authors engaged at the forefront of cellular mobile systems development and standardization /2-5/.

The following sections highlight the fundamental issues of convergence and competition on the way toward 4G, based primarily on the referenced articles /1-5/ that provide extensive reference lists for use by readers interested in more detail. Section 2 highlights the framework for 3G and 4G standards evolution, Section 3 summarizes frequency spectrum availability, Section 4 focuses on the effective spectral efficiency and throughput as key performance metrics, Section 5 highlights the 2G/3G deployment indicators and 4G trends, and Section 6 offers conclusions and comments.

2. Standards development

ITU-R standards development for cellular mobile systems started in 1985 and underwent a number of organizational changes /4/. The current framework consists of "International Mobile Telecommunications-2000" (IMT-2000) and "IMT-Advanced"; the term "IMT" was adopted for both collectively /6/. Two standards deserve particular attention: Recommendation ITU-R M.1457 on specifications of the IMT-2000 radio interfaces /7/, and Recommendation ITU-R M.1645 on objectives of the future development of IMT-2000 and systems beyond IMT-2000 /8/. Both refer to IMT-2000 as "third generation mobile systems". Recommendation ITU-R M.1457, originally adopted in 2000 and updated annually, introduced a family of five different 3G radio interfaces, including the two code division multiple access (CDMA) varieties currently deployed worldwide: wideband CDMA (WCDMA) and CDMA 2000. When Recommendation ITU-R M.1645, adopted in 2003, introduced a new category of mobile systems for more demanding future applications, tentatively named "Systems beyond IMT-2000", it was commonly considered to represent 4G, although this Recommendation does not refer to it as such. Figures 1 and 2 illustrate the concept of systems beyond IMT-2000 as described in Recommendation ITU-R M.1645.

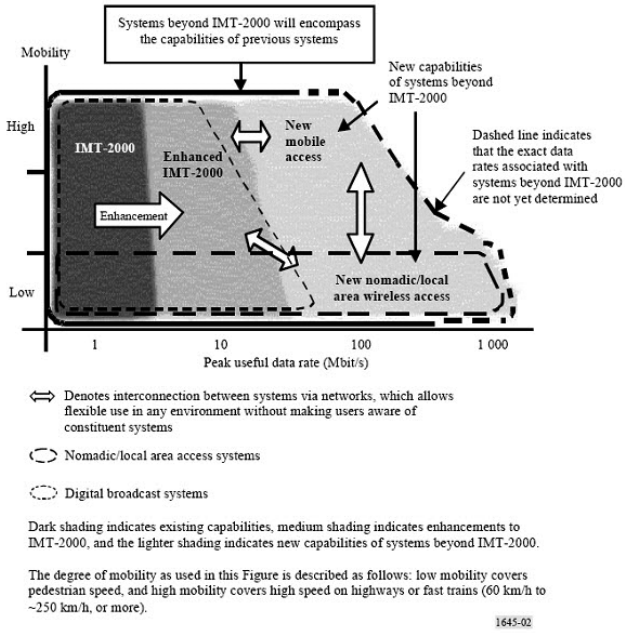

Fig. 1: Illustration of capabilities of IMT-2000 and systems beyond IMT-2000 /8/ (By authorization, ITU Legal Affairs.)

Generational identification was also avoided when "Systems beyond IMT-2000" was renamed "IMT-Advanced", and when Revision 7 of Recommendation ITU-R M.1457 was adopted, both in 2007. Notably, Revision 7 introduced orthogonal frequency division multiple access (OFDMA) radio interfaces. One of them is a new IMT-2000 member based on IEEE Std 802.16, supported by the WiMAX Forum, and the three additional ones represent 3G evolution, e.g. the long term evolution (LTE) and the ultra mobile broadband (UMB) versions that are broadband evolutions from WCDMA and CDMA2000, respectively /2-4/. Since an OFDMA radio interface is commonly considered as a key characteristic of 4G systems, Revision 7 of Recommendation ITU-R M.1457, which was initiated as a vehicle for 3G standardization, actually became a framework for transition to 4G. This unanticipated development seems to justify past avoidance of 4G identification in Recommendation ITU-R M.1645, and it makes it plausible at the current stage of Recommendation ITU-R M.1457 updating. Outside ITU-R, however, the generational terms are in widespread use, and WiMAX, LTE and UMB are commonly considered to represent 4G.

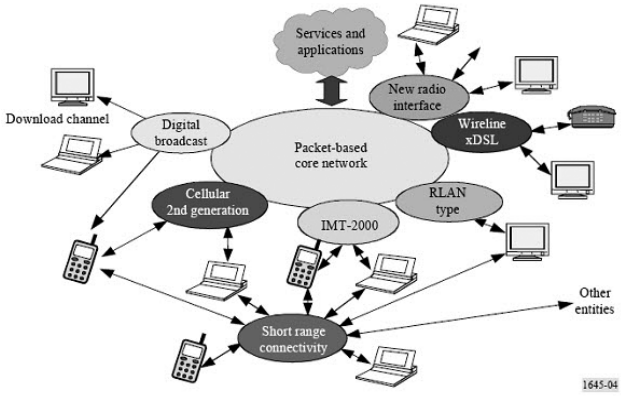

Fig. 2: Future network of systems beyond IMT-2000 including a variety of potential interworking access systems /8/ (By authorization, ITU Legal Affairs.)

The ITU-R framework for IMT-Advanced standardization was defined in 2007 /9/. The schedule calls for submitting proposals for candidate radio interface technologies (RITs) by October 2009, and for developing the necessary Recommendations and Reports by 2011. Foremost among the key features of IMT-Advanced are "target peak data rates of up to approximately 100 Mbit/s for high mobility such as mobile access and up to approximately 1 Gbit/s for low mobility such as nomadic/local wireless access" /8/. The relationship between peak data rates and throughput, which is indicative of expected user experience, is addressed in Section 5.

3. Frequency spectrum availability

Adequate frequency spectrum availability is a prerequisite for satisfactory mobile service provisioning. Growing market demand drives the expanding spectrum needs that are accommodated through appropriate revisions of the Table of Frequency Allocations in the ITU Radio Regulations. This is done at World Radio Conferences (WRCs) that take place every three to four years. In ITU-R terminology, frequency spectrum for IMT is "identified" within bands allocated to the mobile service. After the additions approved at WRC-

07, the frequency spectrum availability for IMT is as follows /1, 5/:

450-470 MHz
698-960 MHz
1 710-2 025 MHz
2 110-2 200 MHz
2 300-2 400 MHz
2 500-2 690 MHz
3 400-3 600 MHz

The current total of 1 077 MHz appears insufficient in view of the consensus estimates of IMT spectrum needs for the year 2010, which range from 1 280 MHz for low demand to 1 720 MHz for high demand, respectively /5/.

The bands 806-960 MHz, 1710-2025 MHz and 2110-2200 MHz are in current use for 2G and 3G services. The bands 450-470 MHz, 698-862 MHz, 2 300-2 400 MHz, and 3 400-3 600 MHz were additionally identified for IMT at WRC-07. There was also a proposal for adding the bands 3600-4200 MHz and 4400-4900 MHz for estimated additional future IMT needs, but it was not adopted due to objections from current users of these bands, foremost the fixed satellite service. No WRC follow up is scheduled at this time; the matter is neither on the WRC-11 agenda, nor on the WRC-15 preliminary agenda. Importantly, a number of regulatory restrictions on spectrum usage apply to specific bands in different regions and countries. The necessary follow-up regulatory proceedings for the newly identified bands for IMT, such as spectrum auctions and radio-frequency channel arrangements, are in progress at various stages in the different regions and countries. Since frequency spectrum is a limited natural resource, spectral efficiency is of particular significance.

Of special interest is the spectrum "refarming" undertaken in Japan to make the bands 3 600-4 200 MHz and 4 400-4 900 MHz available for IMT applications starting in 2012 /5/. This national initiative may stimulate international identification of one or both of these bands for IMT at a future WRC. The beneficial result would be to align spectrum availability closer with the estimated spectrum needs quoted above.

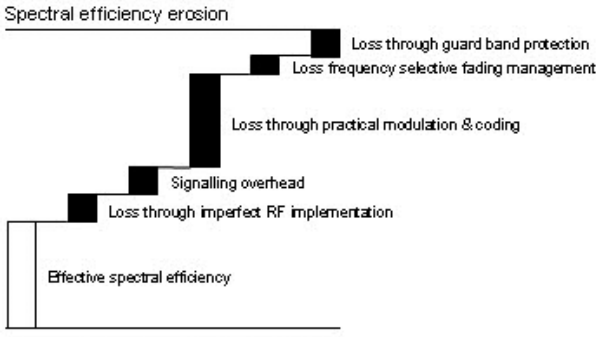

Fig. 3: Illustration of representative spectral efficiency erosion on an approximate dB scale. (Courtesy of Vodafone R&D.)

4. Effective spectral efficiency and throughput

The nominal spectral efficiency, which is the ratio of the peak system data rate to the channel bandwidth, is most commonly quoted. However, the more useful metric for system evaluation is the effective spectral efficiency, which accounts for system implementation losses /2/. Figure 3 illustrates the "erosion" from the nominal to the effective spectral efficiency.

The quantitative erosion of spectral efficiency determines the aggregate per carrier-sector throughput, which is available for sharing by simultaneous cell users. The most informative comparison of representative 3G and 4G systems presented in Table 1 of /3/ reveals the important fact that the effective spectral efficiencies for 4G systems are about double in comparison with 3G systems. Table 1 below, which is an excerpt from the referenced table /3/, compares the current candidate 4G systems, both frequency-division duplex (FDD) and time-division duplex (TDD).

Table 1: 4G comparison (excerpt from Table 1 in /3/). Based on 64 QAM in the downlink (DL), 16 QAM in the uplink (UL), spectrum reuse 1, and signalling overheads included /3/.

		OFDMA + 2x2 MIMO (4G)				
		WiMAX		**UMB**	**LTE**	
TDD (2:1)/FDD		**TDD (10 MHz)**	**FDD (5+5 MHz)**	**FDD (5+5 MHz)**	**TDD (10 MHz)**	**FDD (5+5 MHz)**
Peak data rate (Mbit/s)	DL	37.44	28.63	37.25	47.48	37.5
	UL	5.04	7.56	19.5	9.33	12.5
Aggregate throughput per carrier-sector (Mbit/s)	DL	7.88	5.25	8.1	11.93	7.95
	UL	2.55	3.83	4.0	2.5	3.75
Spectral efficiency (bits/s/Hz/carrier-sector)	DL	1.28		1.62	1.59	
	UL	0.72		0.8	0.79	

The aggregate throughput figures in Table 1 suggest that the user experience with the exemplified candidate 4G systems can be expected to be within the range of current wireline ADSL and cable modem broadband services. The achievable throughput for any individual mobile user depends on a number of parameters, such as specific system characteristics, propagation and interference conditions, traffic patterns, and the number of simultaneous cell users /8/.

5. 2G/3G deployment indicators and 4G trends

The most significant single statistical indicator is that global mobile penetration in terms of subscriptions recently surpassed 50%, which is an impressive achievement in spite of multiple subscriptions that are not accounted for /10/. About 99% of the world's mobile subscribers are served by two 2G/3G system families: GSM/WCDMA and cdmaOne/CDMA2000, respectively /1-3/. Their relative market shares are thus important statistical indicators. The last period for which directly comparable worldwide statistics for both 2G/3G families are available in the public domain as of this writing is the end of the first quarter of 2008 /11-12/. Their combined total number of subscribers amounted to about 3.5 billion. By comparison, the current number of fixed telephone lines totals about 1.3 billion. It is informative to differentiate the total mobile subscriptions in two ways, by system families, and by system generation. The approximate results are:

- market shares by system families were 87% for GSM/WCDMA vs. 13% for cdmaOne/CDMA2000;
- market shares by system generation were 81% for 2G vs. 19% for 3G.

Of particular interest are the market shares of the currently deployed advanced broadband versions of the two system families, high speed packet access (HSPA) and evolution-data optimized (1xEV-DO): 3.7% combined for end Q1 2008; 0.9% for HSPA and 2.8% for 1xEV-DO. Their modest broadband capabilities, e.g. aggregate per sector downlink throughputs of 0.95 Mbit/s in a 1.25 MHz band, and 2.6 Mbit/s in a 5 MHz band, respectively (Table 1 in /3/), indicate that 3G broadband deployment is still in its beginnings. HSPA and 1xEV-DO upgrades in progress are intended to substantially enhance 3G capabilities and improve cost effectiveness.

The above 2G/3G statistical indicators have apparently a bearing on prevailing 4G trends among the leading incumbent mobile service providers. The predominant ones that currently use the GSM/WCDMA system family naturally decided in favor of their own candidate, LTE, and are cooperatively supporting its standardization and development, aiming at commercial LTE launch in 2010 /13/. This includes even Verizon that currently uses the cdmaOne/CDMA 2000 system family /14/. However, another major incumbent service provider currently using the cdmaOne/CDMA 2000 system family, Sprint, is already deploying the commercially available WiMAX, and plans to start offering service in late 2008 /15/. And there are new competitive service entrants that decided to exploit the current time to market advantage of WiMAX, e.g. QU Communications in Japan, with plans to start commercial service in 2009 /16/.

What next for 4G? One possible scenario is a replay of 2G/3G history when cdmaOne was the trailblazer, evolved into CDMA 2000, and was the catalyst for WCDMA, but captured only a minor 2G/3G market share. In the replay, WiMAX is the trailblazer, and apparently the catalyst for LTE, but may likewise end up with a minor 4G market share as a consequence of the existing GSM/WCDMA dominance of the 2G/3G markets. Nevertheless, even a minor 4G market share is attractive. Another possible scenario is WiMAX-LTE convergence that is within reach due to their commonalities. This possibility was already publicly recognized both among service providers and system suppliers, e.g. /17, 18/. The IMT-Advanced framework /9/ offers an opportunity for implementing convergence but, at least as of this writing (September 2008), the IEEE 802.16m and LTE Advanced proposals for IMT-Advanced radio interfaces seem to progress in competition with each other and without apparent attempts toward convergence /4, 19/. Still another possible scenario is the use of a new OFDM radio interface variant, such as the one applying variable spreading factor (VSF) control to OFDM (VSF-Spread OFDM), which experimentally demonstrated 1 Gbit/s peak downlink data rate in a 100 MHz channel using 4x4 MIMO at speeds of up to about 30 km/hr /5/.

6. Conclusions and comments

Synergy between technological progress and service development stimulates convergence through standards development, on the one hand, and competition among both systems suppliers and service providers, on the other. While 3G deployment progressed slower than anticipated and still leaves ample opportunity for broadband upgrading, OFDMA technology push enables leapfrogging to all-IP 4G that offers substantially improved broadband capabilities, spectral efficiencies and cost effectiveness. This increases the service providers' options in satisfying the growing market pull for mobile broadband access with capabilities comparable to those of fixed networks.

The IMT-Advanced peak data rate objective of 100 Mbit/s for mobile applications is within reach of emerging 4G systems. However, their aggregate per carrier-sector throughputs available for sharing between simultaneous users are substantially lower due to system implementation losses. This means that 4G mobile broadband user experience can be expected to be comparable to current ADSL and cable modem broadband services. The IMT-Advanced objective of 1 Gbit/s peak data rate for nomadic applications promises aggregate throughputs that would assure user experience comparable to current fiber optic access,

but pursuit of this objective seems less compelling because usage at such high data rates is more likely to occur in fixed locations. Nevertheless, mobile services are under unabated pressure to offer performance as close as possible to fixed networks, and this pressure is increasing with the growth of the mobile web /20/.

Acknowledgement

The author is grateful to the authors of key references /2-5/, who kindly reviewed the manuscript and provided constructive suggestions: **Dr. Stanley Chia**, Senior Director, Vodafone Group R&D; **Dr. José M. Costa**, Senior Manager, Wireless Access Standards, Nortel, and Vice Chairman, ITU-R Study Group 5 – Terrestrial Services; **Dr. Roger B. Marks**, Senior Vice President – Industry Relations, NextWave Wireless, and Chairman, IEEE 802.16 Working Group on Wireless Access; **Dr. Akira Hashimoto**, Managing Director, Wireless Standardization Department, NTT DoCoMo, and Chairman, ITU-R Study Group 5 – Terrestrial Services.

References

/1/ F. Ivanek, "Convergence and Competition on the Way Toward 4G", *IEEE Microwave Magazine,* vol. 9, no. 4, pp. 6-14, August 2008.

/2/ S. Chia et al., "3G Evolution", *IEEE Microwave Magazine,* vol. 9, no. 4, pp. 52-63, August 2008.

/3/ W. Tong et al., "The Broadband Multimedia Experience", *IEEE Microwave Magazine,* vol. 9, no. 4, pp. 64-71, August 2008.

/4/ R. B. Marks et al., "The Evolution of WirelessMAN", *IEEE Microwave Magazine,* vol. 9, no. 4, pp. 72-79, August 2008.

/5/ A. Hashimoto et al., "Roadmap of IMT-Advanced Development", *IEEE Microwave Magazine,* vol. 9, no. 4, pp. 80-88, August 2008.

/6/ "Naming for International Mobile Telecommunications", *Resolution ITU-R 56,* 2007 /Online/. Available: http://www.itu.int/publ/R-RES-R.56-2007/en

/7/ "Detailed specifications of the radio interfaces of International Mobile Telecommunications-2000 (IMT-2000) ", *Recommendation ITU-R M.1457*, 2007.

/8/ "Framework and overall objectives of the future development of IMT-2000 and systems beyond IMT-2000", *Recommendation ITU-R M.1645*, 2003.

/9/ "ITU global standard for international mobile telecommunications 'IMT-Advanced'", *ITU Radiocommunication Sector (ITU-R)* /Online/. Available: http://www.itu.int/ITU-R/index.asp?category=information&rlink=imt-advanced&lang=en

/10/ "Mobile phones for half the world's population", *ITU News*, no. 1, Jan.-Feb. 2008 /Online/. Available: http://www.itu.int/itunews/manager/main.asp?lang=en&ciYear= 2008&ciNumber=01

/11/ "Subscriber connections Q1 2008", *GSM World* /Online/. Available: http://www.gsmworld.com/news/statistics/pdf/gsma_stats_q1_08.pdf

/12/ "1Q 2008 Subscriber Statistics", *CDMA Development Group (CDG)*, /Online/. Available: http://www.cdg.org/worldwide/cdma_world_subscriber.asp

/13/ "Towards Global Mobile Broadband", *White Paper, UMTS Forum*, February 2008 /Online/. Available: http://www.3gpp.org/news/2008_04_LTE_A.htm„

/14/ "Verizon Selects LTE as 4G Wireless Broadband Direction", *Verizon Investor News*, /Online/. Available: http://investor.verizon.com/news/view.aspx?NewsID=872

/15/ "Sprint and Samsung Declare Mobile WiMAX Technology is Now Ready for Commercial Service", *Sprint News Release*, May 15, 2008 /Online/. Available: http://newsreleases.sprint.com/phoenix.zhtml?c=127149&p=irol- newsArticle_newsroom&ID=1146239&highlight=

/16/ M. Nohara, "Mobile WiMAX to Become Real in Japan", *IEEE Microwave Magazine,* vol. 9, no. 4, pp. 36-42, August 2008.

/17/ "Sarin calls for simplification", *GSMA Mobile World Congress Daily*, Wednesday 13th February 2008, pp. 1-3 /Online/. Available: http://www.wdisdigital.com/index.php?db=GSMA&jnl=DAILIES&vcab=624

/18/ Brad Smith, "Intel Seeking WiMAX-LTE Marriage?", *WirelessWeek*, June 05, 2008 /Online/. Available: http://www.wirelessweek.com/article.aspx?id=160528

/19/ "Beyond 3G: 'LTE-Advanced' Workshop, Shenzen, China", *3GPP News Release*, 11th April 2008 /Online/. Available: http://www.3gpp.org/news/2008_04_LTE_A.htm

/20/ "Making Web access from a mobile device as simple as Web access from a desktop device", *W3C Mobile Web Initiative*, August 2008 /Online/. Available: http://www.w3.org/Mobile/

Ferdo Ivanek
Palo Alto, California, USA

Prispelo (Arrived): 01.09.2008 *Sprejeto (Accepted): 15.09.2008*

FIXED-MOBILE CONVERGENCE

Marko Jagodič

RASKOM d.o.o., Ljubljana

Key words: fixed communications, mobile communications, device convergence, service convergence, network convergence, trends, long term perspectives

Abstract: Fixed-mobile convergence (FMC) is a phenomenon which is dominating at present the development of fixed as well as mobile communications around the world. The article tries to clarify the background for different understanding of FMC and the main reasons which started it and influenced its evolution. The article also addresses some of the more important FMC supporting technologies like Unlicensed Mobile Access (UMA), IP Multimedia Subsystem (IMS) and Femtocells, describes and discusses the most important development phases of FMC as well as the rationale for investing in it.

Fiksno-mobilna konvergenca

Kjučne besede: fiksne komunikacije, mobilne komunikacije, konvergenca naprav, konvergenca storitev, konvergenca omrežij, razvojne smeri, dolgoročna perspektiva

Izvleček: Fiksno-mobilna konvergenca (FMC) je pojav, ki trenutno obvladuje razvoj tako fiksnih kot tudi mobilnih komunikacij po svetu. Članek poizkuša najprej pojasniti ozadja za različno razumevanje FMC in glavne razloge, ki so sprožili njen začetek in vplivali na njen razvoj. Članek tudi predstavi nekatere za razvoj FMC najbolj pomembne tehnologije, kot so Unlicensed Mobile Access (UMA), IP Multimedia Subsystem (IMS) and femtocelice, predstavi in komentira najbolj pomembne razvojne faze FMC in razloge za njeno uvajanje.

1. Introduction

Fixed-Mobile Convergence (FMC) is a process which started when mobile communications, based primarily on voice services, reached a worldwide maturity and mobile customers began to look for new more complex services involving voice, data, and video. One of the most important technologies behind, which persistently expands the availability of these new services to fast growing number of mobile users, is microelectronics, the domain in which Prof. Lojze Trontelj excelled producing innovative products of worldwide importance.

The article will try first to explain the different perceptions of FMC by different players in the area of electronic communications. The description of current evolution towards FMC will follow complemented by some important technological aspects as well as development phases of FMC. The rationale for introducing FMC will be addressed at the end of the article.

2. What is Fixed – Mobile Convergence?

Mr. Ilkkka Nakaniemi from Nokia Siemens Networks made an excellent summary of FMC at OECD Forum in October 2006 /1/saying that FMC is rather complex process which does not involve only service and application convergence. Device and network convergence are equally if not more important and all of them are leading to industry convergence as shown in Fig. 1

Different people understand FMC quite differently. For an operator such as Iceland Telecom, a hosted PBX Centrex service focused on SMEs understands FMC as a combination of PSTN, ISDN and GSM to provide an identical set of services for mobile and fixed workers. An operator like BT views FMC as a new and over-reaching integrated wireline/wireless business opportunity, with variations to serve both consumer and corporate customers. Ryan Jarvis, BT chief of convergence products, describes the FMC phenomenon as three dimensional: "One stratum is network convergence which enables devices to move between networks. Then you have service convergence where you

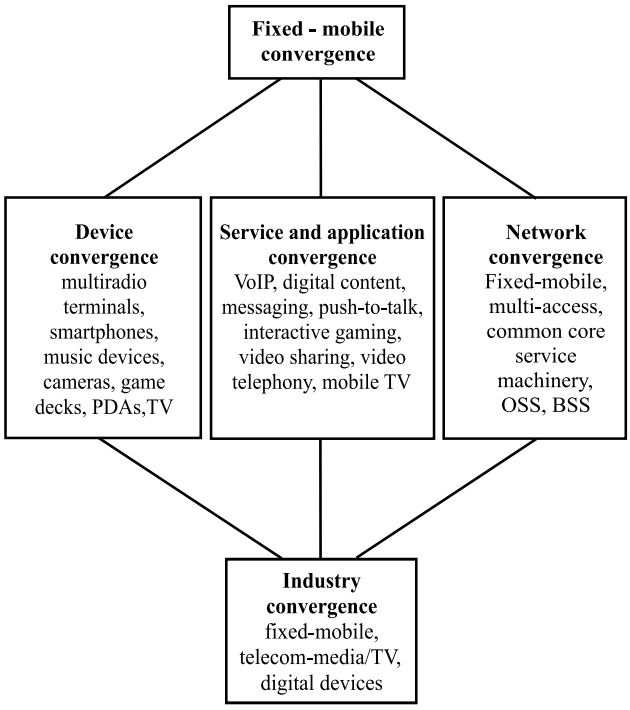

Fig. 1 Fixed – Mobile Convergence elements

have one bill and one customer contact centre that supports that device across multiple networks. And then you have commercial convergence which is usually called bundling – it's effectively one product".

FMC enables really rich set of services using the same device – mobile phone. Users expect and want to have access to all available services on device they have with them at the time (mobile phone, laptop or others) regardless of the operator the device is connected to, fixed or mobile, the one they are subscribed to or another, native or foreign.

3. The evolution towards FMC

The Organisation for Economic Co-operation and Development (OECD) has come up with the following findings related to the evolution of FMC /2/:

- Dual-mode cellular/Wi-Fi handsets exist using Wi-Fi modems in the home environment to access VoIP through ADSL connections
- There are less evolved forms of FMC using cellular/ Wi-Fi dual-mode handsets that do not have a handover function or have a handover function but do not utilize a fixed voice or broadband network in the home.
- Services also exist linking both fixed and mobile networks which are not technologically converged, such as those offering a single voice mailbox over both fixed and mobile networks.
- Voice and data services for cellular networks are being bundled, although data services are sometimes provided through wireless cards for laptops. In this case, there is no interface between cellular and Wi-Fi networks and those services tend to remain separate.
- Mobile based dual-mode services using home-zones are being provided by offering a virtual fixed line within a designated home-zone area. Prices in the home-zone tend to be in line with prices charged by fixed network operators and lower than cellular rates charged outside the home-zone.

Obviously there are many ways being used to provide FMC services some of which are more technologically integrated than others. FMC services are definitely representing a significant challenge to all telecommunication operators. Bundling of disparate services over separate networks is considered as a marketing step necessary to support customers.

From the viewpoint of services, the fixed network operators are endangered by the penetration of mobile services into their market, while the mobile operators are faced with the saturation of mobile markets based on the second generation equipment and the need to persuade customers to shift to third generation equipment. At the same time, at least in some countries, more and more fixed network operators which traditionally did not provide mobile services are entering into mobile markets through MVNO-s (Mobile Virtual Network Operators). Nevertheless both mobile and fixed telecommunications operators have to compete with IP based services using fixed or Wi-Fi networks and therefore they are forced to invest either into the development of Next Generation Networks (NGN) or into support systems like the IP Multimedia Subsystem (IMS).

Cable operators are also beginning to offer FMC services and are keen to provide multiple play services such as triple play or quadruple play and are becoming direct competitors to PSTN operators. It is expected that this direct competition will increase in the future.

The FMC service called home-zone service is known for more then 10 years already. Here, mobile operators offer through their mobile network a virtual fixed line area called the home-zone (for example: UnoFon service by Sonofon in Denmark from 1997 on). Strictly speaking, this type of service is better described as fixed-to-mobile substitution leading to an increase in the amount of mobile call volumes with respect to all voice volumes.

For better understanding of evolution towards FMC it is very illustrative to take a look at the role Wi-Fi hotspots are playing in promoting FMC. The availability of such hotspots is quite impressive as it can be seen from Table 1.

Wi-Fi hot spots are promoting FMC through VoIP-enabled wireless telephony (VoWi-Fi) by utilizing devices that use

Table 1 Number of Wi-Fi hotspots (as of 11.09.2006)

Top 10 Countries		Top 10 Cities		Top 10 Location Types	
US	41 007	Seoul	2 056	Hotel / Resort	31 887
UK	14 933	London	1 943	Restaurant	25 480
Germany	12 509	Tokyo	1 843	Cafe	15 802
South Korea	9 415	Taipei	1 786	Store / Shopping Mall	14 834
Japan	6 258	Paris	1 204	Other	7 850
France	5 334	Berlin	823	Pub	5 348
Taiwan	2 899	San Francisco	805	Office Building	2 386
Italy	2 549	Daegu	787	Gas Station	1 735
Netherlands	2 517	Singapore	671	Airport	1 580
Australia	2 180	New York	669	Library	1 400

Source: JiWire (http://www.jiwire.com/search-hotspot-locations.htm).

Wi-Fi to connect to a VoIP service such as Skype rather than roam between cellular and wireless LAN systems. Most of the VoWi-Fi operators are at present providing Wi-Fi based only services, but some are starting to offer FMC services by combining cellular services with VoWi-Fi. Mobile telecommunications operators are also challenged by Wi-Fi hotspot operators allied with Skype. Therefore some mobile operators seriously consider connecting their cellular networks with Wi-Fi hotspots. Namely the availability of Wi-Fi hotspots is also continuously growing. For example, in the United Kingdom, the number of Wi-Fi hotspots almost doubled between June 2005 and June 2006. On top of Wi-Fi new wireless technologies are coming such as mobile WiMAX which will definitely influence the delivery of FMC services.

The high penetration of mobile phones in OECD countries has resulted in significant substitution of fixed network traffic with mobile network traffic. For example, in France, the volume of voice calls through fixed networks has decreased while voice calls through mobile networks have increased as indicated in Fig. 2

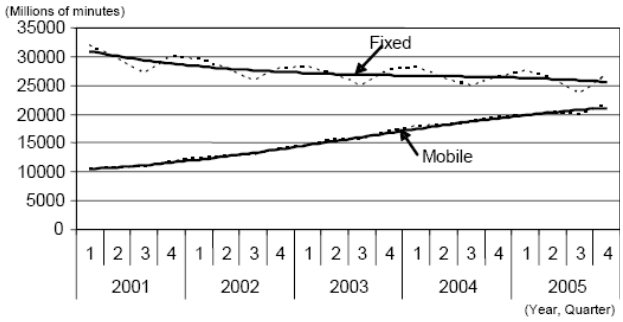

Note: Bold lines are trend lines (3rd order).

Source: ARCEP (*Le marché des services de télécommunications en France*).

Fig. 2 Volume of voice calls in France

In the United Kingdom the substitution was not as extensive as in France. One study indicates that the majority of those examined in the United Kingdom (65%) were not so much in favor to abandon their fixed line services as in other European countries surveyed.

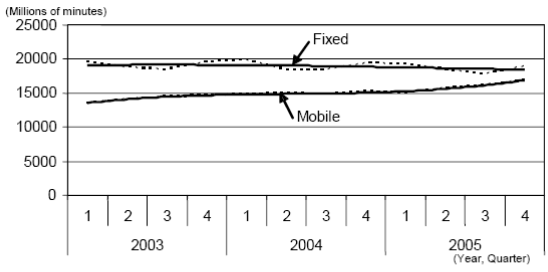

Note: Figures of fixed network were taken from residential 'UK geographic calls' and figures of mobile network were taken from 'UK calls'. Bold lines are trend lines (3rd order).

Source: Ofcom ('The Communications Market 2004 - Telecommunications Appendices' (August 2004), 'The Communications market - Telecommunications Appendices' (January 2005), 'Telecommunications market Data Tables Q4 2005' (June 2006)).

Fig. 3 Volume of voice calls in United Kingdom

To get the right indication of the future trends of FMC services it is necessary to watch the changes in these trends in individual countries. One important variable influencing future trend could be the number of mobile-only households. At present the percentage of households that only use mobile phones within the EU25 countries is 18 %. Another important variable is the ratio of mobile call volumes to all voice volumes. This ratio is close to 70% in Finland, over 50% in Austria, more than 40% in France and around 30% in the United Kingdom. In Germany this it is only 12% which means an opportunity for German mobile operators to take a market share from fixed network operators, especially through the provision of homezone type services. It should be also noted that in the process of transition to NGN or IMS, FMC does not relates to voice calls only but covers a much broader range of services including television and other multimedia services.

Some incumbent fixed operators, that also provide cellular services, are integrating their fixed and mobile operations in order to offer converged services and take advantage of the economies of scope and scale provided by next generation switching systems. Telekom Slovenia has decided to follow this course.

4. Technological aspects

UMA (Unlicensed Mobile Access)

This technology enables access to GSM and GPRS mobile services over unlicensed spectrum using Bluetooth and WLAN 802.11. Subscribers are able to roam and handover between cellular networks and public and private unlicensed wireless networks using dual-mode mobile handsets. The advantage of UMA is its ability to provide FMC capabilities based on existing wireless networks. How UMA works?

IMS

IMS, proposed by 3GPP (3rd Generation Partnership Project), was originally intended to provide IP-based communications over mobile network /3/. Later on it developed into the leading standard for the NGN because it can also be used with fixed IP-based networks. It is based on using SIP protocol. Some operators are still hesitant to decide for IMS mainly because of the still high initial investment cost. However, advanced standards, improved capabilities, and decreasing cost of introducing IMS will convince more and more operators to accept IMS. Namely IMS provides a better method for charging multimedia sessions, because the identity management (IM) is an integral part of the core IMS technology structure and IMS can be used by all kind of operators, fixed, mobile, and integrated operators. It helps to ensure a level playing field among operators and service providers at the technological level. The main reasons to invest in IMS are:

- for mobile operators: deployment of novel services to increase usage

- for fixed operators: reduction of CAPEX and OPEX and capability to offer competitive services
- for integrated operators: achieving service continuity across different domains

Femtocells

A femtocell is a small cellular base station designed to be located inside a home and using a DSL/Cable connection to the backhaul traffic. UMA-enabled cellular/Wi-Fi dual-mode handsets require Wi-Fi access points. This kind of access could be very expensive especially with picocells. Femtocells do not require subscribers to change their mobile handsets into dual-mode handsets, and UMA enabled femtocells, which are at present applicable for 3G or even for 2.5G, can have air interface with existing handsets. Using a single handset improves customer loyalty and reduces churn. In addition, the backhaul traffic from femtocell stations to a mobile core network will run through fixed broadband, thus giving fixed operators a motivation to be involved in this kind of access especially with FTTH as dominating fixed network access technology.

Development phases of FMC

- Service bundling
- FMC using broadband /Wi-Fi connections (cellular/ Wi-Fi dual-mode service)
- Mobile based 'dual-mode' services
- Network convergence

Service bundling

At the very beginning of FMC operators were offering bundling of fixed and mobile services without any technological interface between the two types of networks /2/. While bundling provides subscribers with price discount the use of new technologies brings very little added value for them. Cellular voice and data services can be bundled too, although for data services the use of laptops is generally preferred. Usually without an interface between cellular and Wi-Fi networks those services are not packaged in the way FMC services are offered, since data is regarded as an optional service or may be classified as only for business use. There are also services which link both fixed and mobile networks but are not technically converged like services offering a single voice mailbox over both fixed and mobile networks.

Many offers on the market are based on discounts for calls made between fixed and mobile networks to specific subscribers, but are not based on converged fixed-mobile services.

FMC using broadband /Wi-Fi connections (cellular/ Wi-Fi dual-mode service)

There are several variants of this kind of FMC services /2/:

- Dual-mode services using a mobile handset and Wi-Fi modems in the home environment to access VoIP through ADSL connections (for example "Unik" in France). These are examples of incumbents "cannibalizing" their PSTN traffic. New entrants use the same technology but rely on local loop unbundling (LLU) like "Home Free" in Denmark.
- Services through cellular/Wi-Fi dual-mode handsets that do not have a handover function from one mode to another, offering each mode separately (for example "surf & talk" in Switzerland).
- Cellular/Wi-Fi dual mode voice service which has a handover function from one mode to another, but it does not utilize a fixed voice or broadband network in the home (for example "Hotspot@Home" in USA)

When subscribers are within the Wi-Fi zone, the calling fee is very low or free, and when they are calling within the cellular network, the tariff for cellular calls is applied. With this type of service, the switch between the Wi-Fi and GSM networks is handled automatically.

Mobile based 'dual-mode' services

Mobile-based services using home-zones are a variant of FMC. In this case mobile operators offer their customers a virtual fixed line within a designated home-zone area. Tariffs in the home zone tend to be in line with rates charged by fixed network operators and lower than cellular rates charged outside the home zone. The main incentive for mobile operators to offer this type of services is that they must compete with the fixed line operators encroaching through FMC into the market which was traditionally reserved for mobile operators. Another important incentive for mobile operators to offer dual-mode services is to free up valuable licensed spectrum when the customer is within the home zone area. Many of the fixed operators are doing so through Mobile Virtual Network Operators.

Network Convergence

For the really consequential and sustainable long term network convergence, which is the enabling basis for the fixed-mobile convergence of services and devices, it is not enough to focus only on adopting the principle of all IP networks. This is good enough for the immediate and short term actions in the direction of FMC. For a successful long term FMC much more is needed. With the global acceptance of FMC as the most appropriate mode of electronic communications in the future the existing networks themselves have to be reassessed from the point of view of suitability of their structures to confront with: the exponential growth of traffic, the required geographical coverage, and the need to set up a simple system to support inter-working of the fixed and mobile domains as well as operators.

Photonic technology in the access area has been gaining momentum all the time, driven by the continuous growth of bandwidth, essential for the successful introduction of new services and applications. The most fundamental challenge at this point of evolution of optical networking is to achieve convergence at multiple levels, among them optical – wire-

less being very important to be able to build an integrated optical platform for an efficient end-to-end service delivery with guaranteed performance. It is expected that the total amount of end users and end devices needing broadband connections in the near future will rise to the order of trillions. Therefore a considerable enhancements in the access part of the network are needed including the convergence of optical and wireless technology leading to a hybrid optical – wireless access infrastructure that will facilitate user mobility and support the vast number of connected devices and sensors, while the simultaneous introduction of WDM will help to increase bandwidth and to enhance ability to upgrade networks /6/.

5. The rationale for FMC

The rationale to invest into FMC depends very much on the type of operator /4/, /5/. The fixed network operators see in FMC the opportunity to generate new revenue through quick response to fixed and mobile customers by developing themselves into one-stop-shops for their needs. At the same time FMC is also the best tool to defend them efficiently against mobile substitution.

The mobile network operators have different rationale to invest in FMC. They are faced with market saturation in second generation mobile markets and declining average revenue per user in their existing markets. They are also faced with competition from voice calls made over the Internet and over Wi-Fi or Mobile WiMAX networks. FMC helps them by facilitating the number portability and by reducing the price of mobile calling and access to data using mobile terminals through the provision of cellular/Wi-Fi dual-mode services.

On the other side shifting to an all IP-based network architecture FMC works well simultaneously for both fixed and mobile network operators by reduction of longer-term maintenance costs and allowing the provision of higher value-added services through service bundling. It is expected that the next generation network technology will bring substantial cost reductions which will certainly increase the profitability of most operators.

6. References

/1/ Ilkka Lakaniemi, Views on FMC, OECD Convergence Forum, Oct. 2006

/2/ Report DSTI/ICCP/CISP(2006)4/FINAL, OECD 2006

/3/ Stephen Hayes, Fixed Mobile Convergence – Evolution of IMS, ITU-T Workshop on Multimedia in NGN, Sept. 2007

/4/ Telephony and NXTcomm08, Independent insights: IOC investment and service strategies, June 2008

/5/ Frost&Sullivan and Tekelec, Network Evolution: Migration Strategies for Success, 2007

/6/ Ioannis Tomkos, Kostis Kanonakis, COST DC-ICT Action Proposal: Converged optical network infrastructure in support of future internet and grid services, Sept 2008

Prof. Dr. Marko Jagodič, univ.dipl.ing.
RASKOM d.o.o.
Omersova 62, SI-1000 Ljubljana, Slovenia
E-mail: jagodic.marko@guest.arnes.si

Prispelo (Arrived): 08.05.2008 Sprejeto (Accepted): 15.09.2008

DESIGN GUIDELINES FOR A ROBUST ELECTROMAGNETIC COMPATIBILITY OPERATION OF APLICATION SPECIFIC MICROELECTRONIC SYSTEMS

Janez Trontelj jr.

Faculty of Electrical Engineering, Ljubljana, Slovenia

Key words: Electromagnetic compatibility, EMC, EMI, ASIC, GTEM,

Abstract: Proper operation of microelectronic systems is often influenced by electromagnetic interference. While the geometry and power supply voltage of the microelectronic structures are decreasing, the demand for emission robust integrated circuits is increasing. Designing the integrated circuit for electromagnetic compatibility is therefore necessary, to achieve the desired functional performance, as well as to meet legal requirements. Example here can be automotive market, where several strict regulations must be fulfilled. It is a good practice, to incorporate known guidelines and use simulation tools for electromagnetic compatibility from the beginning of the project. Later redesign of the microelectronic system, to fulfill the electromagnetic compatibility test, is very expensive and can cause serious product delays and consecutive market loss. Conversely, incorporating all the best electromagnetic immunity practice at the beginning, can lead to the product being over engineered and expensive to produce. In this article several electromagnetic compatibility design guidelines and practical solutions for microelectronic systems are presented.

Priporočila za načrtovanje elektromagnetno robustnih mikroelektronskih sistemov po naročilu

Kjučne besede: Elektromagnetna združljivost, EMC, EMI, ASIC, GTEM,

Izvleček: Na pravilno delovanje mikroelektronskih sistemov pogosto vplivajo elektromagnetne motnje. Z zmanjševanjem velikosti mikroelektronskih struktur in njihovih napajalnih napetosti, so se povečale zahteve za elektromagnetno robustnost integriranih vezij. Upoštevanje elektromagnetne združljivosti, je torej potrebno tako zaradi pravilnega delovanja vezja, kot tudi zaradi upoštevanja predpisanih zakonov elektromagnetne združljivosti. Dober primer je tržišče avtomobilske elektronike, kjer je potrebno striktno upoštevati strogo zakonodajo. Priporočila in rezultate simulacijskih orodij za elektromagnetno združljivost je smiselno upoštevati že od samega začetka projekta. Popravljanje končanih, elektromagnetno nezdružljivih mikroelektronskih sistemov je drago opravilo. Običajno povzroči tudi veliko zamudo izdelka in posledično izgubo tržišča. Po drugi strani pa lahko preveč striktno upoštevanje vseh faktorjev glede elektromagnetne združljivosti po nepotrebnem podraži izdelek. V članku smo navedli priporočila in praktične rešitve za elektromagnetno združljivost mikroelektronskih sistemov.

1 Introduction

The technique of electromagnetic compatibility (EMC) is very important engineering process, to ensure that various electrical devices may operate simultaneously without interfering with each other. EMC is mostly influenced by internal or external electromagnetic emissions that are usually caused by pulsing electrical current. The transition time of such pulse is very important. It determines the spectral image of possible electromagnetic interference (EMI), which may disturb the normal operation of another device or microelectronic system. Fast transition time generates wider spectral image that can more easily cause electromagnetic interference at certain frequencies. This phenomenon may degrade the quality of analog signals or corrupt digital signals. Some claim, that only fifteen percents of devices that have not been designed for EMC, are likely to pass EMC testing for the first time.

We can say, that device is electromagnetically compatible, when it is capable to satisfy all the operating specifications in electromagnetic environment and meet all legal requirements about electromagnetic emissions. More precisely, microelectronic system is electromagnetically compatible with its environment, when it satisfies the following criteria:

- It does not cause EMI to other systems.
- It is not sensitive to EMI from other systems
- It does not cause EMI to itself.

Various EMC standards for different applications specify levels and test methods to minimize these problems. EMI occurs, if the received amount of energy is strong enough, to cause the receptor to behave in erratic way. Electromagnetic energy can be transferred via different coupling modes:

- Radiated coupling (electromagnetic field)
- Inductive coupling (magnetic field)
- Capacitive coupling (electric field)
- Conductive coupling (electric current)

Figure 1 presents such system with emitter, coupling path and receiver. The sensitivity to electromagnetic interference of the receiver is also quite important.

Therefore the first step to reduce the amount of transferred electromagnetic energy would be to suppress the emis-

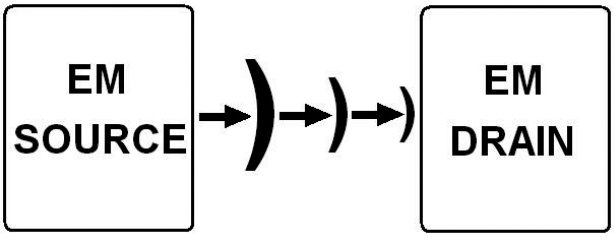

Fig. 1: EMC radiated coupling path with emitter and receiver

sion at its source. Further improvement of the problem, is to make the coupling path as inefficient as possible and the next step is, to make the receptor less susceptible to EMC. Minimizing the cost factor of the selected solution is also quite important. For example, to shield low cost systems with simple and effective conductive enclosure is usually too expensive.

EMC Directive in general is that electrical devices shall be so designed and manufactured, having regard to the state of the art and as to ensure that the electromagnetic disturbance generated does not exceed the level above which radio and telecommunications equipment or any other equipment cannot operate as intended and it has a level of immunity to the electromagnetic disturbance to be expected in its intended use which allows it to operate without unacceptable degradation of its intended use.

The European Union's harmonized EMC Standards provide guidelines and limits for testing and include descriptions of test layout and methods, as well as defined maximum permissible limits of electro-magnetic emission and immunity levels.

2 Methods for better EMC compatibility of the integrated circuits

When designing an application specific integrated circuit (ASIC), we must consider several aspects of EMC. The most common trouble spots are EMI influence on power supply lines and input connections. Here we treat digital and analog input pins differently. Output emissions can be most efficiently suppressed by pulse shaping.

2.1 EMC and power supply lines

Power supply usually delivers to an integrated circuit some kind of AC signal, superimposed on the DC power line. Such AC signals can reach up to 100Vpp. Influence on power supply is presented on Figure 2. It is needless to say, how the difference in power supply for 1 or 2 volts affects modern low power and low voltage microelectronic systems.

The solution here is to properly increase the decoupling on the Vdd. High frequencies and transient currents can flow through a capacitor, in this case in preference to the

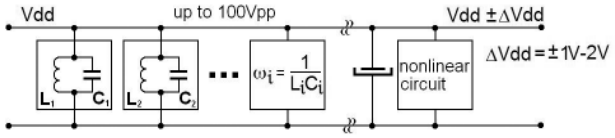

Fig. 2: EMC and power supply lines

harder path through the decoupled circuit, but DC cannot go through the capacitor, so continues on to the decoupled circuit. Some additional LC filters on power supply lines are also helpful. The best way to avoid this problem is to design the ASIC in a way that minimizes the influence of alterations in power supply voltage. In other words, we must guarantee by design as high as possible power supply rejection ratio (PSRR) at high frequencies.

2.2 EMI influence on digital input pins and solution

Figure 3 presents similar situation on digital input pin. Electromagnetic interference can easily generate additional ones and zeroes. Beside digital communication protocol automatic error correction, the solution of the problem is presented on figure 4. Each digital input pin should have some protective structures that will rectify at much higher voltages. For example, this solution is typical for automotive IC market.

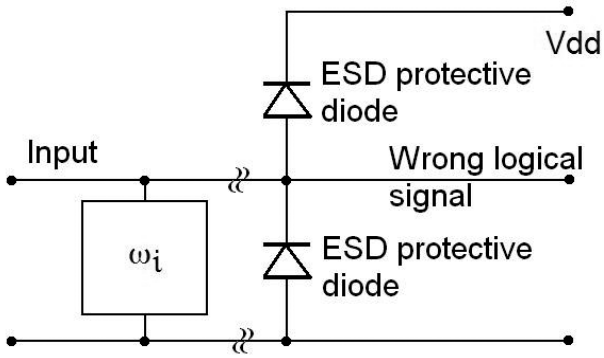

Fig. 3: EMI influence on digital input pin and solution

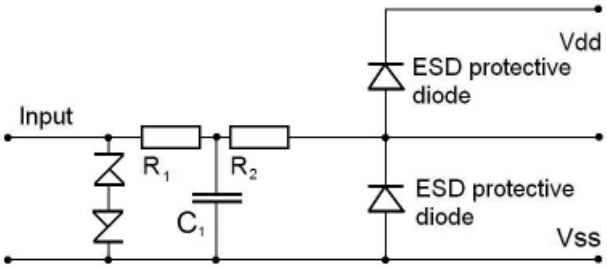

Fig. 4: Solution of EMI influence on digital input pin

2.3 EMI influence on analog input pins and solution

The biggest problems for EMC are analog input pins. If possible, the problem should be solved by an external LC

filter. Figure 5 presents the solution for analog input pins. The protective structure is quite similar to that for the digital input pins. The difference is that here the integrated filter consist from LC and RC part.

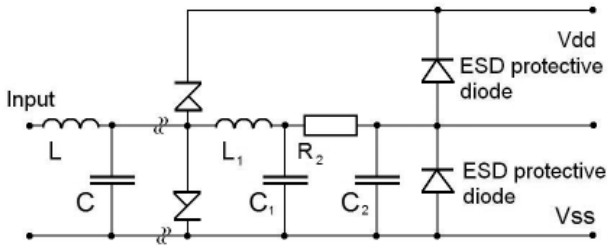

Fig. 5: EMI influence on analog input pins and solution

2.4 Methods to decrease electromagnetic emissions

The straight edge of the digital pulse (if perfectly vertical = zero rise time) represents a sinewave of almost infinitely high frequency. The faster the digital signal gets, wider is the slot of the frequency spectrum it occupies. Unfortunately such digital signals will radiate and cause interference in pretty much the same way, as may some intentional analog wave transmitters. The solution is presented on figure 6. By increasing the rise and fall time, such emissions can be drastically improved. It is also a good idea to keep the clock frequency as low as possible and rather to use some parallelism for speeding up the circuit.

$$t_r = t_f = \frac{C \cdot Vdd}{I_s} \quad (1)$$

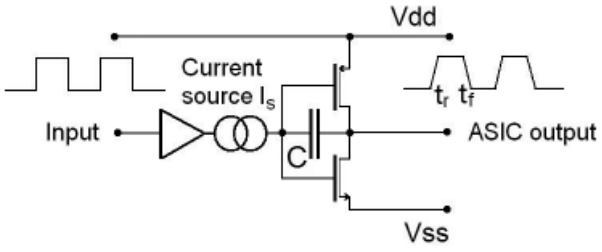

Fig. 6: Decreasing EMI with signal shaping

Another method to decrease the influence of the electromagnetic emission is in proper partitioning and positioning of the integrated circuit components. The topology of the ASIC and of the corresponding printed circuit environment should consider some of the following rules:

- Reduce the serial inductance to avoid resonance (package)
- Place Vdd and Vss supply as close as possible (use Vdd and Vss pad pairs)
- Use a grid of power supply network on chip
- Decoupling capacitance should be used for each active part of the circuit
- Identify and isolate noisy blocks – use separate supplies

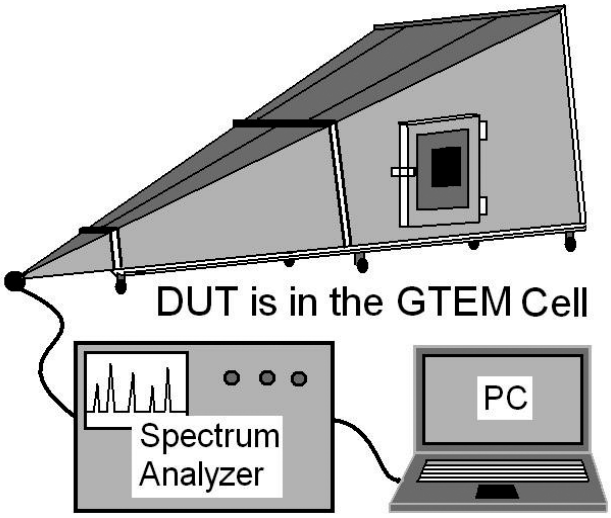

Fig. 7: GTEM cell with typical RF emissions test setup

- High frequency interconnections should be as short as possible
- Very sensitive analog or digital lines should be short
- Sensitive interconnections should be shielded – with ground wires or other layers if possible
- It is better to use two capacitors than one with the same nominal value
- High frequency interconnections should be away from the input and output structures

2.5 Measuring methods

Almost all EMC measuring methods require some generation of low and high frequency, high density electromagnetic field. Some tests require immunity of up to 300V/m. Testing should be done in an environment that allows measurements without disruption from external environment. For both, electromagnetic emission and immunity debugging purpose it is quite important to have a reflection and radio frequency free area for proper accommodating our device under test (DUT).

For small components there are several EMC compliance test cells with field strength sensor available on the market. They are basically divided in TEM (Transverse Electro Magnetic) and GTEM (Gigahertz Transverse Electro Magnetic) cells.

TEM cell is a small enclosure, to be used in normal laboratory environment for emission and immunity analysis. They are relatively inexpensive and do not require a high power amplifier; the drawback is that they can not operate at very low frequencies. By increasing its size, the lower frequency limit can be extended.

GTEM cell is larger. The tapered point and anechoic absorbers at the larger side of the pyramid shape, allow GTEM cell to operate well into the gigahertz range. Figure 7 presents GTEM cell with typical RF emissions test setup and figure 8 presents GTEM cell with typical RF immunity

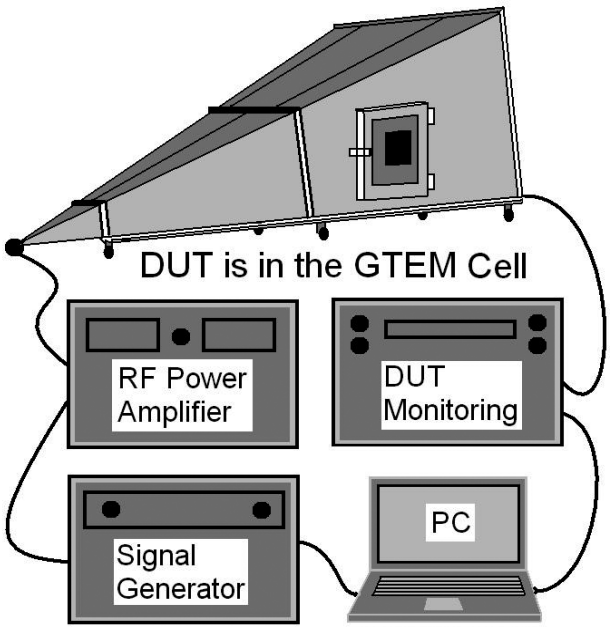

Fig. 8: GTEM cell with typical RF immunity test setup

test setup. A small, from 30W to 100W power amplifier with bandwidth from approximately 100 MHz to 1GHz will do the basic job. It boosts the spot frequency signals to achieve the required field strength. Tested device is exposed to each field for a fixed amount of time. Operation within specifications is checked and procedure is repeated for another, different DUT orientation within the test cell.

For emission compliance, the equivalence between testing in GTEM cell and testing in open area test site (OATS) has been formerly endorsed. On the other hand, the RF immunity testing in GTEM cell can be more or less used only as a pre-compliance verification. Final RF immunity verification should be done in an anechoic chamber. Better is the pre-compliance verification, shorter is the time in expensive anechoic chamber.

Alternatively, the radiated immunity can also be tested in somehow cheaper reverberation chambers. Entire truck or bus can be proofed for EMC in such chambers. They usually have a rotating tuner on the ceiling. Technically they are like a big microwave oven. RF energy is injected into a corner of the chamber and allowed to reflect off the walls, ceiling, floor and rotating tuner. At each reflection the wave loses a little of its magnitude. Consequently the reflected waves arrive at our measuring point inside the chamber with different magnitudes. The revolving tuner also changes the path lengths and the number of reflections of the waves. From few Hz to several GHz can be generated. The larger are the dimensions of the reverberation chamber the lower is the chamber's minimum operating frequency. The maximum useable frequency seems to be related only to the maximum power available to drive the chamber. Figure 9 presents such chamber.

However, measuring a field in a reverberation chamber looks more like measuring a noise and it doesn't give the

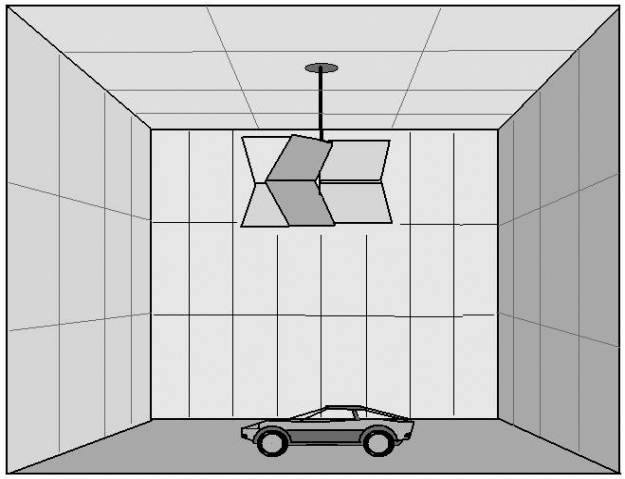

Fig. 9: Reverberation chamber with tuner on the ceiling

operator any information about the direction and polarization. In the reverberation chamber we can measure only the total radiated power and not the electric field at a specified distance, as required by most test standards.

The full compliance EMC testing can be usually done in anechoic chambers. The materials used on the walls and ceiling of an anechoic chamber are such that there is a little, or no reflection of electromagnetic waves. This is accomplished by the geometry and the absorptive nature of these materials. They usually have a rotating platform for DUT. Such anechoic chambers are quite expensive and EMC measurements may take a considerable amount of time. So it is a good idea, to do some pre-compliance EMC measurements with ordinary laboratory equipment, when it is possible.

3 Examples of EMC measurements and solutions

3.1 Example of pre-compliance testing for EMC of automotive airbag sensor

Sensor for automotive airbag was developed in Laboratory of Microelectronics at University of Ljubljana. As guideline for measurements we used EMC standard MIL-STD-461E (5.18.4 RS 101 alt. test procedure AC Helmholtz coil). Sensor was measured in magnetic field that was generated by two opposite coils. Sensor was rotated in six different positions. Two such positions with the coils for the magnetic field generation are presented on figure 10. Frequency was varied from 50Hz to 10 kHz. Sensor passed the later EMC measurements successfully.

3.2 EMC solution for automotive steering wheel sensor

Automotive steering wheel sensor was also developed in Laboratory of Microelectronics at University of Ljubljana. The principle of sensor operation is to determine the automotive steering wheel position on the maximum interfer-

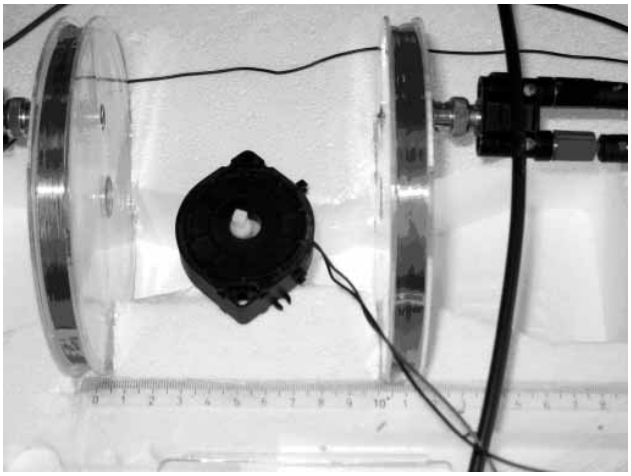

a

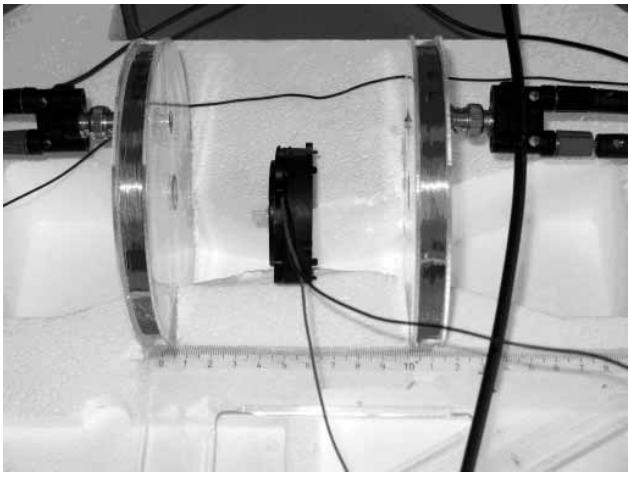

b

Fig. 10: Example of different sensor positions while doing pre-compliance measurements of automotive airbag sensor for EMC

ence basis. The EMC problem here was that sensor was very susceptible to electromagnetic interference. Employment of shielding for the entire sensor did not satisfy the EMC, as well as extensive blocking of input and output pins. The problem was solved by modifying the sensor in a way, that sensor actually detects, when the electromagnetic interference happens on its momentarily operating frequency. Then it automatically switches to another frequency and continues an undisturbed operation. Figure 11 presents such disassembled, steering wheel sensor.

4 Conclusions

The situation about EMC is getting worse, since we are using more and more wireless electrical equipment. That equipment operates at higher and higher frequencies and data rates. For example, the basic clock frequency of the common personal computer nowadays is higher than the transmission frequency used by cellular phones. Scaling down the integrated circuits and decreasing operating voltages to reduce power consumption makes modern elec-

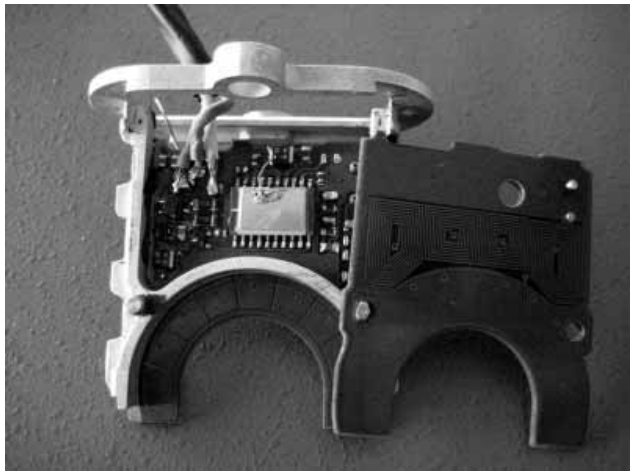

Fig. 11: Automotive steering wheel sensor with capability of switching operating frequencies to avoid EMI

tronic much more vulnerable to interference. Lower is the supply voltage, less tolerance we have for transients. And not at least, more and more digital transmission signals are cleverly packaged to fit as many separate channels as possible in the available spectrum. Such signals are usually hopelessly complicated mesh of the fundamental frequency, a load of harmonics, switching transients, sidebands and music from the local radio transmitter. Beside that, also heavy equipment is drawing large currents and strong electrical motors in particular, may cause transients that can propagate very far over the power supply network. Fortunately all kind of modern data communications protocols include at least some type of error checking and correction. Few lost bits in home DVD player may not cause a serious problem, yet few lost bits in medical or military equipment may be catastrophic.

The problem is also with standards compliance. It is often left up to the manufacturer to choose the most appropriate standard and the selected one may not be the most stringent one available, to match the electromagnetic environment of the product. So, like every other aspect of EMC, the standards compliance is no guarantee that the product will actually work in all circumstances. Therefore we may say in the end, that we have some good design guidelines, but there is no way of knowing exactly what will happen in real life of the product. However, it is possible in theory to design the product that will not make or accept any interference from other products, but it will be bulky, expensive and hard to sell. On the other hand, if we design cheap and for electromagnetic interferences sensitive electronic devices, nobody would buy them either. So designing for electromagnetic compatibility may be extremely convoluted, unpredictable and difficult business, and above all, it is always a subject of compromise. Furthermore always keep in mind that a user, manufacturer or even a provider of electrical device that caused material loses or any other harm to a third party due to electromagnetic compatibility, may be prosecuted.

5 References

/1/ C. R. Paul, Introduction to Electromagnetic Compatibility, John Wiley & Sons Inc., New Jersey, 2006, ISBN-10:0-471-75500-1.

/2/ M. I. Montrose, E. M. Nakauchi, Testing for EMC Compliance, John Wiley & Sons Inc., New Jersey, 2004, ISBN 0-471-43308-X

/3/ S. B. Dhia, M. Ramdani, E. Sicard, Electromagnetic Compatibility of Integrated Circuits, Springer US, 2006, ISBN 978-0-387-26600-8.

Dr. Janez Trontelj jr.
University of Ljubljana, Faculty of Electrical Engineering
Laboratory of Microelectronics
Tržaška 25, SI-1000 Ljubljana, Slovenia
Tel.: +386(0)14768471
e-mail: janez.trontelj-jr@fe.uni-lj.si

Prispelo (Arrived): 26.06.2008 *Sprejeto (Accepted): 15.09.2008*

A MICRO-BOLOMETER FOR FAR INFRARED (FIR) APPLICATIONS BASED ON BORON DOPED POLYCRYSTALLINE SILICONE LAYERS

Radko Osredkar[1], Marijan Maček[2]

[1]University of Ljubljana, Faculty of Computer and Information Science, Ljubljana, Slovenia
[2]University of Ljubljana, Faculty of Electrical Engineering, Ljubljana, Slovenia

Key words: bolometer, FIR, thin films, doped poly Si, noise, micro electronic technologies

Abstract: Sources if noise in moderately doped (n_d = 10^{18} 10^{20} cm^{-3}, r = 0.002 – 1 Wcm) *p*–type (boron doped) poly Si resistors, used as a bolometer sensing element, at low frequencies are analysed. We demonstrate that the *1/f* noise in such resistors is well described by the Hooge relationship, and that parameter a_H is linearly proportional to the energy barrier height E_b. The noise generated in the contact areas of the *p*type resistors does not contribute significantly to the overall noise of the device. The test bolometer chip characteristics, developed at our laboratory specifically for evaluating the resistor film performance, closely follow the theoretical predictions of the accepted theory, making the design and fabrication of a usefull FIR detector possible.

Mikro bolometer namenjen uporabi v daljnem IR območju, zgrajen na osnovi tanke, polikristaline silicijeve plasti dopirane z borom

Kjučne besede: bolometer, tanke plasti, popirani polisilicij, šum, mikroelektronske tehnologije

Izvleček: V prispevku analiziramo izvore šuma pri nizkih frekvencah v zmerno dopiranem z borom (n_d = 10^{18} – 10^{20} cm^{-3}, r = 0.002 – 1 Wcm) polisilicijevem uporniku tipa *p*, ki je uporabljen kot seznorski element v bolometru. Pokažemo, da šum *1/f* v takšnih upornikih dobro opisuje Hoogeova enačba, da je parameter a_H v njej linearno odvisen od veliksto energijske bariere E_b med zrni polisilicija. Šum kontaktv upornikov tipa p ne prispeva znatno k skupnemu šumu celotne bolometrske naprave. Lastnosti testnega bolomotra na silicijevi tableti, ki smo ga v laboratoriju razvili posebej z namenom okarakterizirati lastnosti uporovne plasti, dobro opisuje veljavna teorija, kar nam omogoča načrtati in izdelati uporaben detektor za EM valovanja v daljnem IR območju.

1. Introduction

Due to the small photon energies photonic detector are unsuitable for detection of electromagnetic (EM) radiation with wavelengths longer than 12 ěm and therefore can not be used for detection of far infrared (FIR) and terahertz (0.1 to 10 THz, i.e. wavelengths between 10 ěm to several millimeters) waves. But in this range of the EM spectrum heat detectors are available, offering several advantages: their response is in principle not dependent on the wavelength of the incoming radiation, and are relatively simple to use and maintain as they do not require cooling to low temperatures, if temperature resolution of the order of ~0.1 $K \cdot Hz^{-1/2}$ is sought. Such detectors have often been used for remote temperature measurements and in different motion sensors, however, advances in materials science and micromachining technologies have made fabrication of arrays of heat detectors possible that are used in thermo vision systems /1, 2/. All heat detectors absorb IR radiation and consequently their temperature rises. This temperature change is converted by the detector to a change of the output signal /2/ via a change of resistance of the device (e.g. in metal, semiconductor, or ferroelectric bolometers), a change in thermo-voltage, pressure (e.g. Golay cell), pyroelectric effect, etc. In this paper we present a study of the sensing materials for a bolometric type of heat detector, together with an example of the detector.

2. Bolometer parameters

The bolometric principle and several devices based on it have been studied in detail /3, 4/. The basic parameter of a bolometric device is its sensitivity (*S*). It is a function of the temperature coefficient TC of the device, its heat conductivity *G*, heat capacity *C*, and the time constant $\hat{o} = C/G$. Under the influence of the incident EM radiation of frequency $\hat{u}$ and intensity P_o, the sensitivity of the bolometer is given by

$$S = \frac{V_s}{P_0} \approx \frac{TC \cdot V_d}{G\left(1+(\omega\tau)^2\right)^{1/2}} \qquad (1)$$

For a large response of the device to the incident EM radiation thus a material with as large as possible *TC*, and as low as possible heat conductivity *G* is needed. These may be conflicting requirements as the TC is determined by the materials used, and G, on the other hand, is basically determined by the fabrication technology employed. Its val-

ue can be lowered if the sensing element of the device is positioned in vacuum, whereby the heat losses are minimized. From (1) it would appear that the sensitivity could be conveniently increased by increasing the voltage drop V_s over the bolometer sensor, however, the signal voltage to noise voltage ratio of the bolometer must be also be considered.

Generally, there are three sources of voltage noise present in all types of resistors: the Johnson noise V_J , caused by the thermal motion of the charges in the sensing element, noise due to temperature fluctuations (the so called phonon noise), and the $1/f$ noise, due to recombination – generation effects in semiconductors and/or effects on grain boundaries /5/. The first two types of noise are frequency independent (white noise) and also independent of the current through the resistor, but not the $1/f$ noise. At low frequencies or/and high applied currents the $1/f$ noise becomes predominant. The Johnson noise is a white noise with a constant spectral distribution S over the entire frequency range. It is described by the well known equation

$$S_j = 4kTR \tag{2}$$

where k is the Boltzmann constant, 1.38 10^{-23} J/K. The spectral density of phonon noise is given /1/ by the equation

$$S_T^{1/2} = I(TC) \cdot R \cdot \sqrt{\frac{kT^2}{G}} \tag{3}$$

and is linear with respect to the current through the bolometer structure. If the heat conductance G of the device is sufficiently small (below 0.1 mW/K), the phonon noise of the device approaches the Johnson noise. A much more serious source of noise in bolometers is the $1/f$ noise as the devices usually operate at frequencies of several 10 Hz and a relatively high voltage over the device. This contribution to the noise is described by the Hooge semi-empirical equation

$$\frac{S_H}{V^2} = \alpha_H \frac{1}{f \cdot N} \tag{4}$$

where $\acute{a}_H$ is the Hooge constant, f the frequency and N the number of charge carriers. The total noise spectral density (energy) is the sum of all 3 contributions,

$$S_n = S_j + S_T + S_H \tag{5}$$

The measured noise V_n is therefore the integral of spectral density S_n over the frequency range of interest

3. Experimental: polycrystalline silicone film properties

In designing a bolometric device with a polycrystalline silicon (poly Si) resistor the properties of the resistor film should be understood in extensive detail. Poly Si has been used in semiconductor manufacturing for decades as material for transistor gates, resistors, capacitors, etc. Due to its well established technology, and its electrical and mechanical properties it is also a very attractive material for a wide range of micro–machined devices and sensors. Unfortunately, there is a serious draw back in poly Si properties, if used in a bolometric device: its *1/f* noise /6, 7/ is large. Excessive *1/f* noise can seriously degrade sensor properties, especially in case of bolometers, where heating and sensing are combined in the same material. For instance, detectivity of bolometers fabricated on *n*-doped poly Si, as reported in /8, 9/, was by an order of magnitude lower than expected.

Poly Si films in this study were deposited on the top of an oxidized (50 nm) 100 mm Si wafers. The poly Si deposition was performed in a commercial LPCVD reactor by the decomposition of SiH_4 at the standard conditions, T = 625°C, p = 350 mtorr. Doping of 0.38 mm and 1.0 mm thick films was performed by ion implantation of boron (D_{ii} = $3 \cdot 10^{14}$ – $5 \cdot 10^{15}$ cm^{-2}, E = 40 keV). After poly Si patterning (two resistors geometries: 375 · 75 mm^2, and 375 · 5 mm^2) wafers underwent process steps typical for the standard CMOS processing with 2 mm minimal geometry, including annealing at 920°C and a 1000°C reflow. The final step was alloying in the forming gas at 420°C. The noise measurements were performed according to the technique described in ref. /10/, using a low noise spectrum analyzer HP 3585A.

It is known that the energy barrier between small Si grains in the poly Si film is a function of dopant concentration. As a first approximation the dopant concentration n_d is proportional to the ratio of the dose to the poly Si film thickness. In Fig. 1 we demonstrate that the energy barrier (E_b) in boron doped (*p*type) poly Si is proportional to $n_d^{-0.59}$ while in phosphorous doped (*n*type) the E_b µ $n_d^{-0.85}$. According to ref. /8/ the power of the concentrations above the critical concentration, ~$5x10^{17}$ cm^{-3}, should be be-

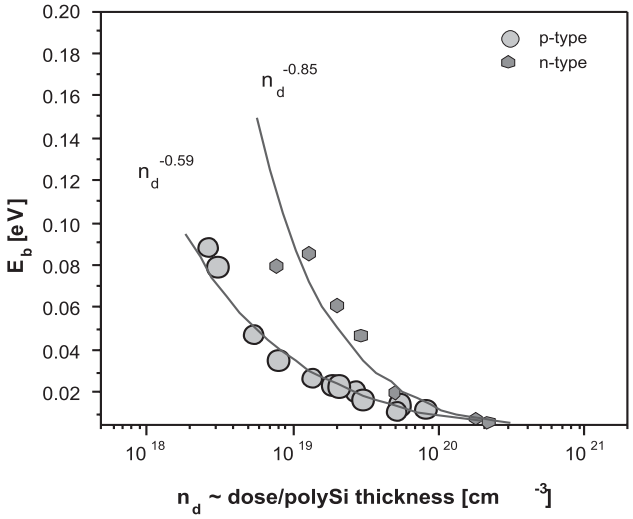

Fig. 1: FigEbConc:: Energy barrier height E_b *as a function of doping for* p– *and* n–*type poly Si. Concentration of dopant is defined as:* n_d *H" Dose/poly thickness.*

tween −0.85 and −1. Our measured values for the E_b of *p*−type correspond to the values given in /8/. On the other hand, the relationship between the resistivity *r* and the barrier E_b shows the same relationship for both types of poly Si.

The noise measured in a poly Si resistor, as described above, is the sum of the thermal and Johnson noise, *1/f* noise, and the noise of the measuring system. Spectral density $S_{1/f}$ of the noise is proportional to the square of the applied bias voltage or current I_o flowing trough the resistor. This relationship is demonstrated in Fig. 2, where the $S_V^{1/2}$ vs. I_o is plotted for convenience. For the particular resistor (n_d ~ $3\cdot10^{18}$ cm^{-3}, *R* = 29.2 *kW,* ?? *f* = 75 Hz) the power of the current was 2.02, which is close to theoretical value /7/. This indicates that the noise is mainly generated in the depletion barrier region of poly Si. If the noise were generated in the grain bulk region the relationship would involve a higher power of I_o.

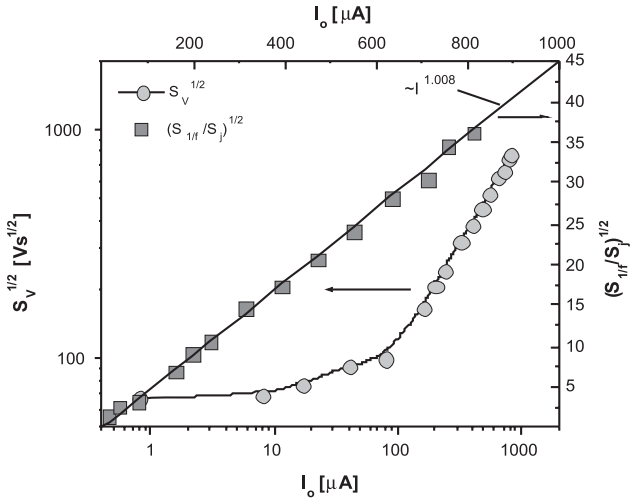

Fig. 2: Measured noise spectral density S_v *and its* $S_{1/f}$ *component at* f *= 75 Hz as a function of the current flowing trough the resistor with* R *= 29.2 kW*

According to the theory the noise spectral density $S_{1/f}$ is inversely proportional to the frequency, $S_{1/f}$ μ f^{-1}. This is demonstrated in Fig. 3, where the frequency dependence of the same resistor as in Fig. 2 is plotted. The measured $S_{1/f}$ is proportional to $f^{-1.09}$, which is reasonably close to the theoretical value and published experimental data /10/: for *p*type resistors the reported values are −1 and −0.85 for *p* and *n*type poly Si respectively. Indeed, we have measured values about −0.9 for n−type poly Si bolometers /9/.

The dependence of the measured *1/f* noise on the current and frequency confirms the accepted notion that the noise is generated within the depletion barrier region of poly Si and not in the bulk of the grain. Data for thin 0.38 mm and thick 1 mm layers demonstrate that the noise is also independent of the geometry, and is influenced by the carrier number only. The main difference between the *p* and *n*type materials is the different energy barriers. Gen-

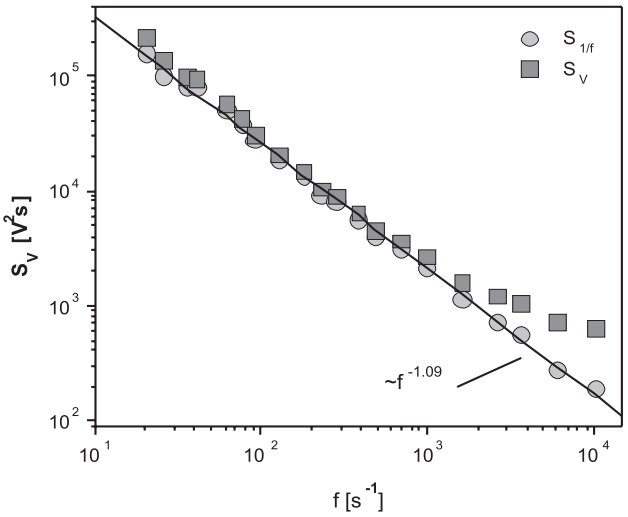

Fig. 3: Measured noise spectral density S_v *and* $S_{1/f}$ *component as a function of the frequency for the same resistor as in Fig. at* I_o *= 200 mA.*

erally, the energy barrier in *n*type semiconductor is higher than in the *p*type for the same doping. And the same is valid for poly Si at low and medium doping levels (<10^{20} cm^{-3}), as indicated by our previous work /11/. Therefore the *1/f* noise is much more pronounced in *n*type material, unless the doping is so high that the segregation of the dopant on the grain boundaries occurs.

For illustration, the specific resistively *ń* of the poly Si film as function of the dopant concentration is shown in Fig. 4.

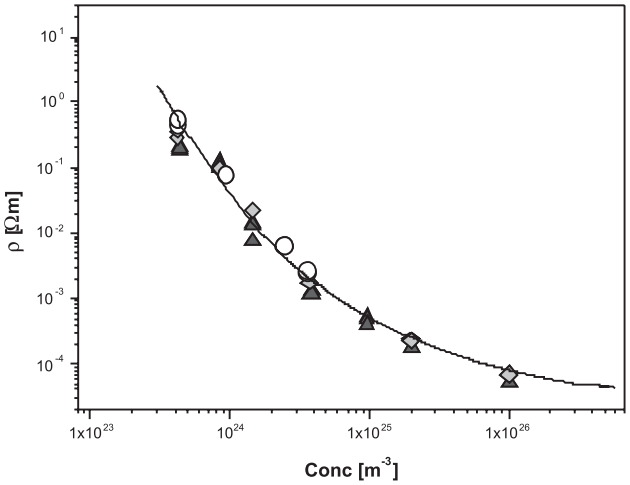

Fig. 4: The dependence of the specific resistivity of the poly Si layer on the the boron concentration, C = D_{ii}/deb$_{Si}$−C_{out}. *During the heat treatment, approximately* $6\cdot10^{23}$ m^3 *boron is lost. (% samples run # 1, f& sample run #2, % bolometer test chip, solid line − theory)*

For the bolometer applications significant Hooge parameter $á_H$, which controls the *1/f* noise of the poly Si, can now be conveniently presented as a function of the specific resistivity of the boron doped poly Si film (Fig. 5).

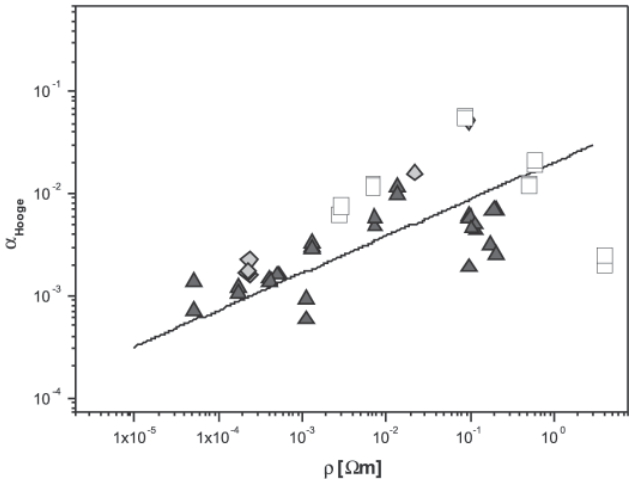

Fig. 5: The dependence of the Hooge parameter á$_H$ *on the specific resistivity of the boron doped poly Si layer (% samples run # 1, f& sample run #2, % bolometer test chip, solid line – theory).*

In step with the dopant concentration, the TC of the film is also changing with its specific resistance. The flow of the current through the film is associated with the tunneling of the charge carriers through the grain boundaries, where, *ń ~ exp(qE$_b$/kT)*, and *E$_b$* is the height of the barrier. In Fig. 6 the dependence of the TC, measured at 25 °C, is shown as a function of the specific resistivity of the boron doped polysilicon.

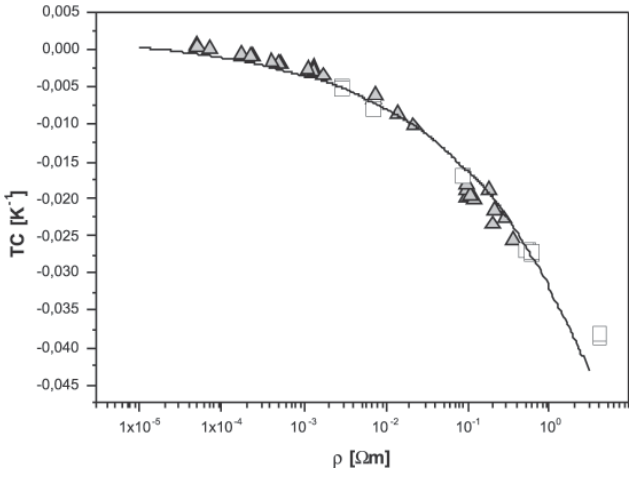

Fig. 6: The dependence of the TC *on the specific resistivity of the boron doped poly Si layer. (% samples run # 1 at 25 °C, % bolometer test chip, solid line – theory)*

Our measurements on contact chains indicate that the noise in the contact area to the *n*–type poly Si is extremely sensitive to the doping ($S_{1/f}$ µ n_d^{-4}) but not in the *p*–type ($\propto n_d^{-0.8}$). This indicates that medium and high resistivity *p*type resistors can be fabricated without additional doping of the contacts, contrary to the *n*type poly Si, where the contacts should be doped above $2 \cdot 10^{20}$ cm^{-3} which is typically done from a $POCl_3$ source.

4. Absorption of the EM radiation by the bolometer

An important consideration in evaluating a bolometer resistor performance is the absorption of the EM radiation by the active surface of the device. In the FIR domain a satisfactory absorptivity of the bolometer surface can be achieved by covering it with passivation films which are standard in the microelectronic fabrication technologies. Such an absorption film is formed by a LPCVD deposited PSG (refractive index n = 1.46) film, and a mixed SiON (n ~ 1.75) and SiN (n ~ 2) film, deposited by the PECVD method /12/. At longer incident radiation wavelengths a different approach is indicated, combining dielectric films with conducting films. The calculated absorption coefficients for PECVD SiON films of different thicknesses are shown in Fig. 7. Absorption at even higher wave lengths can be achived (up to 35 mm for PECVD a-Si with n=3.4) by increasing the index of refraction.

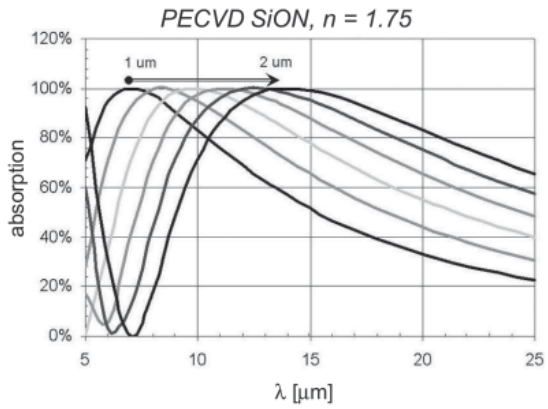

Fig. 7: The absorption of the bolometer surface as a function of the incident EM radiation wavelength at sheet resistance Z$_o$ *= 377 Ů/ square for PECV SiON,* n *= 1.75, for 1 ěm to 2 ěm film thicknesses (in increments of 0.2 ěm).*

5. Bolometer fabrication

In the test bolometer fabrication, designed to analyze the poly Si films performance, special care was taken to consider only fabrication steps that are compatible with a standard CMOS technology with 2(3) layers of the poly Si. The fabricated test IC is shown on Fig. 8. The test chip enabled us to characterize the poly Si properties as described above.

6. Conclusion

Noise in moderately doped (n_d = $10^{18}10^{20}$ cm^{-3}, *r* = 0.002 – 1 Wcm) *p*–type (boron doped) poly Si resistors at low frequencies is dominated by *1/f* noise. Its spectral density $S_{1/f}$ is proportional to the square of the current flowing through the resistor, and we conclude that the *1/f* noise is generated within the depletion barrier region, not in the

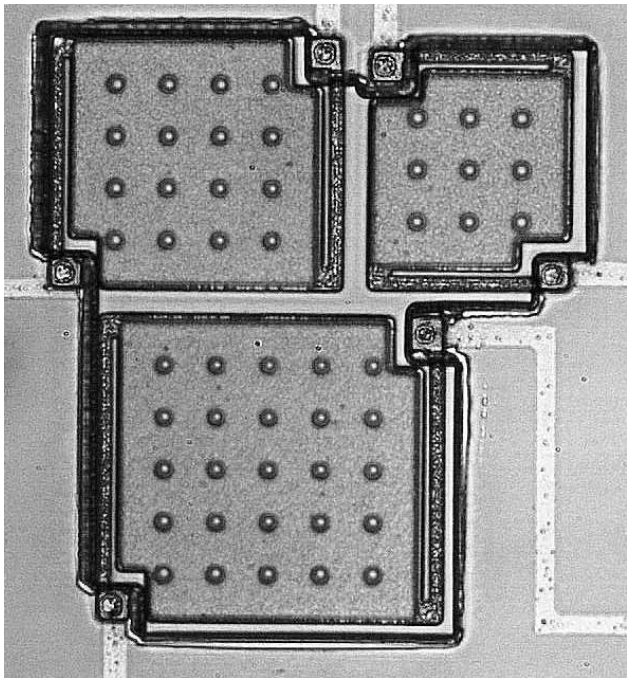

Fig. 8: The test bolometer device, comprising of three, 40·40, 50·50, and 70·70 ěm^2 bolometers. The resistor is supported by 2 ěm wide supports; the holes in the detector areas enable consistent under-etching of the structure during fabrication.

bulk of grains or in the contact areas. Spectral density $S_{1/f}$ is also inversely proportional to the frequency, and frequency dependent noise is well described by the Hooge relationship. Parameter a_H is linearly proportional to the energy barrier height E_b which itself is proportional to the doping, $E_b \mu n_d^{-0.59}$. Its values are from 10^{-2} to 310^{-3} for doping levels 10^{18} to 10^{20} cm^{-3}. Measured values for a_H are similar to the reported values for *p*–type boron doped poly SiGe /13/ and lower than reported for the *n*–type poly Si /7, 10/. The noise generated in the contact areas of *p*type resistors does not contribute significantly to the overall noise of the resistors. Therefore there is no need for additional doping of the contacts. The test bolometer chip characteristics, developed at our laboratory specifically for evaluating the resistor film performance, closely follow the theoretical predictions of the accepted theory, thus assuring us that the design and fabrication of a usefull FIR detector is within our reach.

7. Acknowledgement

This work was supported by the Ministry of Education, Science and Sports of the Republic of Slovenia.

8. References

/1/ P.W. Kruse, Design of Uncooled Infrared Imaging Arrays, SPIE 2746 Infrared Detectors and Focal Plane Arrays IX, Orlando, FL. April 1996

/2/ P.W. Kruse, Uncooled IR Focal Plane Arrays, AeroSense 1996, Los Angeles 10.Apr.1998

/3/ M. Maček, Inf. MIDEM, 1998, **86**, pp. 77-89 (1998)

/4/ P.L. Richards, J. Appl. Phys, **76** (1), 1994, pp. 1-24

/5/ F.N.Hooge, T.G.M. Kleinpenning, L.K.J. Vandamme, Rep.Prog.Phys, 44, 479(1981)

/6/ H.C. de Graff, M.T.M. Huybers, J.Appl.Phys, **54**, pp. 2504-2507, (1983)

/7/ M.Y. Luo, G. Bosman, IEEE Trans.Electro Devices, **3**7, pp. 768–774 (1990)

/8/ J.Y.W. Seto, J.Appl.Phys, **46**, 5247–5254 (1975)

/9/ M. Maček, Inf. MIDEM, 1998, **86**, pp. 77-89 (1998)

/10/ M.J. Dean, S. Rumyantsev, J. Orchard-Webb, J.Vac.Sci.Tecnol.B, **16**, pp.1881–1884(1998)

/11/ M. Maček, 40th International Conference on Microelectronics, September 29. – October 01. 2004, Maribor, Slovenia. Proceedings. MIDEM - Society for Microelectronics, Electronic Components and Materials, 2004, str. 81-85

/12/ M. Maček, Inf. MIDEM, 1998, let. 28, **86**, pp. 81-89

/13/ X.Y. Chen, C. Salm, Appl. Phys. Lett. **75**, pp. 516–518

Radko Osredkar
University of Ljubljana, Faculty of Computer and Information Science
Tržaška 25, 1000 Ljubljana, Slovenia
Tel:01/4768-358; Email: radko.osredkar@fri.uni-lj.si

Marijan Maček
University of Ljubljana, Faculty of Electrical Engineering
Tržaška 25, 1000 Ljubljana, Slovenia
Tel:01/4768-473; Email: marijan.macek@fe.uni-lj.si

Prispelo (Arrived): 08.05.2008 Sprejeto (Accepted): 15.09.2008

TEMPERATURE BEHAVIOUR OF CAPACITIVE PRESSURE SENSOR FABRICATED WITH LTCC TECHNOLOGY

Darko Belavič, Marina Santo Zarnik, Marko Hrovat*,
Srečko Maček*, Marija Kosec*

HIPOT-RR d.o.o., 8310 Šentjernej, Slovenia
*Jožef Stefan Institute, 1000 Ljubljana, Slovenia

Key words: sensor, pressure sensor, capacitive pressure sensor, thick-film technology, temperature behaviour

Abstract: This work is focused on capacitive pressure sensors designed as ceramic capsules, made with low-temperature cofired ceramic (LTCC), consisting of a circular edge-clamped deformable diaphragm that is bonded to a rigid ring and the base substrate. This construction forms the cavity of the pressure sensor. The diaphragm, with a diameter of 9.0 mm has a thickness of 200 ěm, and the depth of the cavity is from about 70 µm. The principle of capacitive pressure sensor is based on changes of the capacitance values between two electrodes. One thick-film electrode is deposited on the diaphragm and the other on the rigid substrate. The distance between electrodes and the area of electrodes define the initial capacitance of the capacitive pressure sensor, which is around 10 pF. The distance between electrodes and together with the geometry and flexibility of the diaphragm define the sensitivity of the sensor, which is about 4 fF/kPa. We investigated the temperature dependence of the sensors' characteristics of capacitive thick-film pressure sensors. The sensor is based on changes the capacitance values between two electrodes: one electrode is fixed and the other is movable. The displacement of the movable electrode depends on the applied pressure. The main influence on the temperature dependence of the sensor characteristics is from the temperature coefficient of the elasticity and sensor's geometry, while the temperature coefficient of the Poisson's ratio and the temperature expansion coefficient have only a minor effect.

Temperaturne lastnosti kapacitivnega senzorja tlaka narejenega v LTCC tehnologiji

Kjučne besede: senzor, senzor tlaka, kapacitivni senzor tlaka, debeloplastna tehnologija, temperaturna odvisnost

Izvleček: V prispevku so prikazani raziskovalni rezultati na kapacitivnem senzorju tlaka narejenemu v LTCC tehnologiji. LTCC (Low Temperature Cofered Ceramic) je keramika z nizko temperaturo žganja. Ta keramika se žge pri temperaturah med 850 in 950°C. Da se pri teh razmeroma nizkih temperaturah zasintra, vsebuje precej steklene faze. LTCC tehnologija temelji na tankih keramičnih folijah, ki se jih sestavlja v večplastne strukture. Na ta način je možno zgraditi tridimenzionalno strukturo za kapacitivni senzor tlaka. Osnovo take strukture predstavlja tanka okrogla in upogljiva membrana. Rob membrane je pritrjen na obroč, ta pa na trdo (neupogljivo) podlago. Ena elektroda kondenzatorja je na membrani, druga pa na podlagi. Merjeni tlak upogne membrano, kar spremeni razdaljo med elektrodama. S tem dobimo spremembo kapacitivnosti. Senzor tlaka za tlačno področje do 100 kPa ima membrano s premerom 9,0 mm in debelino 200 mm. Pri razmaku med elektrodama okoli 70 mm je začetna kapacitivnost približno 10 pF. Razmak med elektrodama ter geometrija in fleksibilnost membrane določata občutljivost senzorja na merjeni tlak. Raziskovali smo temperaturno odvisnost karakteristik kapacitivnega senzorja tlaka. Na njo v glavnem vpliva temperaturna odvisnost modula elastičnosti LTCC materiala, delno pa tudi temperaturni razteznostni koeficient LTCC materiala ter konstrukcija in dimenzije tridimenzionalne LTCC strukture. Na temperaturno odvisnost začetne kapacitivnosti pa je znatno vplivajo zaostale mehanske napetosti v membrani in eventualna predhodna ukrivljenost membrane.

1 Introduction

Pressure is a mechanical quantity defined as the ratio of force to the surface area over which it is exerted. A complete pressure-measurement system consists of a series of components. One of them is the sensing element (a transducer) that responds to the pressure applied to it and converts the pressure into a measurable signal, which in most cases is an electrical signal. In most cases the sensing elements in pressure sensors are based on strain-gauge, capacitive, piezoelectric or optical principles to convert the physical quantity (pressure) into an electrical signal. The majority of pressure sensors on the market is based on piezoresistive principle. This is mainly due to the fact that that the piezoresistive pressure sensors are relatively sensitive to an applied pressure and their analogue output is linear in a wide pressure range while the output impedance is low. For capacitive pressure sensors the pressure sensitivity is essentially higher than that of piezoresistive pressure sensors, and the power consumption is much lower. The major disadvantages are their small sensing capacitance, high output impedance and nonlinearity of the sensors response. The small capacitance makes them highly susceptible to parasitic effects.

Most pressure sensors are made by micro-machining silicon /1,2/. On the other hand, complex sensor systems combine different materials (silicon, ceramic, metal, polymer, etc.) and technologies (semiconductor, thin and thick film, etc.). In some demanding applications thick-film technology and ceramic materials are a very useful alternative /3-6/. In many cases low-temperature cofired ceramic (LTCC) is used for the fabrication of thick-film pressure sensors. In comparison with semiconductor sensors they are larger, more robust and have a lower sensitivity, but they operate over a wider operating-temperature range /3,5/.

This contribution includes the study of sensing principle, investigated materials, and designing a capacitive pressure sensor using thick-film and LTCC materials and technology. The special attention is focused on the temperature dependence of sensor's characteristics

2 LTCC materials

The low-temperature cofired ceramic (LTCC) technology is a rapidly growing segment of the hybrid electronic-module market. The LTCC technology is a three-dimensional ceramic technology utilizing the third dimension (z) for the interconnects-layers, the electronic components, and the different three-dimensional (3D) structures, such as cantilevers, bridges, diaphragms, channels and cavities. It is a mixture of thick-film and ceramic technologies. Thick-film technology contributes the lateral and vertical electrical interconnections, and the embedded and surface passive electronic components (resistors, thermistors, inductors, capacitors). Ceramic technology contributes the electrical, mechanical and dielectric properties as well as different 3D structures /6,7/.

LTCC materials in the green state (called green tapes, before sintering) are soft, flexible, and easily handled and mechanically shaped. A large number of layers can be laminated to form high-density interconnections and three-dimensional structures. The fabrication process of LTCC structures includes several steps, which are named LTCC technology. The separate layers are the mechanical shaping of meso-size features (0.1-15 mm), and then the thick-film layers are the screen-printed. All the layers are then stacked and laminated together with hot pressing. This laminates are sintered in a one-step process (cofiring) at relatively low temperatures (850–900°C) to form a rigid monolithic ceramic multilayer circuit (module). Some thick-film materials need to be post-fired; thick-film pastes are screen-printed on the pre-fired laminate and have to be fired again. The whole LTCC process saves time, money and reduces the circuit's dimensions compared with conventional hybrid thick-film technology.

The important advantage for pressure sensors applications is the lower Young's modulus (about 100 GPa) of LTCC materials in comparison with alumina (about 340 GPa). As example Figure 1 shows the comparison of deflections of the diaphragms made with alumina and LTCC materials. The calculated deflections as a function of the distance from the diaphragm centre (r) are presented for the pressure sensors with the same dimensions at an applied pressure of 100 kPa. The diameter of the circular edge-clamped diaphragm is 9.0 mm, and the thickness is 200mm. The biggest deflection, of 8.5 µm in the middle of the circular diaphragm, was observed for the LTCC, and the lowest deflection, of 2.7 µm, was exhibited by the alumina diaphragm.

The LTCC tapes consist of ceramic and glass particles suspended in an organic binder. The materials are either

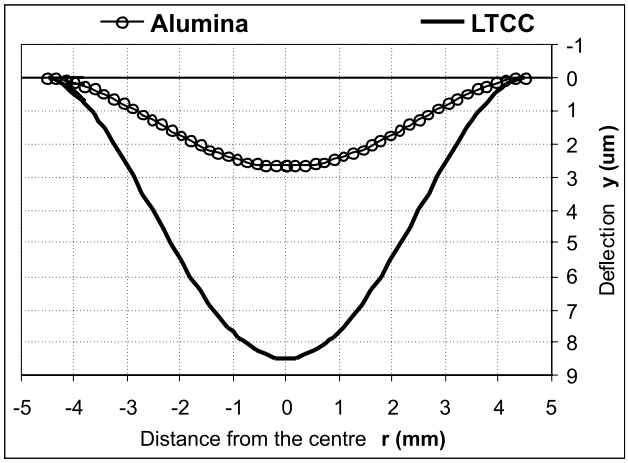

Fig.1: The calculated deflections of diaphragms made with alumina and LTCC materials at an applied pressure of 100 kPa.

based on crystallisable glass or a mixture of glass and ceramics, for example, alumina, silica or cordierite ($Mg_2Al_4Si_5O_{18}$) /8/. The composition of the inorganic phases in most LTCC tapes is similar to, or the same as, materials in thick-film multilayer dielectric pastes. To sinter to a dense and non-porous structure at these, rather low, temperatures, it has to contain some low-melting-point glass phase. This glass could presumably interact with other thick-film materials, leading to changes in the electrical characteristics /8,9/. The composition of a typical LTCC material is shown in Figure 2.

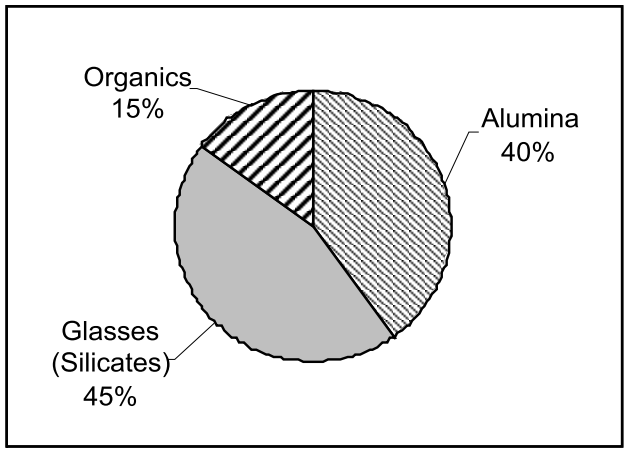

Fig.2: The composition of a typical green LTCC material (wt.%).

The disadvantages of LTCC technology as compared with an alumina are a lower thermal conductivity (about 2.5 to 4 W/mK) in comparison with alumina and the shrinking (about 10 to 15% in x/y-axis and about 10 to 45% in z-axis) of the tapes during firing. Some of the characteristics of alumina substrates and fired LTCC laminates are presented in Table 1.

Table 1: Some characteristics of LTCC material in comparison with Al_2O_3 ceramics

Characteristics	Al_2O_3 (94-99.5%)	LTCC
Thermal expansion coeffi. (10^{-6}/K)	7.6-8.3	5.8-7.0
Density (g/cm^2)	3.7-3.9	2.5-3.2
Flexural strength (MPa)	300-460	170-320
Young's modulus (GPa)	215-415	90-110
Thermal conductivity (Wm/K)	20-26	2.0-4.5
Dielectric constant	9.2-9.8	7.5-8.0
Loss tg (x10^{-3})	0.5	1.5-2.0
Resistivity (ohm.cm)	10^{12}-10^{14}	10^{12}-10^{14}
Breakdown (V/100 μm)	3000-4000	>4000

3 LTCC Structure

Most ceramic pressure sensors are made with deformable diaphragms /5/. The deformation is induced by the applied pressure and then converted into an electrical signal. LTCC technology and materials are suitable for forming a three-dimensional (3D) construction, consisting of a circular edge-clamped deformable diaphragm that is bonded to a rigid ring and a base substrate /3,6,7/. These elements form the cavity of the pressure sensor. The cross-section of ceramic pressure sensor is shown in Figures 3 and 4.

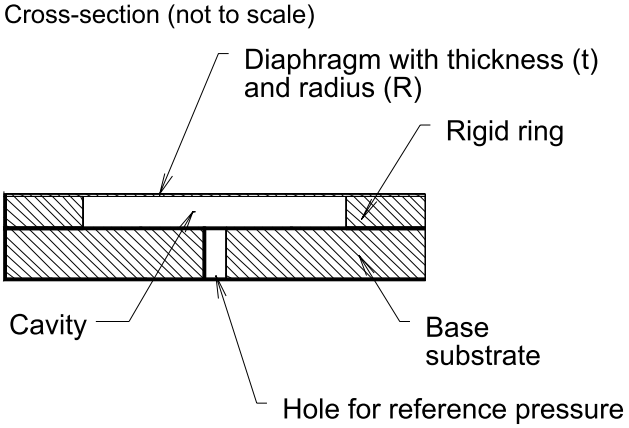

Fig.3: The schematic cross-section of the LTCC structure of a pressure sensor (not to scale).

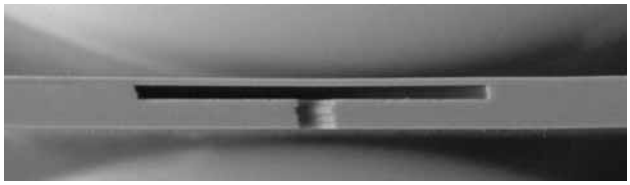

Fig.4: The cross-section of 3D LTCC structure for the pressure sensor.

4 LTCC Capacitive Pressure SENSOR

The LTCC capacitive pressure sensor is based on the fractional change in capacitance (DC/C) induced by the applied pressure. The capacitance change can be due to changes of the distance between the electrodes of the capacitor, to changes of the permittivity of the dielectric materials, or changing both. In this contribution we present the capacitive pressure sensor based on changes of the distance between the electrodes of the air capacitor.

The construction of the thick-film capacitive sensor is very similar to other thick-film pressure sensors /10-13/. The difference is that the distance between the deformable diaphragm and the rigid base substrate is smaller and must be very well defined. The bottom electrode of the capacitor is on the rigid substrate and the upper electrode is on the deformable diaphragm. Therefore, the area of the electrode and the distance between them define the value of the initial capacitance of the pressure sensor. The principle of the construction is shown in Figure 5.

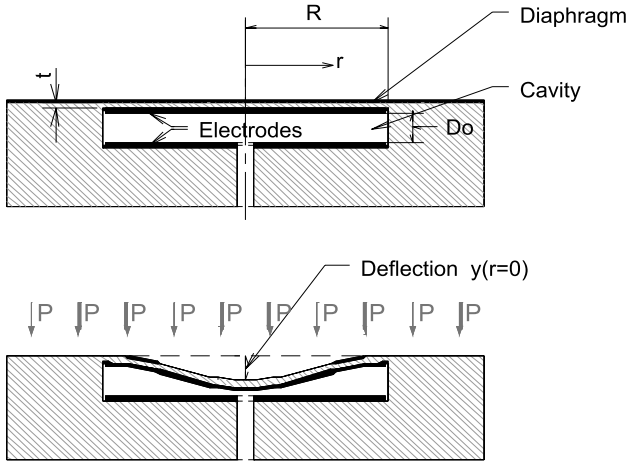

Fig.5: The cross-section of a capacitive pressure sensor without (above) and with (bottom) applied measuring pressure (schematic, not to scale).

The capacitive pressure sensors' characteristics depend on the construction, the dimensions and the material properties (Table 1) of the sensor body and sensing capacitor /10-15/. The influence of the geometry and the material properties of the LTCC structure on the deflection of an edge-clamped deformable diaphragm under an applied pressure is described by equation (1)

$$y(r) = \frac{3P\left(1-\nu^2\right)\left(R^2-r^2\right)^2}{16\,E\,t^3} \quad (1)$$

where the deflection y at the position r from the centre of the diaphragm is a function of the applied pressure, P, the material characteristics (elasticity, E, and Poisson's ratio, n) of the diaphragm, and the dimensions (thickness, t, and radius, R) of the diaphragm (Figures 3 and 5).

The value of initial capacitance (C_0) of the capacitive pressure sensor is defined with the areas of the electrodes and the distance between them. The distance between the electrodes (D) is subtracted from cavity depth and the thickness of both electrodes. When the deflection of the diaphragm y(r=0) under an applied pressure is much smaller than the thickness of the diaphragm and the separation of the electrodes than the capacitance between electrodes is given by equation (2)

$$C(P) = \varepsilon_0 \cdot \varepsilon_r \cdot \int_0^R \frac{2 \cdot \pi \cdot r \cdot dr}{D_0 - y(r)} \quad (2)$$

where C is the capacitance under an applied pressure P, $\acute{I}_0$ is the permittivity in vacuum, $\acute{I}_r$ is the relative permittivity, R is the radius of the electrode, r is the current radius, D_0 is the distance between the electrodes at zero applied pressure and y(r) is the deflection at the current radius r when the pressure P is applied.

The air capacitor of the test samples of the LTCC capacitive pressure sensor was designed as a cavity with a diameter of 9.0 mm and a height of about 80 µm. The thickness of the diaphragm is 200 ěm, and the dimensions of the whole LTCC structure are 18.0 × 12.5 × 1.4 mm. The diameter of the upper and bottom electrodes is 8.6 mm. The test samples of the sensors were fabricated with LTCC materials Du Pont 951. The diaphragm has a thickness of 200 ěm. The fabricated samples, which are shown in Figure 6, were tested in the range from 0 to 70 kPa, where the sensor's response is linear. The test samples were measured at five different temperatures (-25°C, 0°C, 25°C, 50°C and 75°C).

5 Results and discussion

All the test samples were tested at different applied pressures and at different temperatures. The initial capacitances (C_0) of the pressure sensors are between 8 and 10 pF. The relative changes in the initial capacitance of the pressure sensors M2/1 and M3/1) versus the different temperatures are shown in Figures 7 and 8. The calculate temperature coefficients of initial capacitances for two samples M2/1 and M3/1 calculated from experimental results presented in Figures 7 and 8 are about -350×10^{-6}/K and $+300\times10^{-6}$/K respectively. Those selected test samples have extreme values (maximum and minimum) of temperature coefficients of initial capacitances. Other fabricated samples have lower values and mostly located in two

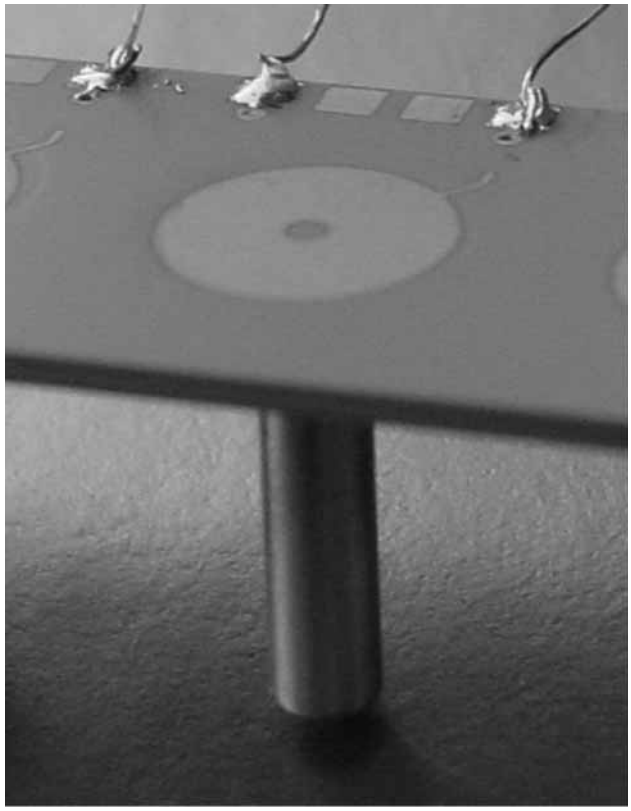

Fig.6: The capacitive pressure sensors made in a 3D LTCC structure.

groups. The first group has average value about -250×10^{-6}/K and the second about $+200\times10^{-6}$/K.

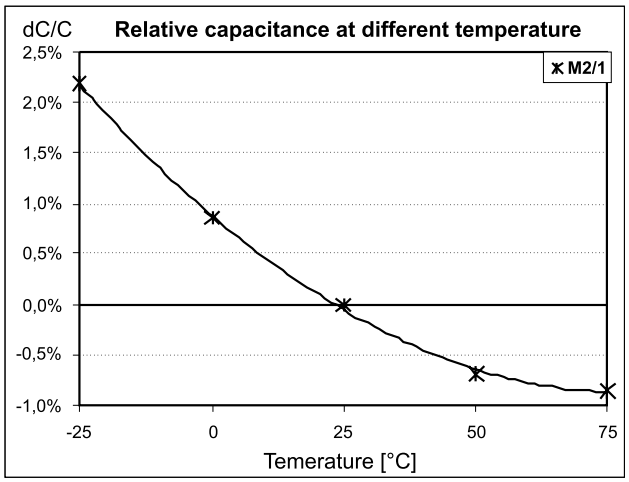

Fig.7: The relative change of initial capacitance at different temperatures for the capacitive pressure sensor M2/1.

The capacitance of the pressure sensors versus negative applied pressure is shown in Figure 9 and the calculated pressure sensitivities from the measured data are between 3.5 and 5.0 fF/kPa. The temperature dependences of sensitivity are not linear and relative high from –700 to 2000 $\times10^{-6}$/K.

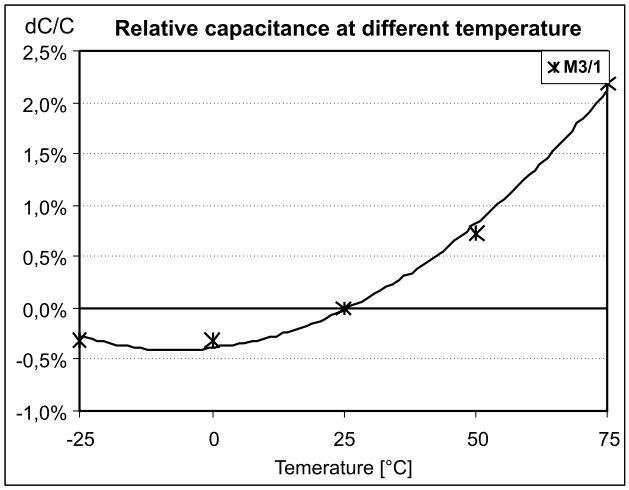

Fig.8: The relative change of initial capacitance at different temperatures for the capacitive pressure sensor M3/1.

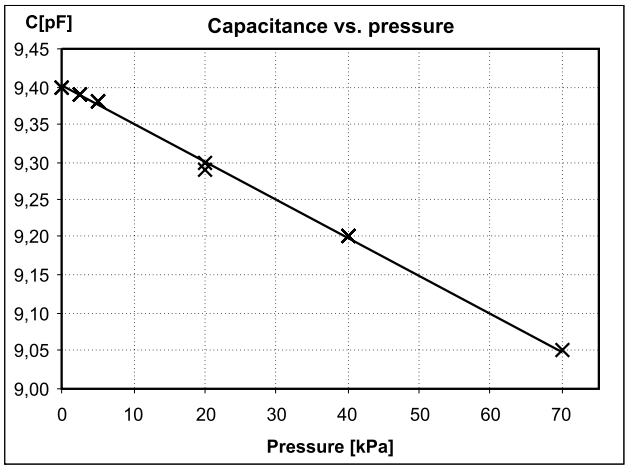

Fig.9: The capacitance versus the negative applied pressure of the capacitive pressure sensor.

The temperature has a noticeable influence on the material characteristics (elasticity and Poisson's ratio) and the fractional changes in the dimensions /8/. The data on the temperature dependence of elasticity of LTCC materials are not available. For this study we presumed that the values of the temperature coefficients of elasticity (TCE) of the LTCC are between the TCE of alumina and the TCE of glass. Therefore, we used a value of -250×10^{-6}/K in our calculations. The data on temperature dependence of the Poisson's ratio of LTCC materials is also not available. The temperature dependence of the Poisson's ratio of alumina is 68×10^{-6}/K. Therefore, 100×10^{-6}/K was used as a rough estimation for the temperature coefficient of the Poisson's ratio of the glassy-alumina-filled LTCC material. The temperature expansion coefficient (TEC) of LTCC materials is 5.8×10^{-6}/K.

Some analytically calculated and experimental values of the characteristics of the LTCC capacitive pressure sensor are presented in Table 2. The main influence on the temperature dependence of the sensor characteristics is from the temperature coefficient of the elasticity, while the temperature coefficient of the Poisson's ratio and the temperature expansion coefficient have only a minor, and opposite, effect on the temperature coefficient of capacitance and the temperature coefficient of sensitivity.

Table 2: Analytically calculated and experimental values of the characteristics of the LTCC capacitive pressure sensor

Characteristics	Calculated Value	Experimental Value
Initial capacitance (pF)	8.7	8÷10
Sensitivity (fF/kPa)	4.0	3.5÷5.0
Temperature coefficient of initial capacitance ($\times10^{-6}$/K)	5.3	-200÷300
Temperature coefficient of sensitivity ($\times10^{-6}$/K)	260	700÷2000

We presume that the significant differences between the experimental and the analytical results of temperature dependences of sensors characteristics lies in the residual stresses and diaphragm pre-bending. Those two effects are not included into the analytical analyses although they have significant influence on the temperature dependences of sensors characteristics. This defectiveness can be corrected by electronic conditioning circuit. For this reason we made the capacitive pressure sensor as the part of the electronic conditioning circuit with the frequency output. The typical output frequency is between 10 and 14 kHz, and depends on the applied pressure. The output frequency versus applied pressure is shown in Figure 10. The calculated pressure sensitivities from the measured data are between 2.5 and 3.5 Hz/kPa. The relative output frequency versus applied pressure at different temperatures is shown in Figure 11. The temperature dependence of initial frequency is relatively high and must be compensated, while the temperature dependence of sensitivity is form –200 to 350 $\times10^{-6}$/K.

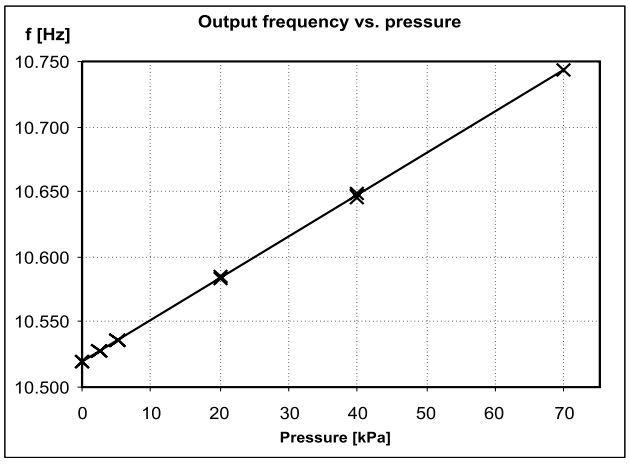

Fig.10: The output frequency versus the applied pressure of the capacitive pressure sensor with the electronic conditioning circuit.

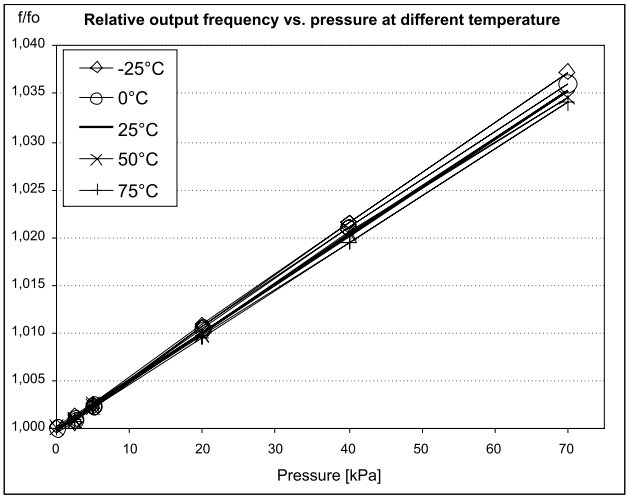

Fig.11: The relative output frequency at different temperatures versus the applied pressure of the capacitive pressure sensor with the electronic conditioning circuit.

Conclusion

The fabrication of capacitive pressure sensors using thick-film and LTCC materials and technology is challenging opportunity for pressure sensors market. The applied pressures generate a relatively small deflection of ceramic diaphragm. This is suitable to use in capacitive pressure sensor because it means that the response of sensors is usefully linear. However, special attention during the fabrication process must be paid to the parallelism of the capacitor electrodes and the repeatability of capacitor dimensions' (areas of electrodes and s distance between them). For the use in the wide temperature ranges the temperature dependences of the sensors characteristics must be compensated by the electronic circuits. The electronic circuits must be used also to minimize the problem of very high output impedance of the pressure sensor. The output capacitance is small, of the order of a few 10 pF, and the changes in this capacitance are of the order of a few fF. This makes it very susceptible to parasitic effects. For capacitive measuring circuits, it is therefore important to minimize the physical separation between the sensing element, i.e. capacitor, and the rest of the circuit.

Acknowledgements

The financial support of the Slovenian Research Agency and the company HYB d.o.o. in the frame of the project L2-7073 is gratefully acknowledged.

The authors wish to thank Mr. Mitja Jerlah (HIPOT-RR) for fabricate test samples.

The paper is dedicated to Professor Lojze Trontelj, Faculty of Electrical Engineering, University of Ljubljana, because of his outstanding and significant contribution in the field of microelectronics and electronic components in Slovenia.

References

/1/ N. M. White, J. D. Turner, "Thick film sensors: past, present and future", Measurements. Sci. Technol., Vol. 8, No. 1, pp. 1-20, 1997.

/2/ M. Pavlin, D. Belavič, M. Santo Zarnik, M. Hrovat, M. Možek, "Packaging technologies for pressure-sensors". Microelectronics International, Vol. 19, pp. 9-13, 2002.

/3/ T. Thelemann, H. Thust, M. Hintz, "Using LTCC for microsystems", Microelectronics International, Vol. 19, No. 3, pp. 19-23, 2002.

/4/ M. Pavlin, F. Novak, "Yield enhancement of piezoresistive pressure sensors for automotive applications", Sensors and Actuators, A, Physical, Vol. 141, No. 1, pp. 34-42, January 2007.

/5/ D. Belavič, M. Hrovat, M. Pavlin, M. Santo Zarnik, "Thick-film technology for Sensor Applications", Informacije MIDEM, Vol. 33, pp. 45-48, 2003.

/6/ L.J. Golonka, A. Dziedzic, J. Kita, T. Zawada, "LTCC in microsystem application", Informacije MIDEM, Vol. 32, No.4, pp. 272-279, December 2002.

/7/ T. Thelemann, H. Thust, M. Hintz, "Using LTCC for Microsystems", Microelectronics International, Vol. 19, pp. 19-23, 2002.

/8/ C.J.Ting, C.S. Hsi, H.J. Lu, "Interactions between ruthenium-based resistors and cordierite-glass substrates in low temperature co-fired ceramics",, Journal of the American Ceramics Society, Vol. 83, pp. 23945-2953, 2000.

/9/ A.A. Shapiro, D.F. Elwell, P. Imamura, M.L. MeCartney, "Structure-property relationships in low-temperature cofired ceramic", Proceedings of the 1994 International Symposium on Microelectronics ISHM-94, Boston, Massachusetts, pp. 306-311, 1994.

/10/ R. Puers, "Capacitive sensors; when and how to use them", Sensors and Actuators A, Vol. 37, pp. 93-105, 1993R. Puers, "Capacitive sensors; when and how to use them", Sensors and Actuators A, Vol. 37, pp. 93-105, 1993.

/11/ C. B. Sippola, C. H. Ahn, "A thick film screen-printed ceramic capacitive pressure microsensor for high temperature applications", Journal of Micromechanics and Microengineering, Vol.16, pp. 1086-1091, 2006.

/12/ J.I. Pavlič, M. Santo Zarnik, D. Belavič, "Feasibility study of a ceramic capacitive pressure sensor", Proceedings. Ljubljana: MIDEM - Society for Microelectronics, Electronic Components and Materials, pp. 95-100, 2006.

/13/ M. Yamada, T. Takebayashi, S. I. Notoyama, K. Watanabe, "A Switched-Capacitor Interface for Capacitive Pressure Sensors", IEEE Transactions on Instrumentation and Measurement, Vol. 41, No. 1, pp. 81-86, February 1992.

/14/ D. Belavič, M. Santo Zarnik, M. Jerlah, M. Pavlin, M. Hrovat, S. Maček, "Capacitive thick-film pressure sensor: material and construction investigation", Proceedings of the XXXI International Conference of IMAPS Poland 2007, Rzeszów, Krasiczyn, Poland, pp. 249-253, September 23-26, 2007.

/15/ D Crescini, V Ferrari, D Marioli and A Taroni, "A thick-film capacitive pressure sensor with improved linearity due to electrode-shaping and frequency conversion", Meas. Sci. Technol. Vol. 8, pp. 71-77, 1997.

Darko Belavič, univ.dipl.eng.el.
HIPOT-RR d.o.o.
c/o Jožef Stefan Institute
Jamova 39, 1000 Ljubljana, Slovenia

Phone: +386 1 4773 479
E-mail: darko.belavič@ijs.si

Prispelo (Arrived): 08.05.2008 Sprejeto (Accepted): 15.09.2008

CALIBRATION YIELD IMPROVEMENT AND QUALITY CONTROL OF SMART SENSORS

Matej Možek, Danilo Vrtačnik, Drago Resnik, Slavko Amon

Laboratory of Microsensor Structures and Electronics (LMSE),
Faculty of Electrical Engineering, University of Ljubljana, Ljubljana, Slovenia

Key words: smart sensor, failure analysis, digital temperature compensation, adaptive calibration

Abstract: Concept and realization of an adaptive closed loop system for calibration of smart pressure sensors is presented. Closed loop concept enables the analysis of sensor properties and optimization of calibration procedure. System quality control mechanisms enable automatic sensor classification. Statistical data enable sensor quality information for failure analysis and quality control of calibrated sensors. System enables optimal digital temperature compensation based on sensor data acquisition and digital evaluation of sensor characteristic. Proposed digital temperature compensation reduces typical sensor temperature error after calibration to 0.05%FS, based on calibration of a lot with 34422 MAP sensors. Calibration yield was improved from 93.7% to 96.8%, achieved by adaptive evaluation of sensor properties such as offset and sensitivity. Proposed calibration system shortens the total time for calibration of smart sensors, by implementing the input testing of sensor parameters as well as final testing of the calibrated sensors, achieving calibration time of 42 seconds per sensor in system current calibration capability.

Izboljšava izplena umerjanja in nadzor kakovosti pametnih senzorjev

Kjučne besede: pametni senzor, analiza napak, digitalna temperaturna kompenzacija, adaptivno umerjanje

Izvleček: V prispevku sta predstavljeni zasnova in realizacija adaptivnega zaprtozančnega sistema za umerjanje pametnih senzorjev tlaka. Predstavljeni zaprtozančni koncept omogoča analizo lastnosti senzorjev in optimizacijo postopka umerjanja. Mehanizmi za nadzor kakovosti senzorjev omogočajo avtomatsko klasifikacijo umerjenih senzorjev. Pridobljeni statistični podatki sistema za umerjanje nudijo vpogled v kvaliteto izdelanih senzorjev, obenem pa omogočajo analizo napak umerjanja senzorjev. Sistem zagotavlja optimalno digitalno temperaturno kompenzacijo na osnovi digitalnega opisa senzorske karakteristike. Na podlagi rezultatov umerjanja serije 34422 MAP senzorjev smo dosegli tipično temperaturno napako senzorjev 0.05%FS. Izkoristek umerjanja se ob uporabi zaprtozančne strukture sistema za umerjanje poveča z 93.7% na 96.8%, kar smo dosegli z adaptivnim ovrednotenjem senzorskih lastnosti kot sta ničelna napetost in občutljivost. Predlagana izvedba skrajša čas umerjanja na 42 s na senzor pri trenutni kapaciteti sistema, kar smo dosegli z vključevanjem testnih parametrov senzorja v zaprtozančno strukturo sistema za umerjanje.

1 Introduction

Smart sensors represent an attractive approach in sensor applications due to their adaptability, achieved by means of digital signal processing. Sensor adaptability can be further turned into a major advantage by introduction of smart calibration systems.

Smart sensors are generally integrated with signal conditioning circuits. Signal conditioning circuits are needed to adjust the offset voltage and span, for compensation of temperature effects of both offset voltage and span, as well as to provide an appropriately amplified signal. The proposed approach is based on a special case of smart pressure sensors, but the developed calibration system is generally applicable for any kind of smart sensor.

In manufacturing of modern electronic devices achieving and maintaining high yield level is a challenging task, depending primarily on the capability of identifying and correcting repetitive failure mechanisms. Yield enhancement is defined as the process of improving the baseline yield for a given technology generation from R&D yield level to mature yield. Yield enhancement is one of the strategic topics of ITRS (International Technology Roadmap for Semiconductors) /1/. This iterative improvement of yield is based on yield learning process, which is a collection and application of knowledge of manufacturing process in order to improve device yield through the identification and resolution of systematic and random manufacturing events /2/. Yield improvement process will consequentially increase the number of test parameters and hence the calibration system complexity. One of advantages of increasing system complexity is the ability to integrate the input testing processes and output final testing processes into the calibration process itself, thus shortening the total time for calibration.

Several types of smart sensors with integrated signal conditioning have been presented over the past few years /3, 4/. The calibration processes and temperature compensating methods for these sensors are based either on analog, digital or mixed approaches. Analog approach usually comprises an amplifier with laser trimmable thin film resistors /5, 6/ or off-chip trimmable potentiometers /7, 8/ , to calibrate the sensor span and offset voltage and to compensate for their temperature drift. Analog compensation techniques are relatively slow, inflexible and costineffective. In digital approach, sampling for raw digital pressure and temperature values is first performed, followed

by an evaluation of the output digital values via polynomials for describing sensor characteristic, and finally converting the computed pressure values to according analog voltages /9, 10/. Mixed approach retains strictly the analog signal conversion path, while smart sensor offset and span are adjusted by setting of operational amplifiers by digital means /11/.

This paper will focus on the problem of adaptive calibration any quality control of smart sensors with digital temperature compensation, which is one of the most time consuming steps in sensor production. In order to advance calibration system performance, smart calibration system is conceived as a digitally controlled closed loop system capable of adaptive learning. Presented concept of calibration system is directly implemented in the iterative yield enhancement process in the production of piezoresistive pressure sensors for automotive applications. The calibration system operation and quality control is illustrated on the case of Manifold Absolute Pressure (MAP) sensors. The emphasis will be on MAP sensors, although the proposed approach can be implemented in other fields of application.

2 Calibration procedure

Main calibration procedure starts with measurement of sensor coarse gain and offset and optimization of sensor parameters to the sensor signal conditioner front end stage. After initial optimization procedure the calibration conditions are set according to calibration scenario. Raw sensor readouts of supplied reference quantities are acquired at each calibration point. After acquisition, digital description of sensor characteristic is evaluated and the results are stored back to sensor. A detailed description of calibration procedure is given in /12/. Calibration scenario defines the sequence of reference quantities, which are applied to sensors under calibration. In case of temperature compensation of pressure sensor, the reference quantities are pressure and temperature. Minimal number of calibration points is 4. This is defined by using the lowest (i.e. linear) degree of polynomial for sensor characteristic description /9, 10/ in the temperature and pressure direction. Maximal number of calibration points is primarily limited by total calibration time. In case of pressure sensors, both calibration axes consist of three calibration points, thus enabling compensation of second order nonlinearity in both directions, as depicted in Figure 1. Maximal number of calibration points for pressure sensor can cover nonlinearities up to third order in pressure direction. Actual number of calibration points is a compromise between calibration precision and total calibration time. To shorten total calibration time, the slower settling axis should be used for definition of the calibration points order. In case of MAP sensor, the temperature axis defines the calibration scenario.

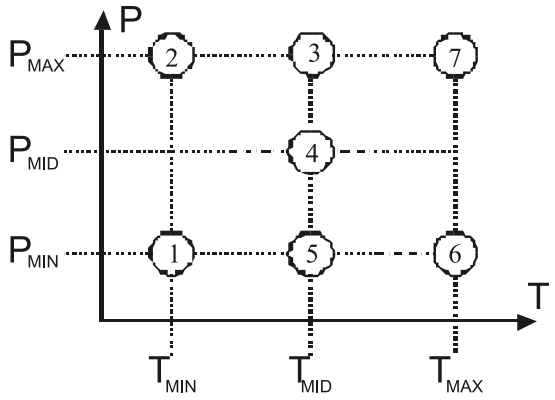

Fig. 1: Calibration scenario.

2.1 Evaluation of parameters at calibration input

Calibration scenario enables the assessment of essential input parameters to calibration procedure, which enables early fault detection on sensors before they enter actual calibration process. Input parameters comprise the properties, such as offset, sensitivity and nonlinearity of uncompensated sensing element (e.g. pressure sensor). Evaluation of such properties is essential for determination of decision criteria for adaptive concept of calibration system.

2.1.1 Pressure sensor sensitivity

Sensor sensitivity can be evaluated at three temperatures. At each temperature, sensitivity is obtained as a difference of pressure sensor voltage response, normalized to corresponding pressure change. Temperature coefficient of pressure sensor sensitivity is evaluated as a difference between sensor sensitivities at two temperature endpoints (T_{MIN} and T_{MAX} in Figure 1). Resulting difference is normalized to temperature corresponding temperature change.

2.1.2 Pressure sensor offset

Sensor offset at room temperature can be evaluated at calibration point 5 as T_{MID} in Figure 1 is normally set at room temperature. Digital sensor offset readout is transformed into voltage according to analog to digital ASIC stage parameters /9, 10/.
Temperature coefficient of sensor offset is estimated from endpoint calibration points offset values normalized to corresponding temperature difference. In presented calibration scenario the calibration endpoints for estimation of temperature coefficient are marked 1 and 6. Obtained result is recalculated to temperature response at 0°C.

2.1.3 Pressure sensor nonlinearity

Nonlinearity is calculated by using calibration points 3, 4 and 5 in Figure 1. Nonlinearity is evaluated as a difference of midpoint pressure response at calibration point 4 from ideal linear sensor response, formed by calibration points

3 and 5. Resulting difference is normalized to calibration span, defined by calibration points 3 and 5. For practical purposes, evaluation of sensor nonlinearity is performed only at room temperature.

2.1.4 Temperature sensor response

Temperature sensor response is evaluated at three different temperatures (T_{MIN}, T_{MID} and T_{MAX}). Acquired data can be used for calibration of auxiliary temperature measurement channel calibration. Temperature sensor offset, sensitivity and nonlinearity can be evaluated from data acquired at calibration points 1, 5 and 6 in Figure 1. Validity of temperature sensor response can be checked at calibration points 2, 3 and 7 in Figure 1.

2.1.5 Insertion of excess test points

In order to avoid additional final testing procedures, further test points can be inserted into calibration scenario, depicted in Figure 1. Raw sensor response is acquired at test points. Acquired data is not used in calculation process of sensor characteristic parameters. Test points are inserted along a faster settling axis. In case of proposed calibration scenario in Figure 1, this is the pressure axis.

Introduction of additional test points imposes a lesser delay in comparison to time required for separate final testing procedure. Moreover, by introduction of additional test points, a more accurate, instant evaluation of total calibration error can be performed immediately after calibration. Total calibration error is essential figure of calibration process quality and gives a direct insight to sensor classification.

2.2 Evaluation of parameters at calibration output

Calibration output parameters are directly related to compensation of unwanted dependencies. In case of presented MAP pressure sensor this is the temperature compensation. Temperature error is evaluated at every calibration point immediately after evaluation of calibration coefficients. It is calculated by calibration computer as a difference between output of ideal characteristic of MAP sensor and the ASIC simulation of sensor characteristic. Total temperature error comprises RSS (root square of sum of squares) of temperature errors, calculated at every calibration point. Total calibration error is comprised of RSS sum of total temperature error and the combined standard uncertainty for output analog stage, if the sensor features analog output.

The ASIC features 16 bit integer arithmetic, therefore a rounding error, which occurs during coefficients calculation, is further minimized by evaluation of total temperature error on all rounding combinations. Rounding combination of calibration coefficients, that yields minimal temperature error at each calibration point is written to ASIC.

2.3 Failure analysis

Failure analysis is used for detection of cause of calibration failure upon calibrated sensors as well as establishing the system related calibration failures. The failure analysis can be used instead of separate input control to calibration process. Therefore, failure analysis procedures must distinguish between system causes of failure and sensor failures and signal conditioner failures. Furthermore, sensor failure causes may be introduced during manufacturing process or are a direct consequence of failed sensor. Sensor related failures can be divided into several categories:

2.3.1 Sensor related causes of failure

Inadequate response of pressure sensor response failure is determined prior to calibration process. It is evaluated by calculating the sensitivity of sensor - if the sensitivity is zero, or out of sensitivity validity interval, then this error is signaled and the sensor is discarded. Excess nonlinearity is determined by calculating the difference of midpoint pressure response and the midpoint derived from ideal linear sensor characteristic, passing through endpoints. If the nonlinearity exceeds more than 2%, the error is signaled.

2.3.2 ASIC related causes of failure

Inadequate response of temperature sensor response can represent a cause of calibration failure. In case of presented MAP sensor calibration, this type of error is attributed to signal conditioner circuit, since the temperature sensor (diode) is located within ASIC.

Another type of calibration failure can be attributed to calibration polynomial coefficient clamping, when the solution of calibration coefficients exceeds the interval of 16 bit integer values. This error can be found after acquisition of raw sensor values, when the sensor characteristic is evaluated.

2.3.3 Calibration system related causes of failure

Inadequate temperature stabilization error can be determined by comparing orthogonality of temperature calibration points. Whenever the corresponding temperature calibration points differ more than 10%, this error is signaled.

Calibration of sensor output stage failure can be detected by comparing the analog to digital values at corresponding calibration points, which have the same output response. If the output values differ more than 10%, this error is signaled. This is a system cause of failure, because the process of output calibration was interrupted.

The sensor output value must not be clamped to maximum at any calibration point. If an error stays clamped to maximum, this can be attributed to signal conditioner failure. However, this error may also indicate improper sensor connection.

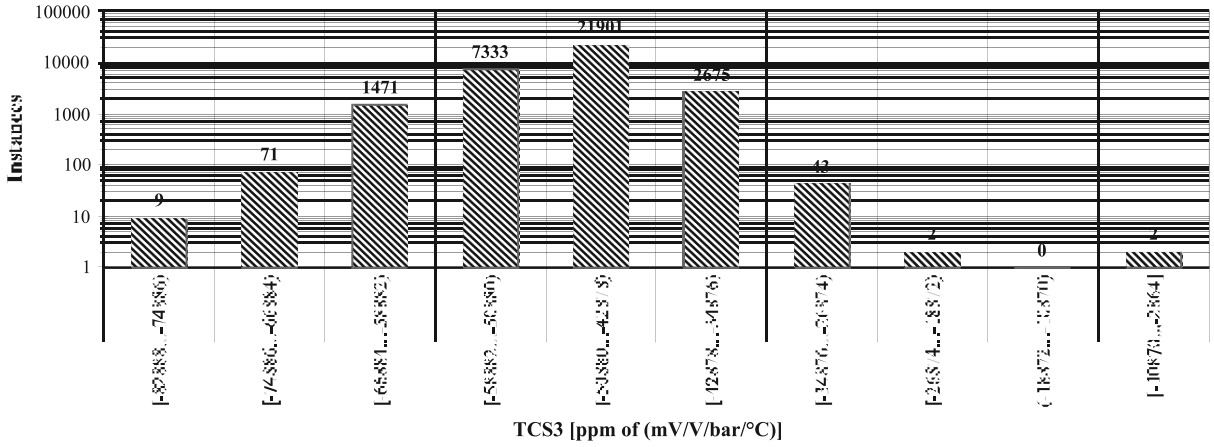

Fig. 2: Input temperature coefficient of sensitivity.

3 Results

Presented results are based on 34422 calibrated manifold absolute pressure sensors. Results comprise analysis of operation of two calibration systems. Input sensor properties investigation is presented on ZMD31020 signal conditioner /9/. Output properties analysis and failure analysis was performed on ZMD31050 signal conditioner /10/.

3.1 Input properties of calibrated sensors

Based on described statistical analysis of sensor properties a histogram, which sets the sensor validity interval was plot. The input temperature coefficient of pressure sensitivity at calibration point 3 in Figure 1 is in the range of /-8% … -0.2%/, which represents a insurmountable span of temperature coefficients, if analog calibration was to be made upon such sensors.

Average value of input temperature coefficient of pressure sensitivity in the histogram, depicted in the Figure 2 is -4.9% (mV/V/bar). Standard deviation from this value is 0.51% of (mV/V/bar). Sensors, based on analog signal conditioners with operational amplifiers /7/, can compensate temperature coefficient of sensitivity up to 0.2%/°C. The latter clearly demonstrates the advantage of the digital temperature compensation based signal conditioners. Input temperature coefficient of offset voltage is depicted in Figure 3. Again, the plotted histogram depicts large variations for temperature coefficient of offset voltage. Analog calibration system could not calibrate the sensor with temperature coefficient of offset voltage in the range of 1mV/°C.

3.2 Output properties of calibrated sensors

In case of calibration of ZMD31050 based MAP sensors, further 11 test points were introduced to calibration scenario. Output temperature error histograms were evaluated at 5%, 10%, 20%, 30%, 40%, 50%, 60%, 70%, 80% and 90% of power supply voltage pressure response at 85°C and 20°C upon a set of 5828 sensors. From initial 5828 sensors, 366 were evaluated as bad. Among them were 182 sensors, lacking the results from testing at 20°C. Calculated histograms are a clear demonstration of effectiveness of digital temperature compensation. The histogram in Figure 4 depicts the magnitude of temperature error in test point 1 (T=85°C, P=17kPa, V_{OUT}=5%VCC). Presented result was subtracted with an ideal value and

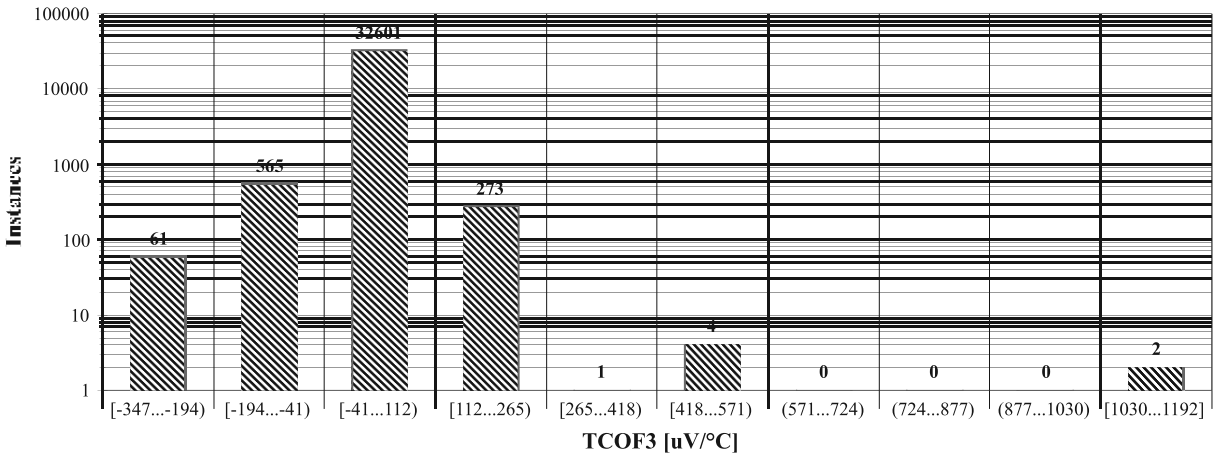

Fig. 3: Input temperature coefficient of offset voltage.

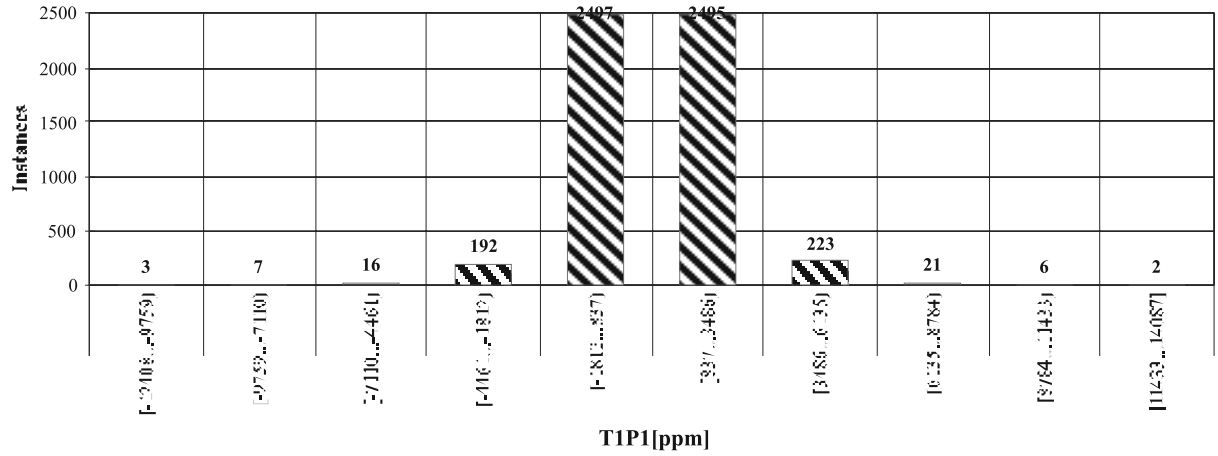

Fig. 4: Temperature error at test point 1.

the resulting error was normalized in ppm. The data in the Figure 4 shows temperature error in the range of /-0.2% … 0.38%/ for 5075 sensors out of 5462 total, whereas the admissible range of temperature errors lies within ±1.7%.

Mean histogram value, representing a typical calibration temperature error is 0.086%. The standard deviation from this value is 0.16%. Similar histogram was evaluated at test point 11 (T=20°C, P=105kPa, V_{OUT}=95%V_{CC}) and the resulting temperature error is depicted in Figure 5. Mean histogram value is now 0.15%, while the standard deviance is 0.19%.

If remaining 184 sensors (366-182) bad sensors are further analyzed, the output stage failure is noted on 82 sensors, which can be attributed to faulty connection of the sensor output, because the sensor output stays the same on every test point. The same cause of error can be attributed to faulty output stage – fault in signal conditioner. The actual cause can be determined with combined insight into calibration database. Remaining 102 sensors were calibrated with temperature error out of MAP sensor specification. One of them (ID=58800) was rejected by calibration process due to inadequate pressure response. Upon analysis of calibration database upon these 101 sensors, it becomes apparent that most of the tested sensors passed the calibration, but failed the test. This indicates a change in sensor properties during packaging step of production. The tests were performed after thermal cycling, therefore the failure was introduced during packaging phase of sensor production. Packaging after calibration was performed in case of MAP sensors based upon ZMD31020 signal conditioner. Temperature error values are summarized in the Table 1. First column summarizes the test pressure points, second column lists the maximum error margin in parts per million and the next two columns summarize the typical temperature error at temperatures 85°C and 20°C. For each pressure test point, a temperature error histogram was statistically evaluated by calculating first four statistical moments. Table 1 lists the temperature error average and its standard deviation (ó).

Results from Table 1 can be interpreted as a figure of quality of calibrated sensors for MAP sensor application.

Next, the analysis of maximal sensor temperature error was performed on all tested temperatures. Resulting maximal

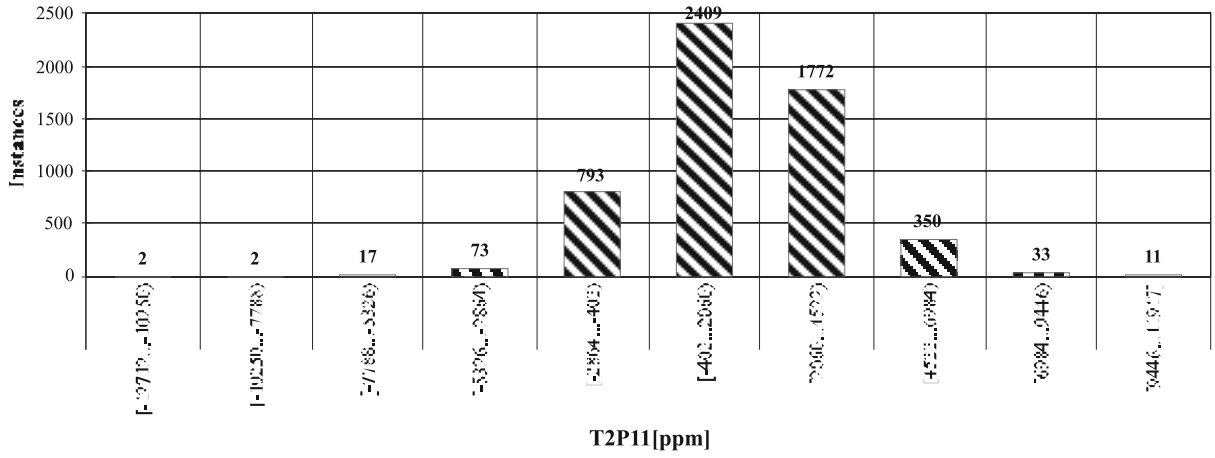

Fig. 5: Temperature error at test point 11.

Table 1: Temperature error for MAP sensors.

P (kPa)	error limit (ppm)	error @ 85°C		error @ 20°C	
		avg. (ppm)	σ (ppm)	avg. (ppm)	σ (ppm)
17	±17000	861	1686	2527	2048
20	±16300	548	1461	2067	2075
30	±14200	-294	1497	2087	2124
40	±12000	-707	1613	1898	2013
50	±12000	-1076	1559	1621	1960
60	±12000	-895	1508	1832	1935
70	±12000	-560	1480	2167	1904
80	±12000	-538	1433	2146	1891
90	±12000	-729	1436	1899	1923
100	±13500	-848	1451	1639	1960
105	±15000	-876	1449	1535	1996

errors were divided into 10 bins and the result was evaluated in the histogram. Resulting histogram is summarized in Table 2. The histogram depicts sensor classification in ten classes. The majority (5189 of 5462) of sensors are well within 0.7% limit of temperature error.

Important is, that classification can be performed on each and every calibrated sensor. Because of complete sensor traceability, we are able to identify the class and quality for each calibrated sensor. The calibration yield upon 5462 sensors is 98.1%.

Table 2: Classification of calibrated sensors.

Class	Limit (ppm)		Sensors
	upper	lower	
1	767	2239	992
2	2239	3711	2190
3	3711	5183	1477
4	5183	6655	530
5	6655	8127	182
6	8127	9599	44
7	9599	11071	24
8	11071	12543	16
9	12543	14015	4
10	14015	15490	3

The cause of failed sensors is attributed to change of sensor properties after calibration during packaging process. This was counter measured by performing the packaging process prior to calibration and performing the calibration as a last step of production process. Advanced signal conditioners (ZMD31050) enable calibration of packaged sensors by one-wire communication. The change of sensor properties can also be monitored by the signal conditioner itself. Advanced signal conditioner ZMD31050 measures not only the differential sensor voltage, but also the common mode voltage. This voltage changes if a single bridge resistor value changes. The change is compared to limits, measured during calibration. When the common mode falls out of stored limits, an alarm is signaled and sensor output is disabled, making sensor unusable. The calibration yield was further improved by discarding the faulty sensors during sensor pretesting phase.

3.3 Demonstration of adaptivity concept

The adaptivity of the system is based upon determining the limits of all system parameters, which define the criteria for quality of calibrated sensors. The result from criteria adaptation is the calibration interval for a given sensor property, based on sensors which comply with predefined output response.

The limit optimization process is performed upon every sensor that enters the calibration process. Primary acquired sensor parameters are obtained directly from acquisition – raw pressure and temperature sensor readouts. The raw values are recalculated to analog measured quantity according to preamplifier settings, including sensor offset compensation and preamplifier gain.

An illustrative case of sensor limit adaptation is presented when a new sensor enter the calibration process. After initial acquisition of raw values the new sensor response is evaluated and its response is inserted in the histogram, which depicts the raw sensor readouts at the first calibration point (17kPa, -20°C). Entering sensor was assigned identification number (ID=31326).

From the histogram on Figure 6, it is obvious, that the tested sensor extremely deviates in raw response from all other sensors. However, an automated analysis must establish other sensor properties in order to determine whether a given sensor will enter a full calibration process or not. Sole evaluation of the magnitude of raw pressure response is not sufficient for final estimation, because the sensors at the input can be e.g. from different manufacturers and their responses may vary. The calibration system is designed to adapt also to new type of sensor with different input properties. The system needs to find the explanation for this raw pressure response. If several pressure points are scanned, the sensor properties can be evaluated (sensitivity, offset and nonlinearity). First, the sensor sensitivity is calculated as a difference of two pressure responses. If the sensor readout is approximately ten times larger than normal, then the sensitivity should be in proportion with raw readouts. Otherwise, the sensor response can be considered inadequate – this indicates failure in offset or gain optimization process. The system calculates the sensor sensitivity and depicts the result in the histogram for comparison with other sensors. The resulting histogram is depicted in the Figure 7. The sensitivity was evaluated in the range between 300 and 338, which is in proportion with sensor readouts.

Therefore, further analysis is performed and sensor nonlinearity is evaluated and the results are depicted in the Figure 8. When the sensor nonlinearity is compared to other sensors in histogram, it becomes obvious, that the sen-

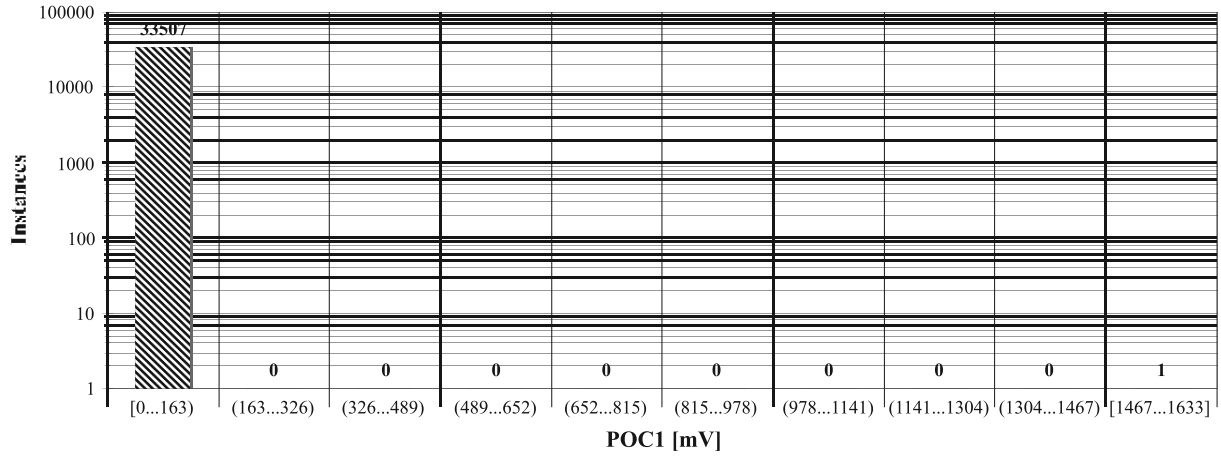

Fig. 6: Raw pressure sensor response at calibration point 1.

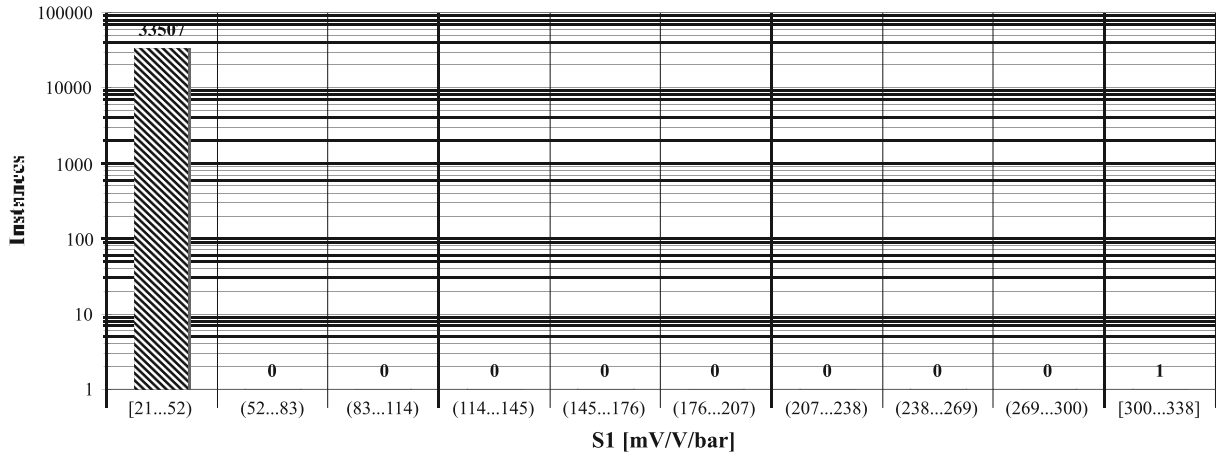

Fig. 7: Sensitivity at calibration point 1.

sor is highly nonlinear (55.8%). Therefore, the sensor is discarded from further calibration process.

The sequence of high sensitivity and excess nonlinearity failures implies that a pressure sensor was not designed for calibration on a high pressure range: A low pressure sensor was exhibited to calibration on a high pressure range. Such a low pressure sensor exhibits larger sensitivity but also nonlinear response, when exposed to overpressure.

Sensors such with nonlinearity can be calibrated, but not with the seven point calibration scenario, which was used during calibration process of manifold absolute pressure

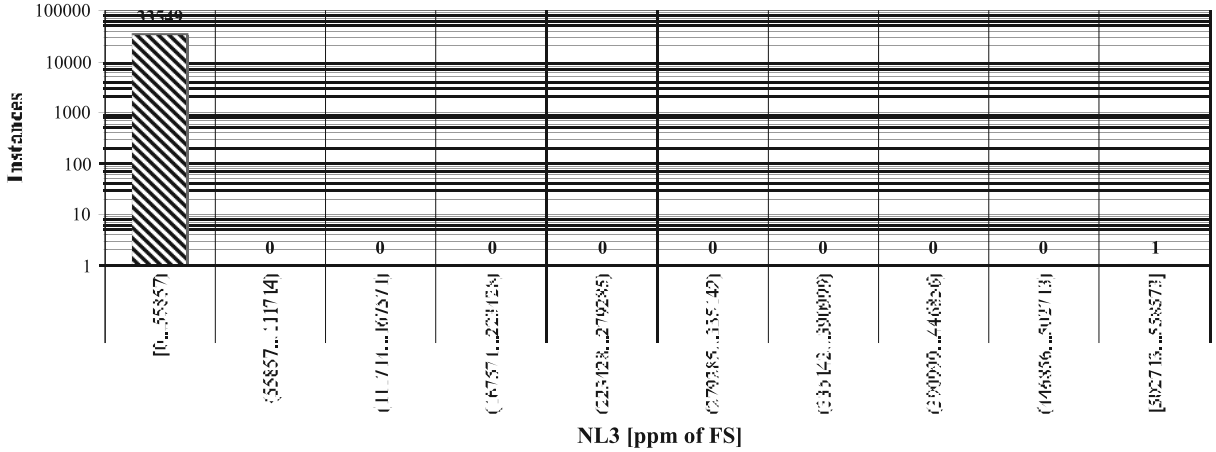

Fig. 8: Nonlinearity at calibration point 1.

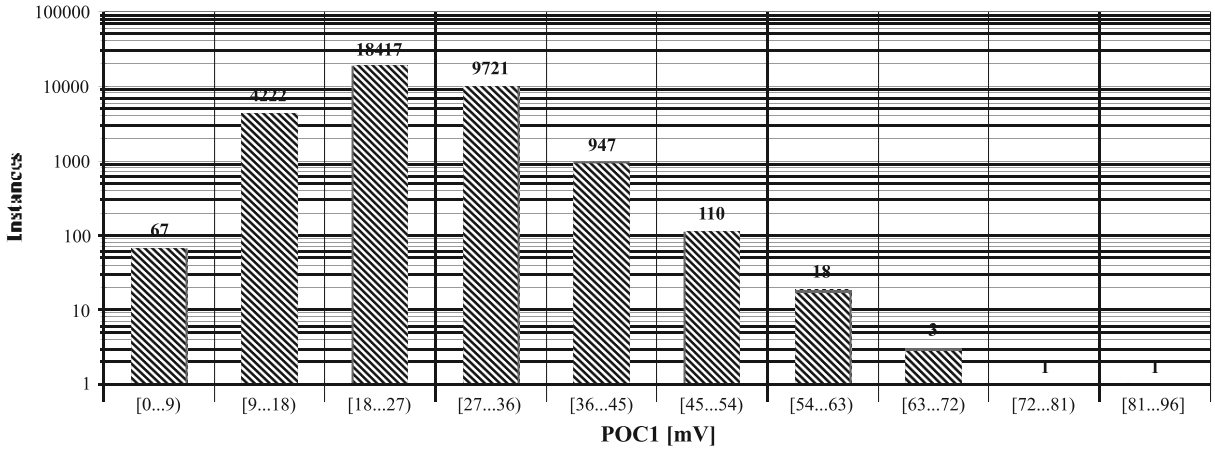

Fig. 9: Corrected raw pressure sensor response at calibration point 1.

sensor. Maximal nonlinearity of uncalibrated pressure sensors was limited to 2%

Sensor is discarded from further calibration and resulting histograms of raw pressure readout are evaluated again. Resulting histograms after discarding are depicted in Figure 9 and Figure 10.

The resulting limits for raw pressure response stay between 0 and 96mV as can be seen in the Figure 13, and for the pressure sensitivity in interval /21…41mV/V/bar/.

3.4 Failure analysis of calibrated sensors

Failure analysis was performed upon a set of calibrated sensors. A detailed insight of failure analysis results is summarized in Table 3. Calibration yield, which would be calculated disregarding failure analysis, would yield 93.7%, since there are 2289 failed sensor out of 36711 calibrated. However, the calibration database stores everything including failed attempts related to system causes, which are not caused by failed sensors. Most of system failures are attributed to improper sensor connection (operator

Table 3: Failure analysis of calibrated sensors.

Cause of failure	Origin of failure	Nr. of sensors
Inadequate response of pressure sensor	Sensor	220
Inadequate response of temperature sensor	Conditioner	81
Calibration coefficients clamped	Calibration	373
Communication failure	System	1108
Inadequate temp. stabilization	System	34
Excess nonlinearity	Sensor	384
Tolerance error during coefficient calculation	Calibration	36
Calibration of sensor output stage failure	System	20
Output stage clamped to maximum level	Conditioner	33
Total		2289

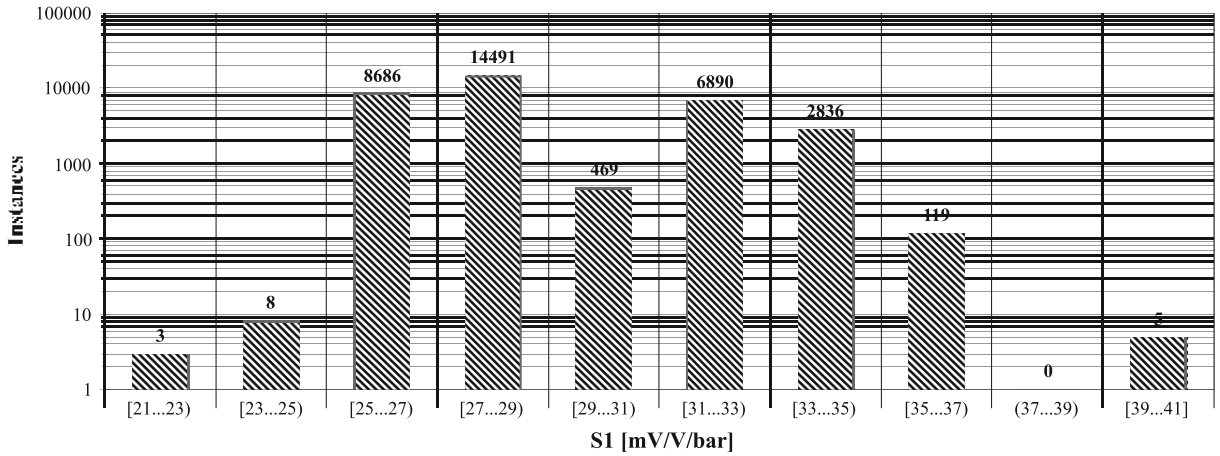

Fig. 10: Corrected pressure sensor sensitivity at calibration point 1.

error). Therefore the system related causes must be removed from analysis to obtain actual yield of calibration. After this, the calibration yield improves to 96.8%, since there are only 1127 failed sensors of 35549.

4 Conclusion

Adaptive calibration and quality control of smart pressure sensors were presented. Presented digital temperature compensation reduces typical sensor temperature error after calibration to 0.05%FS, based on calibration of 34422 MAP sensors. During initial calibration stage, early detection of faulty sensors has proven essential for the calibration yield improvement. Yield improvement is achieved by thorough analysis of sensor properties such as offset, sensitivity, nonlinearity and temperature coefficients of sensitivity and offset. Further refinement of calibration failure causes gives a detailed insight into sensor related failure causes, system related failure causes and signal conditioner failure causes. Described quality control mechanisms enable automatic sensor classification. Proposed calibration system shortens the total time for calibration of smart sensors, by implementing the input testing of sensor parameters as well as final testing of the calibrated sensors. Final testing was achieved by inserting additional test points into the calibration scenario. In current calibration system configuration, the calibration time was 42 seconds per sensor. In system maximal extension, enabling simultaneous calibration of 2048 sensors, calibration time would be reduced to 3 seconds per sensor.

Acknowledgments

This work was supported by Ministry of Higher Education, Science and technology of Republic of Slovenia within research programme R-252 and industrial partner HYB d.o.o. Trubarjeva 7, 8310 Šentjernej, Slovenia.

References

/1/ International technology roadmap for semiconductors: 2006 update - Test And Test Equipment Electronic file available at: http://www.itrs.net/Links/2006Update/FinalToPost/03_Test2006Update.pdf, 2008.

/2/ International technology roadmap for semiconductors: 2006 update - Yield Enhancement Electronic file available at: http://www.itrs.net/Links/2006Update/FinalToPost/13_Yield2006Update.pdf, 2008.

/3/ Yoshiaki Takashima, Tsuneo Adachi, Toshiyuki Yoshino and Tetsuya Yamada, Temperature compensation method for piezoresistive sensors, JSAE Review, Volume 18, Issue 3 (1997), pp. 317 319.

/4/ IEEE Std. 1451.2 D3.05-Aug1997 "IEEE standard for a smart transducer interface for sensors and actuators – Transducer to microprocessor communication protocols and transducer electronic data sheet (TEDS) formats" Institute of Electrical and Electronics Engineers, September 1997.

/5/ M. -T. Chau, D. Dominguez, B. Bonvalot and J. Suski, "CMOS fully digital integrated pressure sensors", Sensors and Actuators A, Volume 60, Issues 1-3 (1997), pp. 86 89.

/6/ Q. Wang, J. Ding and W. Wang, "Fabrication and temperature coefficient compensation technology of low cost high temperature pressure sensor" Sensors and Actuators A, Volume 120, Issue 2 (2005) 468 473.

/7/ F. V. Schnatz et al., "Smart CMOS capacitive pressure transducer with on-chip calibration capability", Sensors and Actuators A, Volume 34, Issue 1 (1992), pp. 77 83.

/8/ Bo-Na Lee et al., "Calibration and temperature compensation of silicon pressure sensors using ion-implanted trimming resistors." Sensors and Actuators A 72 (1999), pp. 148 152.

/9/ ZMD31020 Advanced Differential Sensor Signal Conditioner Functional Description Rev. 0.75, (2002) ZMD AG.

/10/ ZMD31050 Advanced Differential Sensor Signal Conditioner Functional Description Rev. 0.75, (2005), ZMD AG.

/11/ MLX90269 Absolute Integrated Pressure Sensor datasheet, June 2006, Melexis- Microelectronic Integrated Systems Inc., rev 2.

/12/ Možek, Matej, Vrtačnik, Danilo, Resnik, Drago, Aljančič, Uroš, Penič, Samo, Amon, Slavko. "Digital self-learning calibration system for smart sensors". Sensors and Actuators A. 141 (2008), 141, pp. 101 108.

dr. Matej Možek
doc.dr. Danilo Vrtačnik
doc.dr. Drago Resnik
mag. Uroš Aljančič
Samo Penič, univ. dipl. inž. el.
prof.dr. Slavko Amon

University of Ljubljana,
Faculty of Electrical Engineering,
Laboratory of Microsensor Structures and Electronics
Trzaska 25, Ljubljana 1000, SLOVENIA
e-mail: matej.mozek@fe.uni-lj.si
Telefon: 01 4768 380, Telefax: 01 4264 630

Prispelo (Arrived): 08.05.2008 Sprejeto (Accepted): 15.09.2008

Prof. dr. Lojze Trontelj (1934 – 2008)

Pionir mikroelektronike

Marca letos nas je vse, ki mo ga poznali, pretresla vest, da je umrl profesor Lojze Trontelj, zaslužni profesor Fakultete za elektrotehniko Univerze v Ljubljani. V čast mi je, da lahko v reviji, ki je namenjena njemu tako ljubemu področju elektrotehnike, mikroelektroniki, v njegov spomin napišem nekaj besed. Prof. Trontlja sem prvič srečal leta 1980, ko sem se pridružil njegovi skupi v Laboratoriju za mikroelektroniko na ljubljanski Fakulteti za elektrotehniko, ki ga je tedaj vodil. Iz začetnega službenega odnosa se je med nama sčasoma razvilo dobro znanstvo in celo prijateljstvo, vendar me je vest o njegovi smrti, kljub temu, da sem mislil, da ga dobro poznam, presenetila. Seveda smo vsi, ki smo z njim sodelovali, vedeli, da ima težave z zdravjem, vendar se je zdelo, da jih uspešno obvladuje in da ga pri njegovem delu ne ovirajo znatno. Glede tega se na videz ni veliko spremenilo niti po tem, ko je odšel v pokoj in najini dotlej vsakodnevni stiki, po naravi stvari, niso bili več tako pogosti. Lojze je svoje privatno življenje strogo ločeval od javnega in ni imel navade, da bi drugim tožil o svojih težavah, niti tedaj ne, ko ga je bolezen končno začela premagovati. Od tod presenečenje vseh, razen najožje družine, ob njegovi smrti. Omenjeno najbrž pojasnjuje, da se moram torej omejiti na opisovanje njegove profesionalne poti učitelja, znanstvenika in organizatorja visoke tehnologije, osebno stran njegovega življenja pa bo morda kdaj opisal nekdo, ki ga je bolje od mene poznal tudi po osebni plati.

Profesor Lojze Trontelj je bil rojen leta 1934 v Krškem. Maturiral je na Klasični gimnaziji v Ljubljani in se po maturi vpisal na Fakulteto za elektrotehniko Ljubljanske univerze. Tam je leta 1959 diplomiral z odličnim uspehom s temo iz področja mikrovalovne tehnike pri profesorju Grudnu. Izbira teme diplome se zdi naravna, saj se je že kot študent posvečal področju najvišjih frekvenc in se celo nekaj mesecev dopolnilno izobraževal na področju pri podjetju Siemens na Dunaju. Najbrž še iz tistih časov izvira tudi glo-

A Pioneer of Slovenian Microelectronics

In March professor Lojze Trontelj, professor emeritus at the Faculty of Electrical Engineering of the Ljubljana University, passed away. I am honored to be asked by his friends to write several words in his memory in a journal that is dedicated to the field of microelectronics, which was so dear to him. I have first met prof. Trontelj in 1980, when I joined his group in the Laboratory for Microelectronics at the Faculty of Electrical Engineering. Our at first purely professional relation, with time developed into friendship and I thought I knew Lojze well. However, the news of his death surprised me. Certainly, everybody who knew him was aware of his health problems, but he seemed to handle them well and they did not appear to influence his work. In this respect nothing seemed to change after his retirement in 2000, even though our previously daily contacts, by the nature of things, diminished in frequency. But Lojze strictly separated his private life from his professional life, and was not in the habit of talking to people, even those he knew well, about his private problems. This has not changed even when his health was starting to give up, and thus my surprise at his passing away. With this said, I obviously have to limit myself to describing his professional life of a teacher, scientist, and organizer of high-tech enterprises. The personal side of his life may thus be elucidated sometime by someone who knew him better than me from that side also.

Prof. Trontelj was born in 1934 in Krško, Slovenia. He attended the classical gymnasium (a high school where classical Latin and Greek are taught) in Ljubljana and after graduation enrolled into the Faculty of Electrical Engineering of the Ljubljana University, where in 1959 he completed his studies with honors with a diploma work dedicated to microwaves, with prof. Gruden as his supervisor. His choice of the field of research seems natural, as already as a student he was interested in phenomena at highest frequen-

boko prijateljstvo med prof. Trontljem in prof. Grudnom, ki je vsem postalo očitno šele kasneje, ko je Lojze zvesto skrbel za svojega ostarelega mentorja. Kljub temu, da se je prof. Trontelj po diplomi zaposlil na Inštitutu za elektrozveze v Ljubljani, je bil hkrati imenovan tudi za honorarnega asistenta na Fakulteti za elektrotehniko. Po vrnitvi s služenja vojaškega roka leta 1962, pa je na fakulteti nastopil službo asistenta za predmeta Elektromagnetna nihanja in Mikrovalovi. Le dve leti kasneje, ob uvajanju novega učnega načrta z znatno razširjenim učnim programom, pa je na predlog profesorjev Grudna in Budina postal tudi predavatelj predmeta Mikrovalovi.

Leta 1965 je prof. Trontelj dokončal študij tretje stopnje v smeri Elektronska optika in si z delom *Določevanje širine resonančne krivulje in ostalih mikrovalovnih parametrov pri feritu* pridobil naziv magister elektrotehnike. Leta 1967 je odšel na skoraj polletno specializacijo z mikrovalovnega področja na Tehnično visoko šolo v Stockholmu, kjer je raziskoval nelinearne pojave pri mikrovalovnih feritih, in le leto kasneje na Fakulteti za elektrotehniko uspešno obranil svojo doktorsko disertacijo z naslovom *Metoda za določanje komponent tenzorske permeabilnosti feritov*. Še leto kasneje pa je dosegel vnaprejšnjo habilitacijo za docenta za področje mikrovalov in bil naslednje leto izvoljen za docenta za predmet Mikrovalovi. Hkrati je na povabilo prof. Agdurja ponovno odšel na Tehnično visoko šolo v Stockholmu, kjer se je posvetil integraciji mikrovalovnih feritnih elementov v mikrovalovna integrirana vezja. V izbiri področja morda lahko vidimo zametek zanimanja, ki mu je prof. Trontelj nato posvetil celo življenje – miniaturizacija in integracija elektronskih sistemov. Kakor koli, njegovo sodelovanje z Mikrovalovnim institutom Tehnične visoke šole v Stockholmu je trajalo vse do leta 1971, kjer je vodil projekt Mikrovalovna feritna mikrovezja. Sodelovanje mu je uspelo organizirati tako, da se je velik del projekta dejansko izvajal v mikrovalovnem in mikroelektronskem laboratoriju na FE v Ljubljani, s predvidljivim učinkom, da se je znanstveni in tehnološki nivo laboratorija na fakulteti dvignil na raven modernih raziskovalnih centrov z opaznimi raziskovalnimi dosežki. Vse to gotovo ne bi bilo mogoče, če prof. Trontelj ne bi vztrajal in razvil tesnega sodelovanja laboratorija s tedaj nastajajočo slovensko elektronsko industrijo, ki je za posodobitev laboratorija prispevala znatna sredstva. Ob prenovitvi laboratorija je kot član gradbenega odbora skupaj sprof. Grudnom poskrbel, da je fakulteta leta 1970 dobila novo stavbo (t.i. »elektroniko«) in prizidek, kar je oboje z novimi predavalnicami, laboratoriji in kabineti za učiteljev znatno omililo tedjanjo prostorsko stisko na FE. V dogajanju okoli posodobitve mikrovalovnega laboratorija lahko prepoznamo med univerzitetnimi učitelji zelo redko vrlino – prof. Trontelj je imel včasih komaj razumljivo sposobnost, da je znal svoje tehnične zamisli industrijskemu okolju predstavi tako, da jih je sprejelo za svoje.

Leta 1973 je bil prof. Trontelj na FE izvoljen za izrednega profesorja. V tem obdobju je zamenjal težišče svojega zanimanja ter hkrati tudi težišči svojega raziskovalnega in strokovnega dela: mesto mikrovalov so v središču njegove pocies (highest in the domain of electrical engineering), and had spent several months with the company Siemens in Vienna working in the field. From those times stems the deep friendship between pros. Trontelj and Gruden, which years later became obvious to everyone, when Lojze took loving care of his aging mentor. After graduating prof. Trontelj took a job with the Institute for electro communications, and simultaneously became a teaching assistant at the Faculty of Electrical Engineering. After returning from serving in the army, on recommendations from professors Gruden and Budin he stared lecturing at the Faculty on microwaves.

In 1965 prof. Trontelj was granted the Ms. Sc. degree in the field of electronic optics, with the work *A Determination of the Width of the Resonance Curve and Other Microwave Parameters of Ferrites*, and in 1967 went to the Technical High School in Stockholm, Sweden, to further his studies. He specialized in nonlinear phenomena in microwave ferrites. A year later he completed his Dr. Sc. Studies and was granted the degree for his thesis *A Method for Determining the Components of the Tensor Permeability of Ferrites*. Still a year later he became an assistant professor at the Faculty of Electrical Engineering, responsible for lectures on microwaves. At the same time he was invited by prof. Agdur to Stockholm again, where he initiated research into the integration of microwave ferrite elements into microwave integrated circuits. Perhaps we can see in his choice of the research topic in Sweden the beginnings of an interest, to which prof. Trontelj later dedicated his professional life – miniaturization and integration of electronic systems. His collaboration with the Technical High School in Stockholm, where he led the project Microwave Ferrite Microcircuits, lasted until 1971. He had organized the collaboration in such a way, that a large part of the research was in fact performed at the Laboratory for Microwaves and Microelectronics of the Faculty of Electrical Engineering in Ljubljana. With the perhaps predicable result that the scientific and technological level of the laboratory has been raised to the standard of modern research centers, with notable research results. This achievement would certainly not have been possible, had not prof. Trontelj developed a fruitful collaboration of the laboratory with the emerging Slovenian electronics industry, which contributed considerable financial funds for the modernization of the laboratory. As a member of the Building committee of the Faculty prof. Trontelj, together with prof. Gruden, made sure that the Faculty was able to acquire a new building (the so called »electronics building«) as part of the modernization of the laboratory, which greatly expanded the research and teaching facilities of the Faculty. In these activities concerning the modernization and expansion of the laboratory we can glimpse the extraordinary ability of prof. Trontelj – in fact an ability quite rare among university professors – to present his ideas to the industrial sphere in such a way that they can be accepted as their own.

zornosti nadomestile mikroelektronske tehnologije. Njegov spremenjeni pogled na vlogo elektronike in elektrotehnike v družbi morda najbolje ilustrirajo odgovori na vprašanja v nekem intervjuju z njim, ki je bil objavljen leta 1975:

»Delo, ki ga je opravljal pokojni ustanovitelj naše fakultete dr. Ing. Milan Vidmar sega na nekoliko drugačno področje tehnike, kot jo danes obravnava mikroelektronika. Poenostavljeno rečeno, sodijo njegovi dosežki med stroje, ki pomagajo človeškim mišicam, medtem ko mikroelektronika posega na področje računalništva in informatike, torej ima tu ambicijo, pomagati človeškim možganom. Mikroelektronika pomeni danes tretjo tehnološko revolucijo in ta čas ni videti, skoraj ni mogoče oceniti njenih velikih razvojnih možnosti. Zagotovo je mogoče napovedati le to, da se bo življenje v naslednjem desetletju bistveno spremenilo, ker bo mikroelektronika omogočila tesnejše stike med ljudmi, seveda z omogočanjem najrazličnejših informacij.«

Danes bi lahko njegovo napoved o uspehu in pomenu mikroelektronike ter strojev, ki jih snuje ter tako pomaga človeškim možganom, brez zadrege ocenili kot jasnovidno. Njega samega pa čar elektronske revolucije ni zavedel, »Že na tej stopnji, kakršno ponuja današnji razvoj mikroelektronike, je, politično vzeto, potrebna dobršna mera razsodnosti. … Mikroelektroniko je treba razumeti kot infrastrukturo za celo vrsto tehniških udejstvovanj.« Z vsem žarom in energijo svoje osebnosti se je posvetil novemu cilju.

Prof. Trontelj je bil izvoljen za rednega profesorja leta 1980 in jasnoviden ali ne, je svojo vizijo nove elektronske tehnike poskušal uresničiti. Že v letu 1969 je na Fakulteti za elektrotehniko ustanovil manjši mikroelektronski laboratorij, ki je hitro postal vodilna tovrstna ustanova pri nas. Novi laboratorij pravzaprav ni bil prvi na področju modernih polprevodniških tehnologij pri nas, vendar so se dotlej vsi poskusi delovanja na novem raziskovalnem in tehničnem področju izjalovili. Prof. Trontelj pa je za začetne neuspehe te dejavnosti pri nas med prvimi prepoznal razlog: uspešno delovanje nekega mikroelektronskega laboratorija ni odvisno le od strokovne usposobljenosti raziskovalcev in razvijalcev, ki v njem delajo, in akademske relevantnosti njihovega dela, temveč v veliki meri tudi od tega, da delajo na projektih in nalogah, ki so pomembni za industrijsko okolico družbe v kateri laboratorij deluje in ji lahko neposredno koristijo. Problem delovanja takšnega laboratorija je torej v veliki meri organizacijski. Zato je takoj po ustanovitvi laboratorija začel iskati stike z jugoslovansko in svetovno elektronsko industrijo in z njo sodelovati. Hkrati pa ni spregledal, da je takšen laboratorij živ organizem, ki poleg prostorov, opreme in primernega programa dela, zahteva tudi dobro kvalificirano in uglašeno skupino strokovnjakov, ki v njem delajo. Zbrati takšno skupino na tako zelo interdisciplinarnem področju, kot je mikroelektronika, na področju, ki pri nas ni imelo nikakršne tradicije, ni bilo lahko in še teže je bilo skupino elektrotehnikov, kemikov, fizikov in metalurgov uglasiti. Vendar je prof. Trontlju, predvsem s svojim zgledom in svojo vero v poslanstvo takšnega

In 1973 prof. Trontelj was promoted at the Faculty of Electrical Engineering to the position of associate professor. At this time the center of his research and professional interest also moved: microwaves were replaced by the microelectronics technologies. His changed views of the role of the electrical engineering and electronics in the society are perhaps best illustrated in an interview with him, published in 1975:

»The work of dr. ing. Milan Vidmar, the departed founder of our Faculty, is in a different field of electrical engineering than microelectronics. To simplify somewhat, his achievements aim at augmenting and replacing human muscles with machines, while microelectronics in the realm of computers and informatics aims and has the ambition to help human brain. Microelectronics today is the third technological revolution and today it is no possible to foresee, it is almost impossible to judge, its great development potential. But we can predict that the human life in the coming decade will be fundamentally changed, because microelectronics will make closer contacts between people possible, of course by making the exchange of different information possible.«

Today his prediction of the success and importance of the microelectronic technologies, and the machines that help human brains it makes possible, can be judged nothing less than clairvoyant. But he has not been led astray by the spell of the electronics revolution. »Even at this stage of the development of the microelectronics technology, politically speaking, a good deal of sound judgment is necessary … . Microelectronics must be understood as an infrastructure for a large number of technical activities.« With all enthusiasm and energy of his personality he dedicated himself to the new goal.

Prof. Trontelj was tenured in 1980, and, clairvoyant or not, tried to realize his vision of the new electronic technologies. Already a decade earlier he has established a small laboratory for microelectronics at the Faculty of Electrical Engineering. In fact, this laboratory has not been the first of its kind in Slovenia, but all attempts to establish the new microelectronics technologies in this county came to nothing. Prof. Trontelj was the first to understand the causes of this failure: a successful operation of such an establishment does not depend solely on the professional qualifications of the researchers and other personnel employed, nor on the academic merit of their endeavors, but to a large extend also on the relevance and utility of their projects to its industrial environment. The problem of successfully running such a laboratory is thus to a large extent organizational. Therefore, immediately after the establishment of the laboratory he sought contacts with the electronic industry, in Yugoslavia and abroad. However, he did not overlook the fact that such a laboratory is a live organism that in addition to good facilities and a viable program requires a well qualified group of specialists working in it. To assemble such a group in such an interdisciplinary field of endeavor as is micro electronics that had no tradition in Slov-

laboratorija pri nas, uspelo tudi to. Njegova skupina je v osemdesetih letih skupaj s firmo iz silicijeve doline razvila submikronsko tehnologijo CMOS, izvedla je številne uspešne projekte za slovenske in tuje uporabnike, ter s svojimi izkušnjami tesno sodelovala pri postavljanju Iskrine mikroelektronske tovarne v Stegnah. Prof. Trontelj je bil tedaj avtor koncepta razvoja Iskrine Mikroelektronike in soavtor investicijskih elaboratov za izgradnjo tovarne. Vse to brez široko razpredenega mednarodnega sodelovanja laboratorija, fakultete in podjetja Iskre pravzaprav ne bi bilo mogoče in prof. Trontelj je osebno prevzel velik del bremena, ki ga je tako zastavljeno delo zahtevalo. Navkljub svojemu uglednemu akademskemu položaju bil tako od leta 1986 do 1991 tehnični svetnik v Iskrini izpostavi v Silicijevi dolini v ZDA, in je do upokojitve sodeloval je s številnimi eminentnimi akademskimi ustanovami s področja (Stanford University, ZDA) in podjetji (International Microelectronic Products, Hewllett Packard, Motorola, vse iz ZDA, ter Siemens in AMS iz Avstrije). Za vrhunec organizacijskih uspehov prof. Trontlja danes lahko štejemo gradnjo in prenovo laboratorija za mikroelektroniko na FE. Fakulteta je z novim laboratorijem postala ena sorazmerno redkih akademskih ustanov na svetu, ki lahko razpolaga s takšnim laboratorijem. Hkrati s »prenovo« laboratorija (v resnici je šlo za novogradnjo), se je fakulta ponovno lahko prostorsko razžirila, saj je bil znaten del nove stavbe (t.i. »stolpiča«) s predavalnicami in laboratoriji ponovno namenjen pedagoškemu in drugemu raziskovalnemu delu na fakulteti. Gradnja je bila ob velikih naporih zaključena leta 1990 s sredstvi, ki so jih prispevala Iskra ter slovenska in zvezna, jugoslovanska vlada, slednja v znatni meri zaradi uspehov, ki jih je laboratorij imel pri sodelovanju z JLA. Laboratorij s svojima skupinama za tehnologijo in načrtovanje tako danes lahko nadaljuje pomembno delo na področju mikroelektronike, ki ga je začel prof. Trontelj in zasleduje cilje, ki jih je prvi identificiral. Njegovo organizacijsko delo pa ni bilo omejeno le na FE in laboratorij za Mikroelektroniko. S svojimi izkušnjami je bil ključni člen in član predsedstva skupščine Raziskovalne skupnosti Slovenije, predsednik, odbora za raziskovalno infrastrukturo (RSS), član ekspertne skupine za tehniške vede (RSS), član sveta za tehnologijo in inovacije pri Izvršnem svetu skupščine SR Slovenije ter član predsedstva odbora za sestavne dele in materiale pri ETANu.

Ob vsem tem, če si pomagamo z evfemizmom, napornem organizacijskem delu (naša neprestano tranzicijska družba v resnici nikoli ni dobro razumela pomena tehničnega razvoja in znala prisluhniti njegovim potrebam, zato je takšno delo vedno zahtevalo človeka in pol) je bil prof. Trontelj izvrsten pedagog. Gotovo neprimerno boljši, kot so mu bili to pripravljeni priznati z vsakdanjimi študijskimi težavami obremenjeni študenti ali celo kolegi. Kot rečeno, na FE je predaval premeta Mikrovalovi in Mikrovalovna elektronika ter predmeta s področja mikroelektronike Mikroelektronske tehnologije ter Materiali in tehnologije. Za potrebe svojih študentov je napisal nekaj skript in učbenik s področja mikrovalov, ter s učbenik za področje mikroelektronike. Med učbenike gotovo lahko štejemo tudi njegovo knjigo

enia was not a mean task, and keeping it together was even more demanding. But with his personal example and his faith in the mission of such a group, he managed that too. In the eighties his group, in collaboration with an American company form the Silicon Valley developed a submicron fabrication technology for ICs, successfully completed numerous projects for the Slovenian customers and customers from abroad, and contributed significantly with its expertise in the establishment of the Iskra Microelectronics fabrication facilities at Stegne, Ljubljana. Prof. Trontelj was the author of the Iskra Microelectronics project, and conceived the development plans for the facility. All of this would not have been possible without wide ranging international collaborations of the laboratory, the Faculty in the Iskra Company. Prof. Trontelj personally took a large part of the burden that such collaboration represents, on him. Despite his respectable academic position from 1986 to 1991 he has held the position of the senior Iskra consultant and representative in the Silicone Valley, and until his retirement collaborated in the microelectronics field with prominent academic institutions (Stanford University, ZDA) and companies (International Microelectronic Products, Hewlett Packard, Motorola, all from ZDA, and Siemens and AMS from Austria). Today we can judge that the highlight of his organizational efforts must surely be the building and equipping of the new facilities of the Laboratory for Microelectronics at the Faculty of Electrical Engineering. With this addition the Faculty became one of the relatively few academic institutions in the world with such a facility at its disposal. Not to mention the fact, that during the building of the new laboratory a new building for the academic use has been erected also (the so called tower), with new lecture rooms, laboratories etc. With great efforts all of this has been completed in 1990, with significant financial contributions from Iskra, Slovenian, and Yugoslav governments. The latter no doubt based on the several successfully completed projects in the past by the Laboratory for the Yugoslav army. Thanks to these efforts the Laboratory, with its technology and design groups, remains the leading group working in micro electronics in Slovenia, still following the goals set by prof. Trontelj. His organizational talents and efforts were not limited to the Faculty and its Laboratory for Microelectronics. With his expertise and contacts he was a key and leading member of the presidency of the Slovenian Research Community, chairman of its infrastructure committee, member of the expert group for technical sciences, member of the Technology and Innovations Council of the administration of the Republic of Slovenia, and a member of the presidency of the ETAN professional association.

In addition to all this considerable organizational efforts (to use an understatement: our ever transitional society never quite understood the importance of technological development and never found effective institutional ways to serve its needs, therefore all such efforts were truly titanic), prof. Trontelj was a gifted and exceptional teacher. Certainly much better than his overburdened students and sometimes even his perhaps slightly envious colleagues were

Analog Digital ASIC Design, ki je leta 1989 izšla pri založbi McGraw-Hill Book Company Ltd, (s soavtorjema J. Trontljem in G. Shentonom), kot prva tovrstna publikacija na področju sploh. Delo je sčasoma postalo prava uspešnica, ki jo še danes najdete na seznamih citiranih del. S to knjigo ter svojimi raziskavami na področju načrtovanja in realizacije analogno digitalnih integriranih vezij po naročilu se je tedaj uvrstil med vodilne raziskovalce na področju.

Navajanje učbenikov ob njegovem pedagoškem delu pa je v resnici le tehnična podrobnost. Največja in najimenitnejša pedagoška novost, ki jo je prof. Trontelj uvedel na FE in pravzaprav tudi na Ljubljansko univerzo in ki jo kot pedagog tudi sam še vedno občudujem, so bila njegova predavanja iz mikroelektronskih tehnologij. Že v času, ko o novih načinih podajanja snovi in o bolonjski reformi še ni bilo niti govora, je imel navado ob začetku semestra študentom razdeliti teme, ki so jih nato samostojno in s pomočjo sodelavcev iz Laboratorija za mikroelektroniko ter ob delu v laboratoriju samem podrobno obdelali. Ter nato v okviru učnih ur predmeta predstavili svojim kolegom. Vse to je od študentov, sodelavcev in seveda učitelja samega zahtevalo ogromno dela, ki pa se je izkazalo za izredno plodno. Ravno zaradi v trudu pridobljenega znanja in izkušenj so se številni študenti odločili, da svoje diplomsko delo naredijo na področju mikroelektronike, mnogi s prof. Trontljem kot mentorjem. Številni diplomanti pa so se odločili, da svojo akademsko pot nadaljujejo na FE in tudi v Laboratoriju za mikroelektroniko. Tako lahko Lojzetovi sodelavci danes s ponosom trdimo, da je velika večina slovenskih strokovnjakov za mikroelektroniko šli skozi »Trontljevo šolo«, ki ni obsegala samo dodiplomskega študija, temveč tudi podiplomskega in doktorskega. Pod njegovim mentorstvom je študije zaključilo 35 inženirjev elektrotehnike, 23 magistrov ter 15 doktorjev znanosti. Za sorazmerno specializirano področje, ki je ob ukinitvi Iskrine tovarne mikroelektronike navsezadnje izgubilo dobršen del svojega zaledja, so to impresivne številke. Sam pa je nanje ohranil, kot vedno, trezen pogled in je menil, da jih je bilo očitno še premalo, sicer se zaplet z Iskrino Mikroelektroniko gotovo ne bi bil zgodil. Pedagoška dejavnost prof. Trontlja in njegova »šola« se nista končala na pragu FE. Menil je, da morajo biti prav vsi, ki delajo na področju, primerno strokovno izobraženi in je organiziral tečaje iz mikroelektronike ter na njih predaval na IEVT (Tanke plasti v mikroelektroniki) ter na Iskrini šoli RR (Mikroelektronske tehnologije).

Prof. Trontelj je bil član strokovnega združenja IEEE in društva MIDEM. Za svoje raziskovalno in razvojno delo je prejel številne nagrade in priznanja: nagradi Kidričevega sklada leta 1972 in 1988, nekaj nagrad za iznajdbe in je bil je imenovan za inovatorja leta, če naštejemo le najbolje vidne. S področja mikroelektronike je objavil preko 100 člankov in referatov. S sodelavci je bil nosilec sploh prvega patenta, ki ga je bil kdaj podelil Urad Republike Slovenije za intelektualno lastnino. Po upokojitvi leta 2000 mu je bil za njegov prispevek k razvoju mikroelektronike v Sloveniji podeljen naziv Zaslužni profesor Univerze v Ljubljani.

ready to grant him. As already mentioned, at the Faculty he lectured on microwaves, micro electronic technologies, and modern electronic materials. He wrote several textbooks covering these fields. Among these we can surely count his *Analog Digital ASIC Design*, which he wrote with coauthors J. Trontelj in G. Shenton and was published in 1989 by the McGraw-Hill Book Company Ltd. This was the first book covering the field and with time became a real bestseller, which even today can be still found among frequently cited works. With this book and his research in the field of design and manufacture of the analog-digital custom design integrated circuits, he became one of the most prominent researchers in this field.

But listing textbooks is merely a technicality when talking about his teaching success. The greatest and the most outstanding novelty prof. Trontelj brought to the Faculty, and to the Ljubljana University for that matter, one that I, as a teacher myself, still admire were his "lectures" on micro electronic technologies. Before there was even any talk about new teaching methods, or the Bologna reform of the universities, he was in the habit of distributing among his students the themes pertaining to the course. He expected them to independently and sometimes with the help of the Laboratory staff to study them in detail and then present them in seminars to their fellow students, including with the experiences they gained in actual work in the laboratory. All of this demanded great efforts from the students, the laboratory staff and certainly from the teacher himself. But the results were noting but astounding: many students decided to finish their studies in the field of micro electronics, quite a few of them with Prof. Trontelj as supervisor, many decided to continue their postgraduate studies in microelectronics and the Faculty, and their academic careers there. Today Lojzes's collaborators can proudly claim, that a large majority of the Slovenian experts in microelectronics went through the "Trontelj School", comprising not only undergraduate, but also graduate and doctoral studies. Under his mentorship 35 electrical engineers, 25 Ms. Sc. and 15 Dr. Sc. were granted their diplomas, no mean achievement in a relatively narrow, specialized field that has lost much of its outside attraction after the Iskra Mikroelektronika company was closed. He himself maintained a level opinion with regard to these numbers: there were obviously not enough of them or the closing of the factory would not have occurred, he claimed. His teaching and his "school" actually did not end at the Faculty doors. He was convinced that *everyone* working in the field should be relevantly technically educated and therefore organized special courses on microelectronics for the employees of different companies working in this and related fields.

Prof. Trontelj was a member of the professional societies IEEE, and MIDEM. For his research and development achievements he received numerous prizes and recognitions. To mention just the more illustrious ones: the Boris Kidrič Foudation prizes in 1972 and 1988, several prizes for innovations and was named The Innovator of the Year.

Prof. Lojze Trontelj je umrl 19. marca 2008 in v družinskem krogu so se od njega poslovili na ljubljanskih Žalah 22. marca 2008. Po smrti za njim ostajajo žena Nika ter hčer Helena in sin Janez ter brata Jože in Janez z družinami.

He published over 100 papers on microelectronics, and is, with collaborators, the recipient of the first patent ever granted by the Slovenian Office for Intellectual Property. After his retirement in 2000 he was elected Professor Emeritus of the University of Ljubljana for his achievements.

Prof. Lojze Trontelj passed away on March 19th 2008, and his funeral was held on March 22nd 2008 in Ljubljana. He is survived by his wife Nika, daughter Helena, son Janez and brothers Jože and Janez with their families.

Prof. dr. Radko Osredkar

Prof. dr. Lojze Trontelj
VIZIONAR IN PIONIR SLOVENSKE MIKROELEKTRONIKE

Dr. France Rode, Los Altos, CA, ZDA

Projekti nacionalno-državnega pomena običajno izhajajo iz vizije posameznika, ki je pripravljen stopiti na pot, polno ovir političnega, tehničnega in finančnega porekla, in vztrajati na njej do potrditve najvišjih avtoritet. Po uspešni prebroditvi teh začetnih težav, ki zahtevajo neomajno motivacijo in neutrudno vztrajnost, se postopek realizacije običajno porazdeli na širok krog podpornih organov, ki prevzamejo odgovornost za izvršitev posameznih delov projekta. Redki pa so primeri, ko pobudnik vizije sam prehodi pot prepričevanja, s čimer si pridobi moralno podporo odgovornih organov, nato pa je dolžan najprej ustvariti potrebno domačo ekspertizo. Če takšna ekspertiza obstaja samo v tujini in je varovana kot skrivnost peščice podjetij, bi izgledal njen prenos na domača tla skoraj nemogoč podvig tudi za najbolj motiviranega vizionarja. Dodajmo temu še pomanjkanje denarnih sredstev in težko bi našel kogarkoli drugega kot mojega dobrega prijatelja, profesorja dr. Lojzeta Trontlja, ki bi se bil voljan spopasti s takšnim problemom.

Lojze je spremljal hiter porast mikroelektronike v svetu, ki je bila v 70-tih letih strogo varovana skrivnost pionirskih podjetij Silicijeve doline in nekaterih drugih v ZDA. Podjetja Intel, Fairchild, Motorola, Texas Instruments (TI), MOSTEK in American Microsystems Inc. (AMI) so videla v svoji zvrsti polprevodniškega procesiranja edinstveno tekmovalno prednost, vojaški organi v svetu pa so se nadejali pomembne strateške premoči. Nihče v svetu takrat ni ponujal proizvodnih uslug za procesiranje mikroelektronskih vezij, kakor je to primer danes. Le lastna slovenska polprevodniška usposobljenost je predstavljala v Lojzetovih očeh tisto plovilo, ki bo dvigalo slovensko industrijo s plimo moderne svetovne tehnologije. Podjetje Hewlett-Packard še ni imelo svoje primerne tehnologije in ker sem bil odgovoren za razvoj procesorja za prvi žepni znanstveni računalnik, sem imel dostop do podjetij MOSTEK in AMI, ki sta izdelovala integrirana vezja za HP35. Tako sem lahko leta 1974 omogočil Lojzetu dostop do AMI, ki se je uveljavil že zgodaj v času razcveta Silicijeve doline.

V Silicijevi dolini je bilo dokaj običajno, da so univerze sodelovale z lokalno industrijo. Podjetja so videla v univerzah izvor strokovnih kadrov, ki so bili bolj uporabni, če so bili seznanjeni s procesi razvoja in proizvodnje. Lojze, kot predstavnik univerze, je zato kmalu našel plodna tla za ustvarjanje obojestransko koristnih vezi pri AMI. S svojim globokim poznavanjem področja polprevodniške tehnologije si je pridobil spoštovanje med tehnologi, s svojimi organizacijskimi sposobnostmi pa med menedžerji podjetja AMI. Zato mu ni bilo treba skrivati dejstva, da se je želel seznaniti s celotnim procesom ustvarjanja integriranih vezij z namenom prenosa tega znanja na svojo univerzo. V ta namen so že na prvih srečanjih ustvarili okvirni program, po katerem bi slovenski študentje prihajali k AMI in se tam naučili načrtovanja, izdelave mask za procesiranje, kasneje pa sodelovali tudi pri samem procesiranju. Za te začetne podvige je Lojze uspel dobiti sredstva od Iskre in od JLA. Seveda takrat še ni bilo govora o prenosu kakšne tehnološke skrivnosti v Slovenijo, saj se je ta vrednotila v ogromnih vsotah denarja.

Kar kmalu so slovenski strokovnjaki zasloveli pri AMI po svojih sposobnostih. To je odprlo vrata za ustvaritev skupnega projekta pod imenom Joint Developmet Team (JDT). Naši slovenski inženirji so pri tem projektu opravili levji delež in so s svojim delom po pogodbi odplačali pravico do prenosa AMI-tehnološkega procesa v Slovenijo. To je bil verjetno eden izmed najpomembnejših Lojzetovih doprinosov. Omogočil je uporabo procesirnih naprav, ki jih je Iskra Mikroelektronika bila pripravljena nabaviti, a to le pod pogojem, da bo univerza imela usposobljeno osebje in preizkušen tehnološki proces.

Lojze se je dobro zavedal potrebe po usposobitvi čim večjega števila ekspertov v načrtovanju in procesiranju polprevodniških proizvodov, saj je predvideval eksponencialen porast te tehnologije v vseh panogah industrijskega in akademskega gospodarstva. Zato je obnavljal pogodbe z AMI z minimalnimi stroški za Slovenijo in v letu 1986 tudi pričel sodelovanje z novoustanovljenim podjetjem International Microelectronik Products (IMP). V naslednjem desetletju sta Lojze in njegov brat, profesor Janez Trontelj, imela v Silicijevi dolini skupine študentov in inženirjev, ki so ne samo pridobivali znanje o najmodernejši tehnologiji, ampak so tudi dvigali ugled Slovenije s svojo intelektualno sposobnostjo. Vodja razvojnega laboratorija pri AMI je izjavil, da bi bil z veseljem sprejel v službo vsakega Slovenca, ki je delal pri njih v tistem obdobju.

Eden prvih uspešnih proizvodov novoustanovljene slovenske mikroelektronike je bilo integrirano vezje, ki je omogočalo brezkontaktno identifikacijo nosilca. Namenjeno je bilo programiranim elektronskim ključavnicam, ki bi brezžično spoznale legitimnega lastnika. Integrirano vezje, ki je bilo potrebno za delovanje te naprave, bi normalno zahtevalo baterijo, za katero pa ni bilo prostora v osebni identifikacijski kartici. Slovenski načrtovalci so zato zgradili elektronsko vezje, ki je ob približanju ključavnici sprejelo od nje potrebno energijo brezžično in tako omogočilo identifikacijski proces.

Te vrste integrirana vezja morajo kombinirati analogne in digitalne komponente na istem silicijevem čipu, kar je topološko zelo zahtevno. Preprečiti je treba medsebojne mot-

nje obeh vrst vezij, ki so po vseh merilih praktično v neposredni bližini. Lojze in Janez se nista izgubila v morju birokratskih dolžnosti in sta se osebno spoprijela s temi problemi med letoma 1984 in 1988 ter v letu 1998 skupno s soavtorjem Grahamom Shentonom izdala knjigo *Analog Digital ASIC Design*. V njej sta orisala osnovne principe pa tudi mnogo konkretnih primerov uspešnega načrtovanja kombiniranih analognih in digitalnih vezij. Kot edinstvena publikacija te vrste je njuna knjiga požela veliko zanimanje po vsem svetu, saj se je tehnologija mobilnih telefonov in globalnih navigacijskih sistemov prav takrat spoprijemala s problematiko sožitja analognih in digitalnih vezij na istih čipih. Bogat obisk njunih predavanj je pričal o pomembnosti njunega doprinosa k znanosti načrtovanja kompleksnih integriranih vezij.

Poleg pomembnega števila izvajalcev Lojzetove vizije, ki so se usposobili v Silicijevi dolini, se je pod njegovim akademskim programom usposobilo še mnogo večje število mladih študentov elektronike v teoriji in praksi polprevodniške tehnike, med njimi tudi akademikov, ki se danes uvrščajo med vrhunske v svetu. Ti strokovnjaki skupaj tvorijo pomembno jedro slovenskega znanja, ki bo vedno omogočalo ustvarjanje inovativnih slovenskih integriranih vezij. Dejstvo, da se ta v sedanji dobi pretežno izdelujejo v za to prirejenih procesirnih delavnicah, ne zmanjša Lojzetovega uspešnega lastnoročnega prenosa ene najpomembnejših tehnologij stoletja v slovensko okolje.

Informacije MIDEM
Strokovna revija za mikroelektroniko, elektronske sestavine dele in materiale

NAVODILA AVTORJEM

Informacije MIDEM je znanstveno-strokovno-društvena publikacija Strokovnega društva za mikroelektroniko, elektronske sestavne dele in materiale - MIDEM. Revija objavlja prispevke s področja mikroelektronike, elektronskih sestavnih delov in materialov. Ob oddaji člankov morajo avtorji predlagati uredništvu razvrstitev dela v skladu s tipologijo za vodenje bibliografij v okviru sistema COBISS.
Znanstveni in strokovni prispevki bodo recenzirani.

Znanstveno-strokovni prispevki morajo biti pripravljeni na naslednji način:

1. Naslov dela, imena in priimki avtorjev brez titul, imena institucij in firm
2. Ključne besede in povzetek (največ 250 besed).
3. Naslov dela v angleščini.
4. Ključne besede v angleščini (Key words) in podaljšani povzetek (Extended Abstract) v angleščini, če je članek napisan v slovenščini
5. Uvod, glavni del, zaključek, zahvale, dodatki in literatura v skladu z IMRAD shemo (Introduction, Methods, Results And Discsussion).
6. Polna imena in priimki avtorjev s titulami, naslovi institucij in firm, v katerih so zaposleni ter tel./Fax/Email podatki.
7. Prispevki naj bodo oblikovani enostransko na A4 straneh v enem stolpcu z dvojnim razmikom, velikost črk namanj 12pt. Priporočena dolžina članka je 12-15 strani brez slik.

Ostali prispevki, kot so poljudni cčlanki, aplikacijski članki, novice iz stroke, vesti iz delovnih organizacij, inštitutov in fakultet, obvestila o akcijah društva MIDEM in njegovih članov ter drugi prispevki so dobrodošli.

Ostala splošna navodila

1. V članku je potrebno uporabljati SI sistem enot oz. v oklepaju navesti alternativne enote.
2. Risbe je potrebno izdelati ali iztiskati na belem papirju. Širina risb naj bo do 7.5 oz.15 cm. Vsaka risba, tabela ali fotografija naj ima številko in podnapis, ki označuje njeno vsebino. Risb, tabel in fotografij ni potrebno lepiti med tekst, ampak jih je potrebno ločeno priložiti članku. V tekstu je treba označiti mesto, kjer jih je potrebno vstaviti.
3. Delo je lahko napisano in bo objavljeno v slovenščini ali v angleščini.
4. Uredniški odbor ne bo sprejel strokovnih prispevkov, ki ne bodo poslani v dveh izvodih skupaj z elektronsko verzijo prispevka na disketi ali zgoščenki v formatih ASCII ali Word for Windows. Grafične datoteke naj bodo priložene ločeno in so lahko v formatu TIFF, EPS, JPEG, VMF ali GIF.
5. Avtorji so v celoti odgovorni za vsebino objavljenega sestavka.

Rokopisov ne vračamo. Rokopise pošljite na spodnji naslov.

Uredništvo Informacije MIDEM
MIDEM pri MIKROIKS
Stegne 11, 1521 Ljubljana, Slovenia
Email: Iztok.Sorli@guest.arnes.si
tel. (01) 5133 768, fax. (01) 5133 771

Informacije MIDEM
Journal of Microelectronics, Electronic Components and Materials

INSTRUCTIONS FOR AUTHORS

Informacije MIDEM is a scientific-professional-social publication of Professional Society for Microelectronics, Electronic Components and Materials – MIDEM. In the Journal, scientific and professional contributions are published covering the field of microelectronics, electronic components and materials.
Authors should suggest to the Editorial board the classification of their contribution such as : original scientific paper, review scientific paper, professional paper…
Scientific and professional papers are subject to review.

Each scientific contribution should include the following:

1. Title of the paper, authors' names, name of the institution/company.
2. Key Words (5-10 words) and Abstract (200-250 words), stating how the work advances state of the art in the field.
3. Introduction, main text, conclusion, acknowledgements, appendix and references following the IMRAD scheme (Introduction, Methods, Results And Discsussion).
4. Full authors' names, titles and complete company/institution address, including Tel./Fax/Email.
5. Manuscripts should be typed double-spaced on one side of A4 page format in font size 12pt. Recommended length of manuscript (figures not included) is 12-15 pages
6. Slovene authors writing in English language must submit title, key words and abstract also in Slovene language.
7. Authors writing in Slovene language must submit title, key words and extended abstract (500-700 words) also in English language.

Other types of contributions such as popular papers, application papers, scientific news, news from companies, institutes and universities, reports on actions of MIDEM Society and its members as well as other relevant contributions, of appropriate length , are also welcome.

General informations

1. Authors should use SI units and provide alternative units in parentheses wherever necessary.
2. Illustrations should be in black on white paper. Their width should be up to 7.5 or 15 cm. Each illustration, table or photograph should be numbered and with legend added. Illustrations, tables and photographs must not be included in the text but added separately. However, their position in the text should be clearly marked.
3. Contributions may be written and will be published in Slovene or English language.
4. Authors must send two hard copies of the complete contributon, together with all files on diskette or CD, in ASCII or Word for Windows format. Graphic files must be added separately and may be in TIFF, EPS, JPEG, VMF or GIF format.
5. Authors are fully responsible for the content of the paper.

Contributions are to be sent to the address below.

Uredništvo Informacije MIDEM
MIDEM pri MIKROIKS
Stegne 11, 1521 Ljubljana, Slovenia
Email: Iztok.Sorli@guest.arnes.si
tel.+386 1 5133 768, fax.+386 1 5133 771

MIDEM
DRUŠTVO-SOCIETY
IMAPS Slovenia Chapter

M I D E M

Strokovno društvo za mikroelektroniko,
elektronske sestavne dele in materiale
MIDEM pri MIKROIKS
Stegne 11, 1521 Ljubljana
SLOVENIJA

TEL.: +386 (0)1 5133 768
FAX: +386 (0)1 5133 771
Email / WWW
iztok.sorli@guest.arnes.si
http://paris.fe.uni-lj.si/midem/

MIDEM SOCIETY REGISTRATION FORM

1. First Name ..... Last Name .....

   Adress .....

   City .....

   Country ..... Postal Code .....

2. Date of Birth .....

3. Education (please, circle whichever appropriate)

   PhD MSc BSc High School Student

3. Profession (please, circle whichever appropriate)

   Electronics Physics Chemistry Metallurgy Material Sc.

4. Company .....

   Adress .....

   City .....

   Country ..... Postal Code .....

   Tel.: ..... FAX: .....

   Email .....

5. Your Primary Job Function

   Fabrication Engineering Facilities QA/QC
   Management Purchasing Consulting Other

6. Please, send mail to a) Company adress b) Home Adress

7. I wil regularly pay MIDEM membership fee, 25,00 EUR/year

MIDEM member recive Journal "Informacije MIDEM" for free !!!

Signature ..... Date .....

MIDEM at MIKROIKS
Stegne 11

1521 Ljubljana
Slovenija

ORGANI DRUŠTVA MIDEM - BOARDS OF MIDEM

Predsednik društva MIDEM
MIDEM President

Prof. dr. Slavko Amon, univ. dipl. inž. el., Fakulteta za elektrotehniko, Ljubljana, Slovenija

IZVRŠILNI ODBOR MIDEM - MIDEM EXECUTIVE BOARD

Podpredsednika
Vice-presidents

Prof. dr. Marija Kosec, univ. dipl. inž. kem., Institut "Jožef Stefan", Ljubljana, Slovenija
Dr. Iztok Šorli, univ. dipl. inž. fiz., MIKROIKS, d. o. o., Ljubljana, Slovenija

Tajnik
Secretary

Igor Pompe, univ. dipl. inž. el., Ljubljana, Slovenija

Člani izvršilnega odbora MIDEM
Executive Board Members

Prof. dr. Janez Trontelj, univ. dipl. inž. el., Ljubljana, blagajnik
Darko Belavič, univ. dipl. inž. el., HIPOT-RR, d. o. o., Šentjernej
Prof. dr. Bruno Cvikl, univ. dipl. inž. fiz., Fakulteta za gradbeništvo, Maribor
Mag. Leopold Knez, univ. dipl. inž. el., Iskra TELA, d. d. , Ljubljana
Dr. Miloš Komac, univ. dipl. inž. kem., ARRS, Ljubljana
Jožef Perne, univ. dipl. inž. el. , Zavod TC SEMTO
Prof. dr. Marko Topič, univ. dipl. inž. el.; Fakulteta za elektrotehniko, Ljubljana
Prof. dr. Anton Zalar, univ. dipl. inž. met., Institut "Jožef Stefan", Ljubljana
Dr. Werner Reczek, Infineon, Avstrija
Prof. dr. Giorgio Pignatel, University of Perugia, Italija
Prof. dr. Leszek J. Golonka, Technical University, Wroclaw, Poljska

Nadzorni odbor
Supervisory Board

Prof. dr. Franc Smole, univ. dipl. inž. el., Fakulteta za elektrotehniko, Ljubljana
Mag. Andrej Pirih, univ. dipl. inž. el., Iskra - Zaščite, d. o. o. , Ljubljana
Dr. Slavko Bernik, univ. dipl. inž. kem., Institut "Jožef Stefan", Ljubljana

Častno razsodišče
Court of Honour

Franc Jan, univ. dipl. inž. fiz., Kranj
Prof. dr. Radko Osredkar, univ. dipl. inž. el., Fakulteta za elektrotehniko, Ljubljana
Prof. dr. Jože Furlan, univ. dipl. inž. el., Ljubljana

Sponzorji MIDEM

MIDEM Sponsors

JAVNA AGENCIJA ZA RAZISKOVALNO DEJAVNOST RS, Ljubljana

INSTITUT "JOŽEF STEFAN", Odsek za elektronsko keramiko, Ljubljana

FAKULTETA ZA ELEKTROTEHNIKO - LMFE, Ljubljana

FAKULTETA ZA ELEKTROTEHNIKO - LMSE, Ljubljana

FAKULTETA ZA ELEKTROTEHNIKO - LPVO, Ljubljana

MIKROIKS, d.o.o., Ljubljana

TC SEMTO, Ljubljana

ISKRA ZAŠČITE d.o.o., Ljubljana

RLS, d.o.o., Ljubljana

Informacije MIDEM, 38(2008)3, Ljubljana, SEPTEMBER 2008, ISSN 0352-9045, UDK 621.3:(53+54+621+66)(05)(497.1)=00

Strokovna revija za mikroelektroniko, elektronske sestavne dele in materiale

Journal of Microelectronics, Electronic Components and Materials

Publikacija informacije MIDEM izhaja po ustanovitvi Strokovnega društva za mikroelektroniko, elektronske sestavne dele in materiale - MIDEM kot nova oblika publikacije Informacije SSOSD, ki jo je izdajal Zvezni strokovni odbor za elektronske sestavne dele in materiale SSOSD pri Jugoslovanski zvezi za ETAN od avgusta 1969 do 6. oktobra 1977 in publikacije Informacije SSESD, ki jo je izdajala Strokovna sekcija za elektronske sestavne dele, mikroelektroniko in materiale - SSESD pri Jugoslovanski zvezi za ETAN od 6. oktobra 1977 do 29. januarja 1986.

Časopis Informacije MIDEM je vpisan v register časopisov pri Ministrstvu za informiranje pod registrsko številko 809.